SOME PHYSICAL PROPERTIES OF IONIC MELTS IN RELATION TO THEIR STRUCTURE

By

William Ewen Smith, B.Sc., A.R.C.S.T.

A Thesis submitted to the University of London for the Degree of Doctor of Philosophy.

Department of Chemical Engineering and Chemical Technology,
Imperial College of Science and Technology,
London, S.W.7.

October, 1965.

Abstract.

The unusual physical behaviour of the melt of potassium nitrate and calcium nitrate had previously been reported. In the present study, the liquid behaviour is defined quantitatively in terms of physical properties, some results are taken on related systems and a structural explanation postulated to explain the data.

A brief review of fundamental liquid theory and theories of viscosity transport are given. A more detailed analysis of the experimental measurements in molten salts most relevant to a structural analysis and a study of previous work in the monodivalent nitrate melts leads to a simple structural model capable of a limited interpretation of experimental behaviour.

Qualitative studies on the nature of the low temperature form of certain compositions of the mixed nitrate melts verifies previous reports of glass formation. A quantitative study in the liquid range of the viscosity of the binary mixtures of sodium, potassium, rubidium and caesium nitrate with calcium nitrate established the essentially non-Arhenius nature of the viscosity plots. An investigation of the electrical conductivity and

U.V. spectra of the melts was then carried out. The conclusions drawn indicated the possibility of anomalous dielectric effects in the supercooled melt. Techniques were developed for this study and results indicating some form of loss mechanism obtained.

Various possible correlations of the data on the basis of simple molecular models were calculated and some conception of the nature of the low temperature liquid form established. A final model explaining the varied behaviour of the properties, including dielectric effects is given.

Acknowledgements.

The author wishes to express his gratitude to Professor A.R. Ubbelohde, F.R.S., for his supervision of this research and for his active advice and encouragement throughout.

Thanks are also due to Dr. Elizabeth Rhodes for her continued help and assistance in all stages of the work.

The support of a Science Research Council Grant and the use of equipment provided by the Ministry of Aviation are also acknowledged.

C O N T E N T S.

	Page
Abstract	2
Acknowledgements	4
SECTION I.	7
Chapter 1 Liquid State Theory and its Application to Transport.	8
1.1. General Theory	8
1.2. Transport Theory	14
1.2.1. Relaxation Theory	15
1.2.2. Vibration Theory of Andrade	16
1.2.3. Hole Theory of Eyring	18
1.2.4. Free Volume Theory	21
Chapter 2 An Experimental Approach to the Problem of Molten Salt Structures.	24
2.1. General Experiments	24
2.1.1. X-ray and Neutron Diffraction Data	24
2.1.2. Ultraviolet Spectroscopy	27
2.1.3. Raman Spectra Studies	30
2.1.4. Thermodynamic and Transport Data	31
2.1. A Review of Knowledge of Binary Alkali-Alkaline Earth Nitrate Mixtures.	33
2.2.1. Preliminary Studies	33
2.2.2. The Work of C.A. Angell	37
2.2.3. The Work of W.A. McAuley	38
2.3. The Simple Volume Model of McAuley, Rhodes and Ubbelohde	39
2.3.1. The size and shape of the ions	40
2.3.2. The model solution	43

(CONTENTS - contd.)

	Page
SECTION II.	45
Chapter 3 General Techniques and Qualitative Studies of the Melts.	46
3.1. General Techniques	46
3.1.1. The Basic Equipment	46
3.1.2. Preparation of Samples	47
3.2. Qualitative Studies of the Melts	50
3.2.1. Chemical and Physical Stability	50
3.2.2. Possible Glass Formation	51
Chapter 4 Results of Quantitative Experiments.	57
4.1. Viscosity	57
4.1.1. Definition	57
4.1.2 Description of Apparatus	60
4.1.3. Description of the Method Used	62
4.1.4. Experimental Error Analysis	64
4.1.5. Accuracy	69
4.1.6. Results	69
4.2. Conductivity	77
4.3. Additions of Chlorides and Bromides to the Melt	82
4.4. Ultraviolet Spectra	85
Chapter 5 Experimental Studies of the Dielectric behaviour of the supercooled melt.	92
5.1. Methods of Measurement	92
5.1.1. Cell Design	92
5.1.2. Transformer Ratio Arm Bridge Circuits	95
5.1.3. The Complete Bridge Measuring Circuit	98
5.1.4. Equipment checks	100
5.2. Presentation of Results	101
5.2.1. Measurements of the dielectric constant	103
5.2.2. Dielectric loss measurements	105
SECTION III.	113
Chapter 6 Explanation of the results in terms of a simple liquid model.	114
Chapter 7 Discussion of the Dielectric Results.	142
7.1. The Standard Interpretation of Polarization phenomena in terms of Molecular Structure.	143
7.2. The Experimental Behaviour	149
References.	157

Section I.

This section deals with a brief survey of general theoretical and experimental results useful in the discussion of the structure of the melts. In Chapter 1, a brief description of liquid theory based mainly on cell and hole theory is given and applied to the case of simple transport theories. In Chapter 2, general experiments helpful in understanding the nature of molten salts are given and are followed by a more detailed discussion of knowledge in the actual systems under analysis.

Chapter 1.

Liquid State Theory and its Application to Transport.

1.1. General Theory.

In both solid and gaseous states, one feature of overriding importance allows the construction of simple, exact models capable of complete solution. In a gas the criterion is the large separation between molecules and in a solid it is the long range order. No similar feature exists in liquids, the size and shape of the molecule, the nature of the intermolecular forces, separation distances, the degree of randomisation and other factors must all be considered. So far, no exact solutions have been obtained and all useful approximations have involved drastic and unrealistic simplifications. The cell and hole theories are considered most likely to provide an eventual solution to the specific problems of ionic liquids, since qualitatively similar conclusions are derived from the experimental studies described in Chapter 2.

X-ray and neutron diffraction data (see 2.1.1.) show that, while there is short range order in a liquid extending to second and third co-ordination shells, no long range order exists. The most effective method of dealing with such

a problem is likely to be by a statistical approach. A direct mathematical solution to the problem is not at present possible due to the complexity of the equations obtained. All theories make some form of assumption either mathematical or physical. While mathematical assumptions are preferable since they can be refined without altering the basic approach, physical models are generally more useful in interpreting experiment and at present more advanced.

The theory starts with the consideration of the molecular partition function,

$$z = \frac{1}{h^{3N} \cdot N!} \int \cdots \int e^{-\frac{H}{kT}} \, dr_1 \cdots dr_N dp_1 \cdots dp_N$$

N is the number of particles considered, $dr_1 \cdots dr_N$ are volume elements of the particles 1 to N at vector distances $r_1 \cdots r_N$ from a reference particle and $p_1 \cdots p_N$ are the momenta terms associated with the particles. Derivations of this equation are given in fundamental texts[1].

The integration for momenta is trivial for structureless particles so that,

$$z = \left(\frac{2\pi \, mkT}{h^2}\right)^{\frac{3N}{2}} \cdot Q$$

Since the basic thermodynamic relationships can be derived from z, the problem is solved if a method evaluating Q, the configurational integral, can be found.

The best known mathematical approximation is due to Kirkwood[2]. He expanded the integral Q in terms of pair distribution functions and higher terms. The series becomes complex and evaluation impossible if it is not terminated drastically. It was assumed that the effect of higher terms was quite small and could be effectively represented by an approximate triplet distribution term. The approximate distribution function was taken as the product of the relevant pair distribution functions. Various authors[3, 4] have since carried out evaluations of these functions but the results do not agree well with experiment.

Physical approximations are of more interest in the current research since they postulate a simple basic structure for the liquid state. The most widely accepted theories are cell theory and a development of it, hole theory. In the cell model, each molecule is assumed to be trapped in a cage or cell fixed by the neighbouring molecules. This gives an overall pattern of a three-dimensional lattice of cells, each of identical size containing one atom. There are no vacant cells and the free volume is accounted for by expanding the lattice. The hole theory allows such vacancies but introduces more adjustable parameters.

Simple cell theory assumes that each cell will contain only one molecule and that each molecule moves independently of molecules in neighbouring cells. The configurational integral is of the form,(5)

$$Q = \frac{1}{N!} \sum^{*} e^{-\frac{u_o}{RT}} . v_f^N$$

where $\sum^{*}$ is the summation over all possible arrangements of the N molecules in N cells, one molecule in each cell so that,

$$\sum^{*} = N!$$

u_o is the zero energy when the centre of each molecule is at the centre of each cell.

v_f is the free volume per molecule.

The free volume term arises from the fact that since each molecule can vibrate in its cell, the volume of the cell is greater than that of the molecule. The essential problem of cell theory is the evaluation of v_f. The solution is simple for molecules consisting of hard spheres but, for real molecules, consideration must be taken of the nature of the potential formed. The most widely accepted solution is that of Lennard-Jones and Devonshire(6, 7).

They expressed the potential energy of a molecule in its cell in terms of the distance from the cell centre and evaluated

v_f as a function of that potential. The shape of the cell used affects the result. It is normal to consider it as spherical. Using the standard 6 : 12 bireciprocal potential function of Lennard-Jones and Devonshire, the configurational integral was calculated by numerical methods.

From these results, the thermodynamic properties of argon, the liquid most likely to fit the theory, were calculated[8]. While the results are approximately correct, they represent more closely solid state results extrapolated into the liquid state region than liquid results.

Three basic assumptions of the theory have been questioned[9]:-

1) that each cell contains only one molecule. This assumption means that poor use is made of the available free volume and that the entropy term will be too low.

2) That each molecule is independent of the vibrations of its neighbours. Such an assumption makes the same error as is inherent in an Einstein crystal but it may be expected to be more serious here.

3) The exact shape of the cell.

Proposed solutions for all three and various other modifications have been studied and agreement with experiment improved, but cell theory remains essentially a theory of the solid state.

The main advantage of hole theory is that it allows a more radical form of disorder while retaining the essential lattice structure so that its analysis can be carried out along similar lines[10]. The excess volume of melting is taken up both by the expansion of the lattice of cells and by the formation of a number of vacant lattice sites or holes. The major problem is to determine the number and size of the holes.

The number of molecules is less than the number of cells available, so that the partition function,

$$Q = \sum_{\lambda} . \pi_i \nu_f^{i.\lambda} . e^{\frac{-u_o}{kT}}$$

is the summation over all possible arrangements of the molecules in the available cells.

$\nu_f^{i\lambda}$ is the free volume of the i^{th} molecule in the arrangement λ.

The term $\nu_f^{i\lambda}$ depends both on the fraction of holes adjacent to position i and on the arrangement of the occupied holes. Various attempts have been made to evaluate this term by approximate methods. Curtiss and Rowlinson achieved this by minimising the energy of the system. Their theory gives the correct values for the second virial coefficient and the correct perfect gas partition function but at higher densities the results are less satisfactory.

Considerable attention has been paid in this analysis to the qualitative development of the models and no attempt has been made either to develop the theories mathematically or to adapt them to fit molten salts. The theories are included to give a simple theoretical model on which transport mechanisms can qualitatively be understood and to compare with the experimental approach of Chapter 2.

1.2. Transport Theory.

Most of the transport data obtained is in the form of viscosity, the remainder A.C. electrical conductivity results. The analysis considered here is of the relation of the macroscopic viscosity coefficient to molecular structure. It is normal to classify theories depending on whether they are based on movement in a gas-like or solid-like model. The lack of knowledge of the relative importance of the many liquid parameters means that basic theories which make only mathematical approximations are extremely general and of little use for practical correlation with experiment. Theories based on a gas-like model are likely to be less applicable to the very dense and highly viscous molten salts. Consequently the gas-like model approach of Enskog [11] and Longuet-Higgins and Pople [12], together with the more comprehensive approaches of Kirkwood [13] and Born and Green [14] are not developed here.

The unsolved nature of the viscosity problem has led to the proliferation of semi-empirical theories, all of which cannot be obeyed. A brief review of the most relevant of these is given. Four approaches are described : relaxation theory, vibration theory and two hole theories, the absolute reaction rate theory of Eyring and the Cohen and Turnbull free volume approach.

1.2.1. Relaxation Theory.

The basic concept of this theory is due to Maxwell, who considered viscosity in a classical manner, neglecting molecular structure. Viscosity was regarded as a combination of an elastic deformation and a simple Newtonian shear effect.

Frenkel[15] developed a similar theory on the basis of molecular interactions. Each molecule vibrates about its equilibrium position and after a time, long compared with the vibration time, it flows into thenext position. This flow process involves the evaporation of the molecule into an interstitial position and its condensation into a new site. The theory gives the expression,

$$\eta = \frac{6\,\tau_0\,kT}{\delta^3} \cdot e^{\frac{w}{kT}}$$

δ is the distance between equilibrium positions.

w is the evaporation energy required to reach the interstitial site.

τ_0 is the period of the equilibrium vibration.

The term δ is temperature dependent and, if the pre-exponential temperature dependence is assumed to be negligible due to compensating effects, the Arhenius expression is obtained.

1.2.2. Vibration Theory of Andrade.

This theory is based on a simple cell model approach although it was developed before it[16]. Each molecule vibrates abouts its equilibrium position in a manner determined by the influence of neighbouring molecules. This environment will change in a time long compared with the time for molecular vibration due to the effect of bulk flow in the liquid. At extreme libration, a molecule may combine with a neighbouring one momentarily, thus allowing for a sharing of momentum parallel to the direction of drift. Andrade derived an expression of the form,

$$\eta = \frac{4}{3} \cdot \frac{\nu . m}{\sigma} .$$

The frequency ν can be approximately determined at the melting point by the use of the Lindemann[17] formula for the corresponding solid

$$\nu = K \sqrt{\frac{T_f}{m\, v^{1/3}}}$$

These results are in good agreement for a range of simple liquids.

The development of these concepts to explain the temperature dependence of viscosity involves four postulates,

1) Momentum transfer occurs only if the mutual potential energy of the molecules is favourable, probably due to their relative position.

2) Some degree of ordering of molecular positions occurs in localised regions of the liquid.

3) This tendency to adopt mutually favourable positions is disturbed by an increase in temperature.

4) The number of molecules possessing a favourable mutual potential energy is determined by a Boltzman distribution function.

Andrade obtained the expression,

$$\eta = A\, e^{\frac{c}{T}} .$$

On considering the effect of volume (v), the above expression was modified to,

$$\eta v^{1/3} = A\, e^{\frac{c'\, f(v)}{T}}$$

assuming that to a first approximation, the potential energy varies as $\frac{1}{v}$, the expression becomes,

$$\eta v^{1/3} = A\, e^{\frac{c}{vT}}$$

which is good agreement with an even wider range of data than the simple Arrhenius equation.

1.2.3. Hole theory of Eyring.

This study of hole theories is based on an extension of the absolute reaction rate concepts developed in chemical kinetics[18]. The volume of a simple liquid at its melting point is about 12% greater than that of the corresponding solid. The excess volume is considered to be taken up mainly by the creation of vacant lattice positions or holes in the liquid and motion is attributed to the ability of a molecule to transfer into such a vacancy.

The following analysis was first prepared by Eyring, considering an arrangement of molecules, each at its cell centre with one cell site unoccupied as shown in diagram I.1.

EYRING MODEL MECHANISM DIAG I.I.

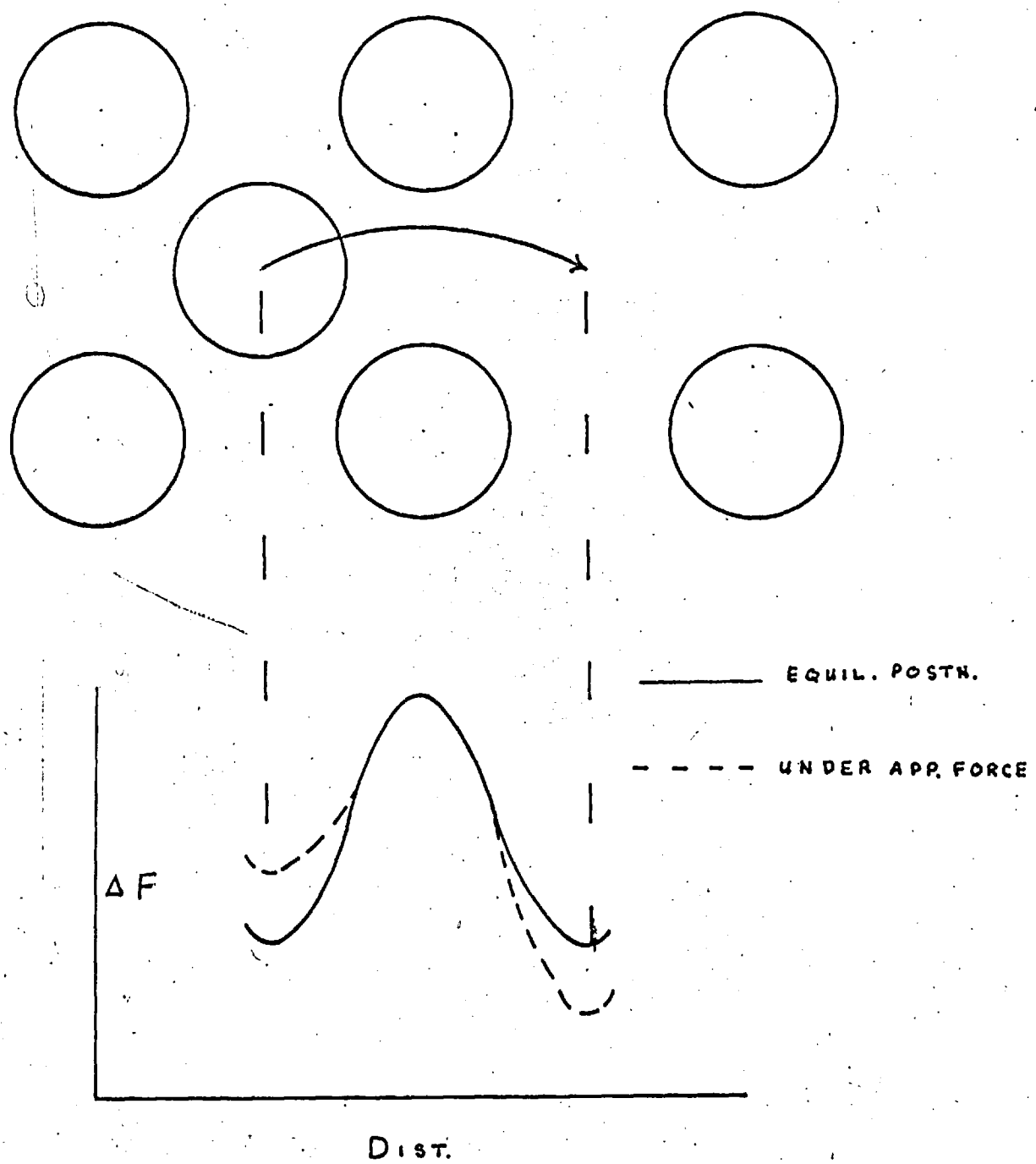

It is assumed that a potential energy barrier prevents motion from an occupied to an unoccupied site. The molecules vibrate in their cell positions until one or other adjacent to the vacant site receives sufficient energy to cross the barrier. Since each lattice site is identical, in equilibrium the potential barrier will be symmetric but if a force (f) is applied to the melt, the potential barrier becomes unsymmetrical, as shown. Under these conditions there is a nett flow of molecules in one direction. By applying the simple concepts of absolute reaction rate theory, Eyring obtained an expression of the form,

$$\eta = \frac{h\,N}{v} \cdot e^{\frac{\Delta F}{RT}}$$

where F is the free energy barrier height, and so,

$$\eta = \frac{h\,N}{v}\, e^{-\frac{\Delta S}{R}\ \frac{\Delta H}{RT}}$$

An expression which contains an entropy term associated with the hopping mechanism. This term is later used to aid in the elucidation of the anomalous transport data obtained.

The fundamental veracity of this theory has been questioned. Nevertheless, it provides a useful and extremely simple basis for comparison of various liquid state systems. It will be used in this manner in later analysis but, as far as possible, the actual physical model from which it was derived will be regarded as oversimplified.

An alternative method of approach was suggested by Eyring on the basis of work by Batchinski, who discovered experimentally that the fluidity of a system is directly proportional to the free volume[19]. Eyring suggested that the viscosity was therefore a function of the number of holes as well as the potential energy barriers in the liquid. This approach has now been embodied by Eyring in the much wider theory of significant structures[20], the concepts of which are not of relevance to this discussion.

1.2.4. Free Volume Theory.

The free volume theory of Cohen and Turnbull[21, 22] has been applied by C.A. Angell (see 2.2.2.) to the anomalous conductivity results for potassium nitrate - calcium nitrate. This is also a form of hole theory which, to some extent, aids in an explanation of glass formation.

The authors consider that all liquids when cooled would become glasses unless crystallization intervened, so that, whether or not a liquid becomes a glass depends on the relative rates of cooling and of crystallization. At the glass point, the thermodynamic properties of a liquid undergo a change of slope without any obvious structural change being detected. Flory and Fox[23] postulated that this change occurred when

the free volume of the system fell below a critical limit. Cohen and Turnbull suggest that this is the point at which a void in the liquid of the size of one molecule becomes energetically impossible.

To explain transport, they consider that the free volume of the liquid is distributed throughout in voids of varying size. Transport occurs when a molecule comes in contact with a void of sufficient size to accommodate it. The molecule may then move into the void but a transport step is only taken provided a second molecule moves into the space vacated by the first one, preventing back diffusion. The problem reduces essentially to discovering the nature of the void distribution. The authors evaluated this statistically and finally arrived at an expression,

$$\phi = A\, e^{-b \frac{v_o}{v_f}}$$

ϕ is the fluidity of the system.

v_o is the minimum volume of one ~~of the ions~~ mole

v_f is the total free volume.

This expression is the empirical equation of Doolittle[24], which is found to hold for a large number of liquids.

The pre-exponential term A contains two fitted parameters characteristic of the theory. Its relationship to the

anomalous melts is discussed in Chapter 2, but the fit is not good.

All the successful theories discussed above appear to contain an exponential term whose behaviour with temperature will be similar to a simple Boltzman distribution function, which might well be expected to describe the liquid state results with reasonable accuracy. The simple Arrhenius theory is therefore used to help reduce the experimental results to simpler proportions. The simple absolute reaction rate theory is preferred for theoretical analysis since the pre-exponential term, directly related to order-disorder analysis, is more informative.

Chapter 2.

An Experimental Approach to the Problem of Molten Salt Structure.

Alternatively to theoretical methods, concepts regarding liquid state structure can be obtained by deduction from experiment. It is in this direction that the specific contribution of molten salts has been most extensively developed. Techniques such as X-ray diffraction are not as informative in the liquid state as in the solid so that spectroscopic properties and thermodynamic and transport data must be considered. Some general experiments apposite to the understanding of molten salt structure and a more detailed account of experimental work on alkali-alkaline earth nitrate mixtures are concluded by a description of the simple structural model for mixed nitrates of McAuley, Rhodes and Ubbelohde.

2.1. General Experiments.

2.1.1. X-ray and Neutron diffraction data.

In the solid state, X-ray photographs give an extremely good method of characterising solid structure, but with liquids the disorder of the system prevents a similar interpretation and only a more limited analysis in terms of radial distribution functions is possible[25]. These distribution functions are

plots of the probability of finding an ion at any given distance from a central reference ion. Typical plots of molten salt data are shown for lithium chloride and sodium nitrate in diagram 2.1. When these functions are corrected for scattering effects, as shown for lithium chloride, the radial distribution functions suggest some form of ordering out to three or four co-ordination shells.

In a simple salt consisting of two simple ions like lithium chloride, a full analysis of the radial distribution function could be made in terms of pair distribution functions Li^+-Li^+, Cl^-- Cl^- and Li^+- Cl^- if three sets of experimental data using different isotopes was available. This analysis has never been successfully carried out for any simple salt. With lithium chloride containing $(Li^7)^+$ ion, however, a comparison with the essentially similar neutron diffraction data, shown in diagram 2.1., gives a partial analysis. The $(Li^7)^+$ isotope has a negative scattering amplitude so that peaks due to $(Li^7)^+$- Cl^- interactions will be negative, those due to $(Li^7)^+$- $(Li^7)^+$ and Cl^-- Cl^- will be positive. The first peak of the distribution is negative, the second positive, so that the charges alternate in the melt.

X RAY AN NEUTRON. DIFFRACTION. DIAG. 2·1

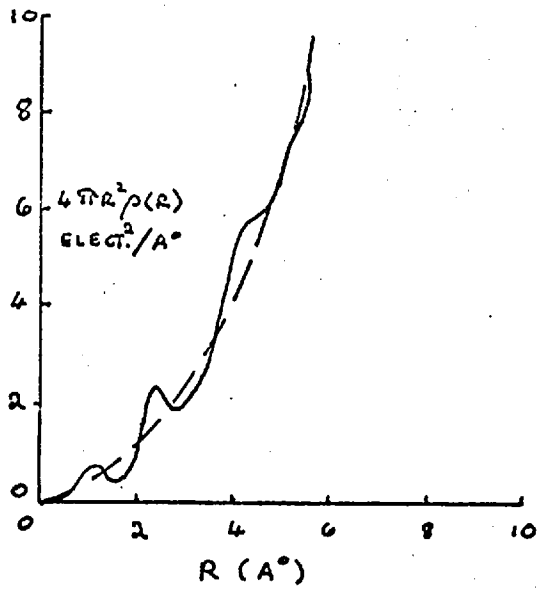

X. RAY. $NaNO_3$ (26)

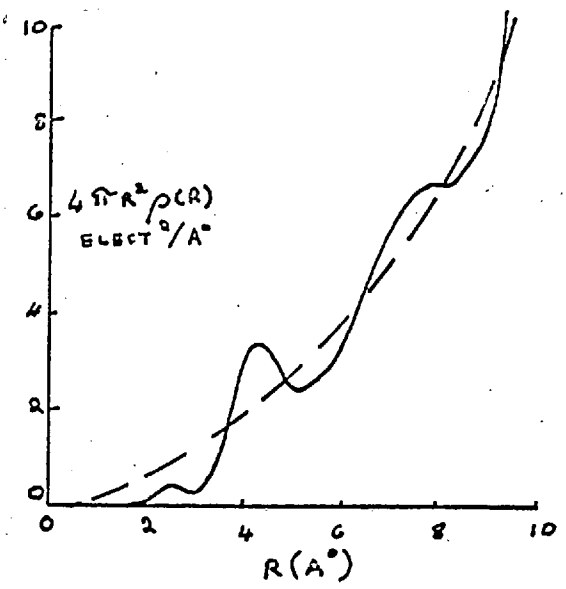

X RAY Li_2Cl_2 (27)

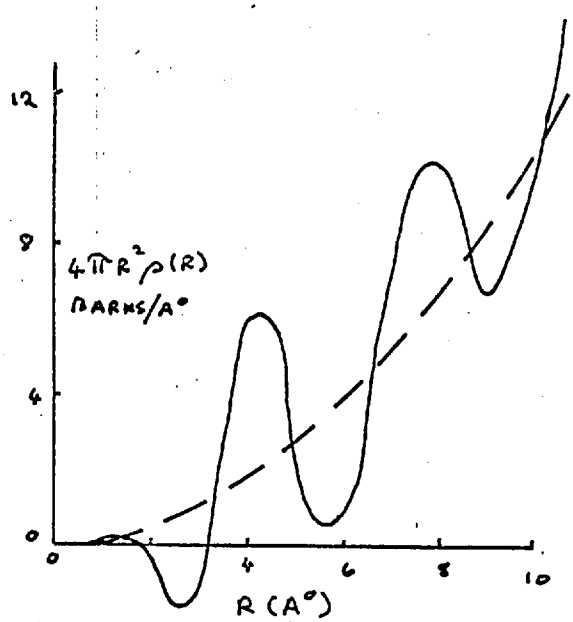

NEUTRON DIF. Li^7Cl

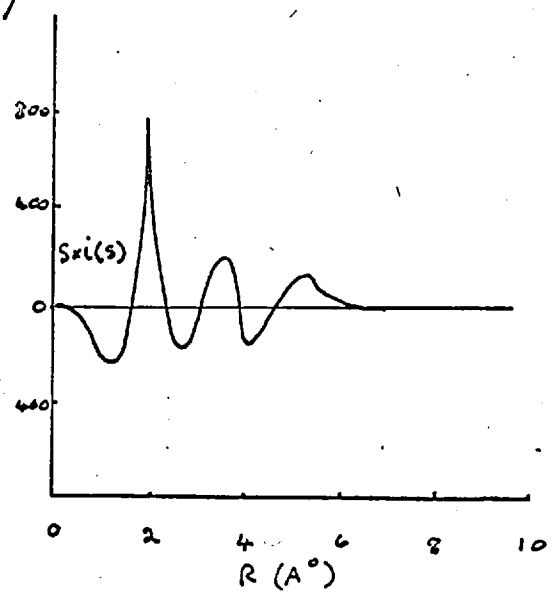

R. D. FUNCTION Li_2Cl_2 (FROM X.RAY)

The nitrate function is more complex, and a fundamental analysis is less possible. The first, extremely sharp peak represents the nitrogen to oxygen distance in the melt and is 1.20 A^{o}, a figure not much different from the value of 1.22 A^{o} in the solid state. The distance of the second peak for sodium nitrate is at 2.35 A^{o} from the origin. This represents the first inter-ionic distance in the melt. There seems no reason to doubt that charge alternation also occurs in nitrate melts and that this represents the $Na^{+} - NO_3^{-}$ distance in the melt.

These results are very sensitive to environmental effects and corrections for such terms as Compton and multiple scattering and adsorption are large and not necessarily well defined. Some of the results obtained are corroborated in the separately developed spectroscopy techniques.

2.1.2. Ultraviolet Spectroscopy.

The u.v. Spectra of the low intensity band of the nitrate ion has been intensively studied in melts since it is environment sensitive. Neither the reason it is sensitive nor the nature of the transition, which is probably $n \longrightarrow \pi^{*}$, is fully understood. One explanation is that the excited electron moves in a strongly anti-bonding orbital formed by a cage of the surrounding ions. Alternatively, it may be assumed that when

when the atomic orbitals are mixed to give a molecular orbital, the difference in electronegativity between the two atoms will give a weighting effect[28]. In either case, the orbital resides at the outside of the nitrate electron shell in direct contact with the cations. The effect of changing cation environment in molten salts on the energy position of the peak of the band has been studied by Smith and Boston[29] and Cleaver, Rhodes and Ubbelohde[30]. The experimental techniques of the latter are described in Chapter 4.

By studying the position of the peak both in the solid and liquid states, it was discovered that, in general, it shifted to higher energies on melting. This indicates that the cation-anion distance in the liquid is rather less than that for the corresponding solid.

In analogy with electrostatic effects it was considered that some function of reciprocal radius of the cations might bear a simple relation to the peak position. In the solid state, the structure and arrangements of the ions is known. Cleaver et al chose three different melt distances, the cation radius, the distance from the centre of the cation to the centre of the nitrate oxygen atom nearest the cation (r_{x-o}) and the distance between the cation centre and the nitrogen centre (r_{x-N}). While the simple reciprocal of all three distances showed approximately linear dependence on E_{max}, the r_{x-o} distance gave the best straight line. (see graph 2.2.).

U.V Spectra Results Graph 2.2.

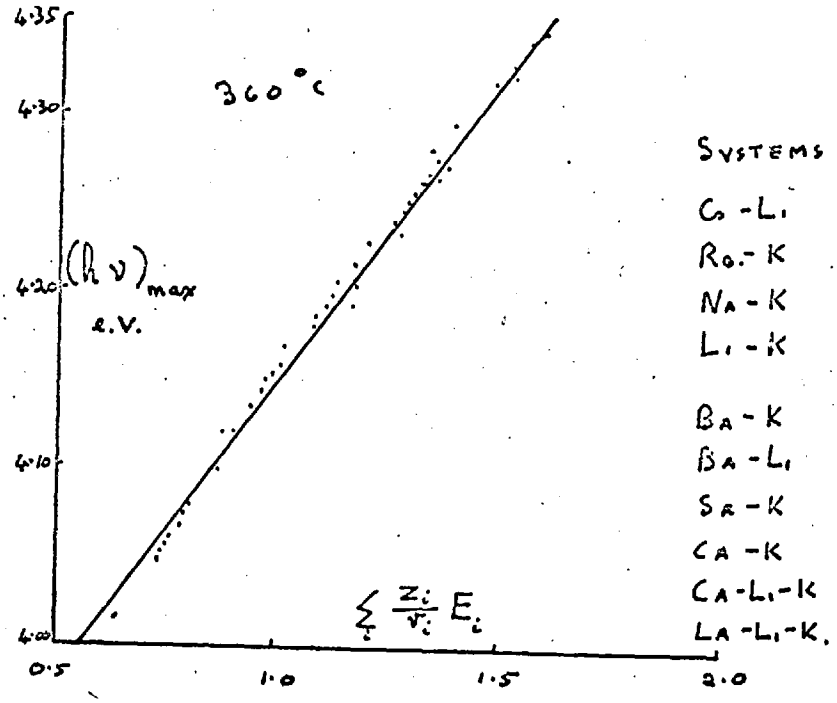

Systems

$C_s - L_i$
$R_b - K$
$N_A - K$
$L_i - K$

$B_A - K$
$B_A - L_i$
$S_R - K$
$C_A - K$
$C_A - L_i - K$
$L_A - L_i - K$.

From,
(29)
Smith + Boston

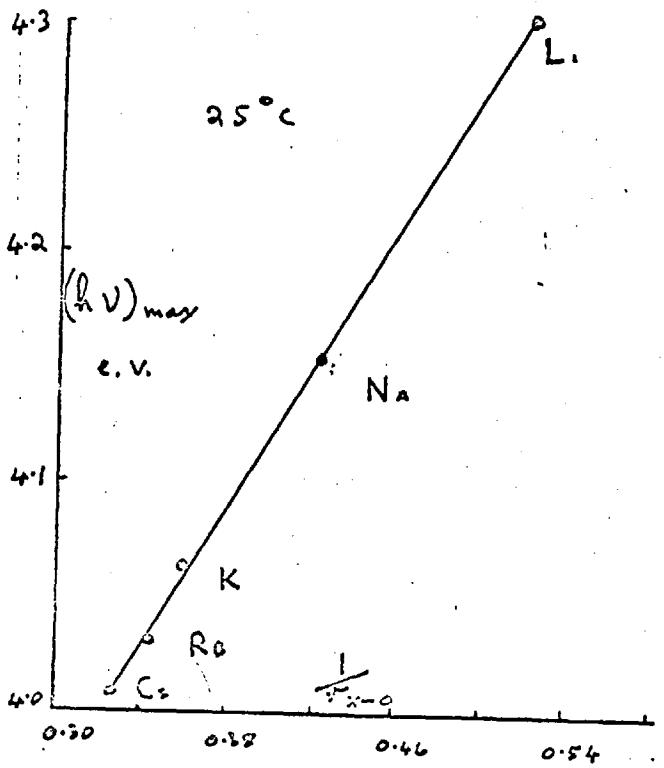

From
(30)
Cleaver, Rhodes & Ubbelonde

In the liquid state, only the cation radius is available, the other distances are unknown. Smith and Boston correlated a wide range of pure and mixed nitrate melts, some of the mixtures containing divalent ions, in terms of a simple potential function. The function is of the form

$$\sum_i \frac{z_i}{r_i} \bar{E}_i$$

where z_i is the cationic charge of the cation species i, r_i is its Pauling radius and E_i is an equivalent fraction term given by,

$$E_i = \frac{z_i n_i}{\sum_i z_i n_i}$$

n_i is the mole number of the cation species i so that $\sum n_i = 1$. The data given by Smith is shown in graph 2.2. The results, taken at 360°C., show approximately linear dependence on E_{max} over a wide range of mixtures.

2.1.3. Raman Spectra Studies.

Janz has analysed the Raman spectra of some pure alkali nitrates[31] and mixtures[32] containing the divalent ions, Ca^{++}, Sr^{++} and Ba^{++}. All the results are taken at temperatures 10° above their respective melting points. They give some indication of the nature of the positional arrangements of the cations relative to the anions.

In the pure nitrates of sodium, potassium, rubidium and caesium, the four fundamental vibrations of the ions are found to be completely degenerate. James and Janz assigned a symmetry of D 3h to the surroundings of the ions suggesting that there is no preferred positional orientation of the nitrates relative to the cations.

With mixtures containing the divalent ions, and with pure lithium nitrate, some degree of splitting of the ν_3 vibration is found. This suggests that some form of preferred orientation occurs reducing the symmetry of the surroundings. Since calculations of the rotational energies of the nitrate ions are impossible due to the lack of knowledge of the intermolecular forces, little more can be deduced with certainty from this data.

2.1.4. Thermodynamic and Transport Data.

A table (2.3.) of the comparative results for some alkali halides and alkali nitrates is shown. The halides represent systems which do not have the steric effects possible with the plate shaped nitrate ions. There are two difficulties in interpreting the thermodynamic melting point data. The wide difference in melting points may affect the actual values and the parameters are dependent on the crystal structures of the various solids.

Table 2.3. Thermodynamic and Transport Comparisons of Chlorides and Nitrates.

Salt.	Melting Point.	Volume Increase on Melting.	Latent Ht. of Fusion.	$E\eta$ K.cals/mole	$E\sigma$ K.cals/mole	$E\eta/E\sigma$
LiCl	613	26.1	4.76	8.8	1.15	7.66
NaCl	801	25.0	6.69	9.4	1.54	6.10
K Cl	776	17.30	6.34	7.8	2.30	3.39
Rb Cl	715				2.83	
Cs Cl	646				3.33	
Li NO_3	255	28.1	6.12	4.23		
Na NO_3	306	11.0	3.49	3.95	2.76	1.43
K NO_3	333	1.0	2.80	4.20	3.94	1.07
Rb NO_3	310			4.60	3.42	1.35
Cs NO_3	414			5.04*	2.70	1.87
References.		33	34	35,36	35,36	

* Value estimated.

The low values compared to the halides of the latent heat of fusion and volume increase on melting suggest however that the nitrate ion is unlikely to be capable of free rotation in the liquid. It is known not to be free to rotate in the solid state.

The transport parameters have been calculated in terms of simple activation energies as suggested in Chapter 1, since little reliance can be placed on any actual model viscosity solutions. The ratio of viscosity to conductivity activation energies is high for halides compared to nitrates.

These results and the results of the spectroscopic and X-ray studies are used in Chapter 6 in conjunction with the experimental work on the binary alkali-alkaline earth nitrates described in later chapters to build up a model of the basic structure of liquid nitrates.

2.2. A Review of Knowledge of binary alkali/alkaline earth nitrate mixtures.

2.2.1. Preliminary Studies.

Rostowski[37] first reported the tendency of liquid mixtures of potassium nitrate-calcium nitrate of certain compositions to form viscous liquids with low ill-defined freezing points. Stevels[38] has since reported other salt pairs rubidium nitrate-calcium nitrate and sodium nitrate-magnesium

nitrate which give similar effects. Bergman[39] similarly reported the ternary system sodium nitrate-potassium nitrate-calcium nitrate as anomalous, although the systems sodium nitrate-potassium nitrate-strontium nitrate and sodium nitrate-calcium nitrate do not show this effect. While the information on the number of systems exhibiting this behaviour is still fragmentary, all the simple binary alkali nitrate-calcium nitrate systems excepting lithium have been investigated in the present studies. While all the systems show similar trends only the potassium nitrate and rubidium nitrate mixtures cool sufficiently to produce the effect and only in the case of potassium nitrate has definitive proof of glass formation been obtained (Chapter 3).

The term glass is now capable of strict characterisation for a simple system as the condition of a liquid whose viscosity has been raised by cooling from normal liquid values to 10^{13} poise without discontinuity[40]. Dietzel and Poegel[41] measured the viscosity of the melt with maximum crystallization time by studying the elongation of a bar of the melt. The glass forming temperature is given by them as 56°C.

Dietzel and Poegel studied crystallization rates in the melt at various temperatures and composition. All the mixtures can be induced to crystallize but times of up to 24 hours

were recorded for a mixture containing 50.4 $^{w}/_{w}$ of potassium nitrate. This disordered structure can be kept stable at room temperature for long periods of time but is sensitive to physical shock.

Using this mixture Urnes[42] compared the viscosity and conductivity of the melt below 160°C. The results are shown in graph 2.4. They suggest that, as the temperature falls, the mechanism governing conductivity and viscosity becomes the same (see Chapter 6).

Gross and Kolesowa[43] measured the Raman spectra of the anomalous melt, results corroborated by Janz, (2.1.3.) and Kroger and Janetzko[44] measured some heats of crystallization.

This work was accompanied by a number of empirical theories. Concurrently with the present research, other workers have carried out more comprehensive studies. Kleppa[45] has measured the heats and volumes of mixing of a number of binary alkali nitrate mixtures, McAuley[46] has analysed the volume changes both with composition and temperature of a number of binary alkali-alkaline earth systems and C.A. Angell[47] has studied conductivity and diffusion in the potassium nitrate-calcium nitrate system.

Viscosity and Conductivity . Results Graph 2.4

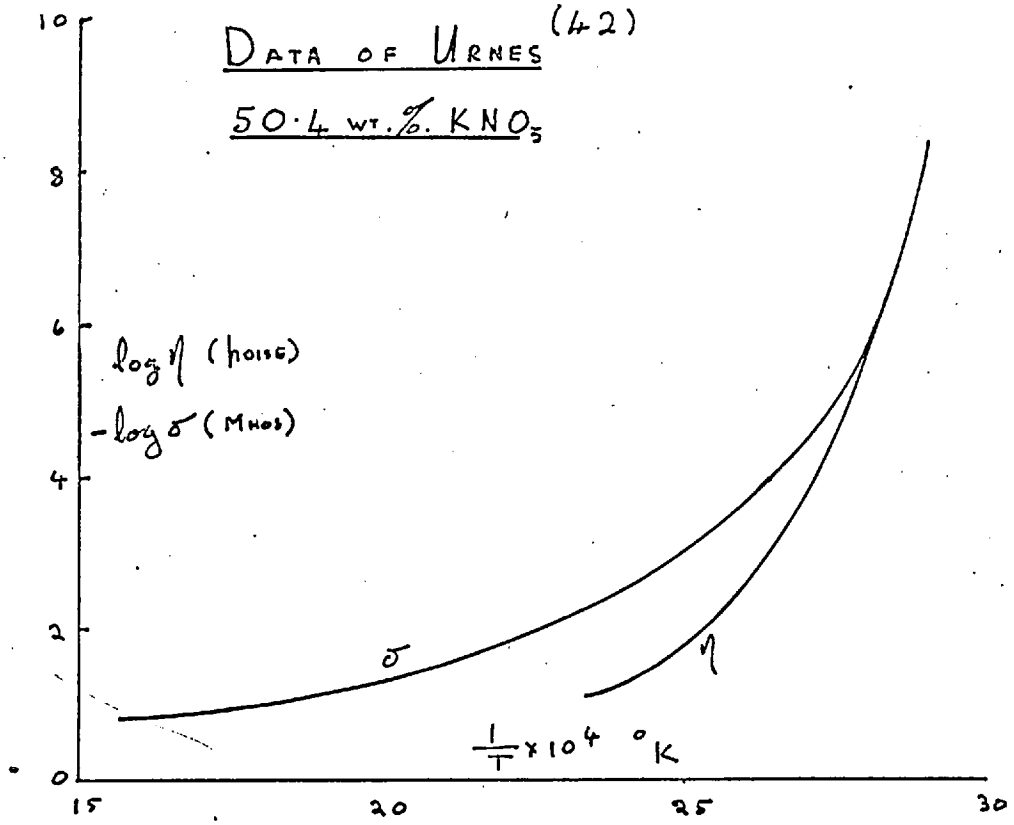

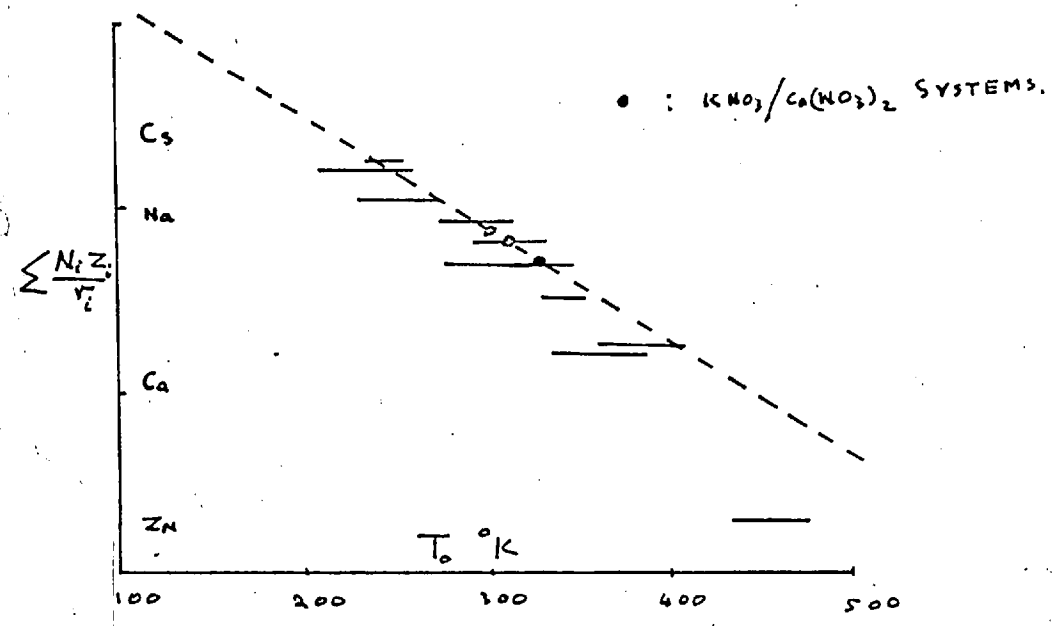

Plot of C. A. Angell (47)

2.2.2. The Work of C.A. Angell[47].

A brief description of the Cohen and Turnbull theory has already been given (1.2.4.). It leads to the result for the diffusion coefficient D,

$$D = A\ e^{-b\frac{v_o}{v_f}}$$

Angell used an approximate method to solve the free volume integral and obtained a result as,

$$\frac{d \ln D}{d \frac{1}{T}} = \frac{E_D}{R} = -\frac{1}{2} T - k\left(\frac{T}{T-T_o}\right)^2$$

The value E_D is the Arhenius activation energy for the diffusion process which is simply related to E_σ the activation energy for conduction. The value T_o is the temperature of the glass transition on the Cohen and Turnbull theory. The results were finally calculated from the expression,

$$E_\sigma = -k\left(\frac{T}{T-T_o}\right)^2 - \alpha RT^2 - \frac{1}{2} RT.$$

If the value of T_o estimated at 56°C. by Dietzel and Poegel from viscosity measurements, is substituted into the equation, the results are not in good agreement with the experimental values of E_σ.

The values of T_o required to give the best agreement with the measured values was calculated. The number and

size distribution of holes in the liquid would be expected to bear a simple relation to the cationic strength of the melt. If a similar parameter to that of Smith (2.1.2.), a cationic potential function, is plotted against T_o the results show linear behaviour but the range of values is small. Attempts to generalise the plot to other systems give small deviations from ideal behaviour, as shown in graph 2.4.

The calculated K and α parameters embodied in the pre-exponential term of the Cohen and Turnbull theory are not in good agreement with experiment and so a more detailed theory is not possible.

Angell has more recently also obtained pure diffusion data for the salts which generally confirm the above analysis.

2.2.3. The Work of W.A. McAuley[46].

During the course of the present research, it became apparent that volume results would be required to aid the elucidation of the melt structure. The work commenced by Al Mahadi[48] was extended and improved by McAuley. Experiments were carried out using a modification of the densitometer of Husband[49], in which excess volume is measured by a simple pressure method. An accuracy of 0.1% is estimated for the equipment. The main results are summarised here.

1) Kleppa discovered a slight excess volume of mixing in mixtures of the monovalent nitrates. Some verification of this, using the techniques of McAuley, have recently been obtained[50].

2) McAuley in a selected series of mixtures of sodium, potassium, rubidium and caesium nitrates with magnesium calcium, barium and strontium nitrates obtained no excess volume effects at all. Since the experimental accuracy is high, the systems may be regarded as thermodynamically perfect mixtures.

3) The mono-divalent melts give linear coefficients of expansion. This was checked and found to be correct even for the anomalous potassium nitrate-calcium nitrate melt down to 160°C. A graph of thermal expansion against composition is also completely linear.

4) As a result of the linear dependence of volume against composition, the results for the pure divalent melts can be obtained by extrapolation. The molar volumes of magnesium and calcium nitrate are identical, the values for strontium and barium nitrate slightly higher.

2.3. The Simple Volume Model of McAuley, Rhodes and Ubbelohde.

While the transport and thermodynamic behaviour of the nitrates is not simple to interpret, a model has been

proposed to explain the volume data of McAuley. Based on geometrical arrangements of the ions, its essential simplicity must be offset against its success in interpreting some interesting features of the volume behaviour.

2.3.1. The size and shape of the ions.

The cations in the melt are regarded as hard spheres having the same repulsion radii as in the crystalline state[51]. This postulate is in approximate agreement with the X-ray data for the molten chloride systems, in which the distance of closest approach is similar to the sum of the Pauling radii of the two ions.

Since the nitrate ions comprise the bulk of the melt, the exact shape and size is more important and also more difficult to ascertain. The X-ray results for molten nitrates show a well defined peak at about 1.2 A° due to the N—O bond distance, which in the solid is 1.22 A°. As well as giving the N—O distance in the liquid state, the existence of the nitrate ion as a single covalently bonded species in the melt is also confirmed.

In the solid state, the nitrogen to oxygen bonds radiate in a plane at 120° angles to each other from the central nitrogen[52]. There is no reason to believe that this arrangement is altered.

The major problem is the determination of the distance from the oxygen centre to the surroundings. Janz[53] assigned a value of 1.1 A^{o} or 1/2 of the O—O bond length as the radius of the oxygen atoms. He assumed that the oxygens were partly spherical, as shown in diagram 2.5., and so arrived at a radius for the nitrate of 2.32 A^{o}. In the solid state, it is well known that intramolecular distances are normally smaller than intermolecular distances. If a suitable intermolecular distance of closest approach from solid state results of the oxygen to the cations of nitrates is chosen, the radius becomes 2.58 A^{o}. In the following argument the Janz radii are used, and are justified since the results agree largely with experiment.

JANZ MODEL NITRATE ION. DIAG 2.5.

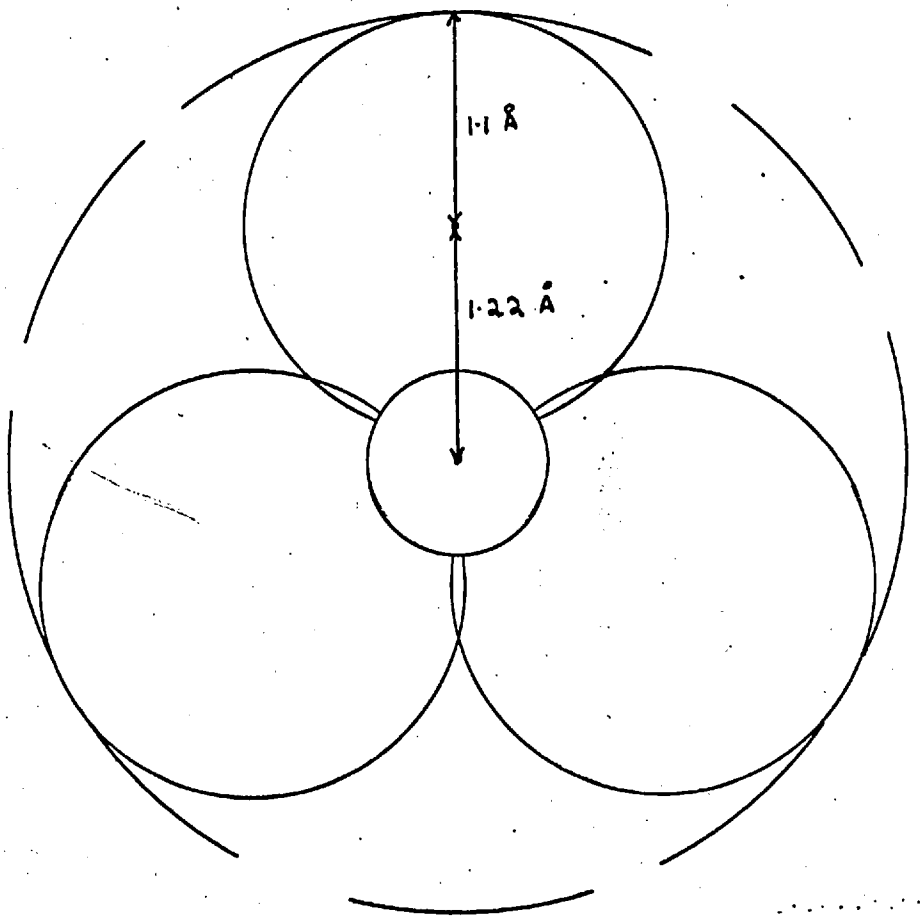

2.3.2. The model solution.

In the liquid state, the nitrate ion would be expected to possess considerable rotational or vibrational energy. Calculations of the energy required for free rotation are difficult[54]. Since direct evidence is not available, the nitrate ion will be assumed here to be a freely rotating disc, whose repulsion envelope is effectively a sphere of radius equal to that of the disc (2.32 A^{o}). This postulate agrees with the Janz results for pure sodium and potassium nitrate but not with the corresponding results for mono-divalent cation mixtures (2.1.3.).

From X-ray and Neutron diffraction data, it is clear that no long range order exists in the liquid but local ordering does (2.1.1.). It is also clear that approximate charge ordering exists at least in the lithium chloride melt and almost certainly in all melts. It is reasonable to assume that a disordered structure will pack as tightly as the short range repulsive forces and kinetic energy will allow. A cubic close packed lattice of nitrate ions with cations at the face centres gives a useful approximation to such packing requirements.

Using the above model, McAuley, Rhodes and Ubbelohde were able to predict fairly exactly the volumes of various

nitrates at their freezing points. The values for sodium, calcium and magnesium which were found experimentally to be identical (42.6 cc) are found to be identical theoretically since the cations can fit completely into the holes in the nitrate lattice. For larger cations, two interpenetrating lattices are required to calculate the volumes. The results of theoretical and experimental methods are compared in Table 2.6.

Table 2.6. Equivalent volumes of the ions of the pure nitrates.

Ion	Li^+	Na^+	K^+	Rb^+	Cs^+	Mg^{++}	Ca^{++}	Sr^{++}	Ba^{++}
radii	0.60	1.01	1.33	1.48	1.68	0.65	0.99	1.13	1.34
V_{liq}	38.7	44.3	54.1	58.6	69.6	41.3	41.3	44.1	44.9
V_{calc}	42.6	42.6	~~45.1~~ 58.6	~~50.9~~ 66.2	~~59.8~~ 77.6	42.6	42.6	42.6	~~43.4~~ 45.6

This model is best regarded as a simple cell model approach to the salt structure and its agreement with experiment is surprising. It allows no form of disorder except the rotation of the nitrates and embodies the essential fallacy of all cell theories that a liquid can be represented by a regular three dimensional lattice. A critique of its failure in explaining more complex properties is given in Chapter 6.

Section II.

The experimental observations are divided into three chapters. In Chapter 3, the general techniques used in handling molten nitrates and some qualitative studies of the nature of the anomalous mixtures are described. The main quantitative experiments were carried out using apparatus already developed and in Chapter 4 a brief description of these techniques, in which particular attention is paid to error effects, is given. The measurements of the dielectric properties of the salts using new techniques specially developed for this study are more fully described in Chapter 5.

Chapter 3.

General Techniques and Qualitative Studies of the Melts.

3.1. General Techniques.

3.1.1. The Basic Equipment.

The initial problems of corrosion and temperature control in molten nitrate experiments had previously been solved. The apparatus in contact with the salt was constructed of pyrex, stainless steel, inconel or ceramics which do not corrode appreciably. The use of pyrex limits the temperature maximum to 500°C., a temperature above the decomposition point of the mono-divalent melt mixtures.

The viscosity and conductivity experiments were carried out in a thermostat bath (diagram 3.1.), consisting of a well insulated pyrex beaker filled with the ternary entectic melt of sodium nitrite, sodium nitrate and potassium nitrate (40 : 7 : 53% by weight) which freezes at 160°C. The main heat is supplied by a 1.25 K.W. inconel heater. Accurate temperature control was obtained using an electronic, "saturated reactor", controller feeding a 500 watt ceramic heater. The controller used a platinum resistance thermometer as a sensing element. The temperature of the bath was maintained for long periods of time at up to 450°C. to ± 0.02°C.

THERMOSTAT BATH GRAPH 3.1

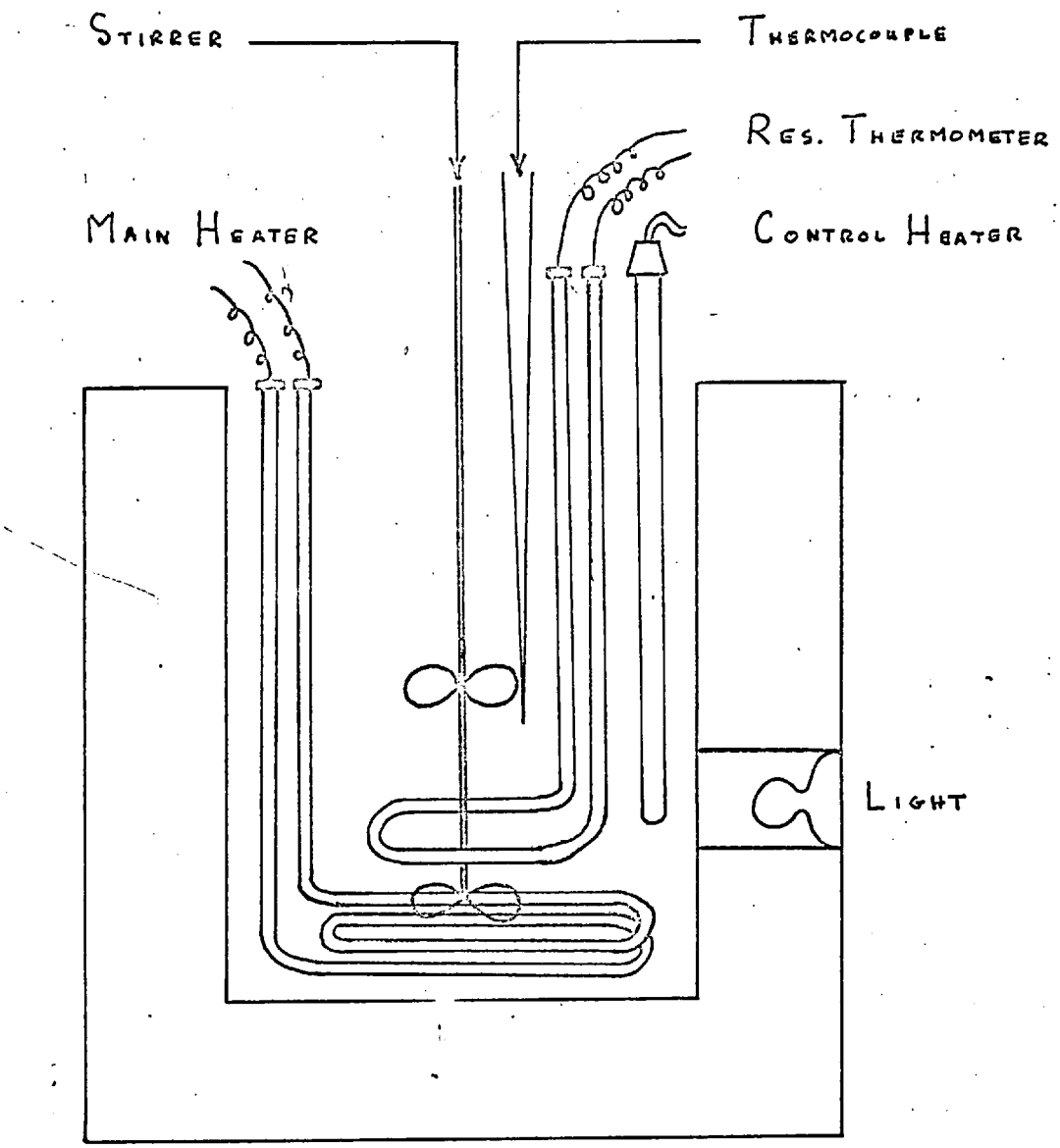

Specially calibrated "pallador" thermocouples were used. Calibration was by direct comparison in the melt bath with a platinum resistance thermometer calibrated by the National Physical Laboratory to ± 0.001°C. The resistance thermometer readings were measured on a Smith's bridge[1] and the thermocouple readings on a potentiometer. The thermocouples were first annealed at 450°C. for 24 hours and the comparative values of the thermocouples and resistance thermometer measured at a large number of controlled temperatures. The results were graphed. It was estimated that the calibration was accurate to ± 0.05°C. but, due to diffusion of gold across the hot junction, frequent recalibration was required to maintain this accuracy.

3.1.2. Preparation of Samples.

To prepare mixtures, the solid components were weighed separately, mixed in a tube and the contents melted by immersing the tube in the thermostat bath. The accurate determination of weights before mixing provides the best method of determining the composition of the melts. So that the composition would be accurately determined, and to prevent decomposition on melting, all solids were carefully dried.

The method of drying depended on the nature of the salt. The treatment of each salt and its purity are given in Table 3.2.

Drying Treatment of Salts.

Anhydrous Salt.	Drying Treatment.	Supplier.	Purity.
$NaNO_3$	Heated to 250°C. for 24 hours in oven.	Judactan A.R.	99.9%
$K\ NO_3$	Shock Dried and heated under vac.	Judactan A.R.	99.9%
$Rb\ NO_3$	Pumped down for 48 hours.	Johnson Matthey.	99.9%
$Cs\ NO_3$	Pumped down for 48 hours.	Johnson Matthey.	99.9%
$Ca(NO_3)_2$	Heated to 250°C. for 24 hours in oven.	British Drug House.	>98.0%

Calcium nitrate is much more hygroscopic than the monovalent salts. After drying, and while still hot, it was transferred to a weighing tube and the tube sealed and allowed to cool in a desiccator. The calcium salt was weighed, sealed and the mixture composition adjusted by altering the weight of the monovalent salt.

Nitrate melts may contain, even after the solid salts are dried, appreciable quantities of water[2]. The most effective method of removal is by bubbling dry clean nitrogen through the melt for about 12 hours. The melts were finally dried by this method using white spot nitrogen (0.01 gms. H_2O/cu.meter gas) which had been passed through a cotton wool filter then a liquid air trap.

For conductivity and dielectric studies, the melts were prepared in the cell containers and dried in situ but, with the smaller viscometer, the melts were dried in separate containers and transferred molten. Initially a completely closed system was used to transfer the salt but it was difficult both to estimate the quantity of salt passing into the viscometer and to prevent decomposition on hot spots on the heated conduit. It was found simpler to use a dropping pipette of sufficiently large thermal mass to prevent the

salt freezing before the transfer was completed. The possibility of some water being absorbed during the process was eliminated by measuring the viscosity before and after final drying in situ. No difference in value could be detected.

For spectroscopy samples, two quartz plates were heated to 250°C. on a small hot plate over which was passed a stream of dry nitrogen. A drop of the melt, prepared and dried as in the above experiments, was smeared on to one plate and the other squeezed quickly on top. Due to the fine film thickness, the rate of water penetration was small and caused no difficulty. After adjusting the thickness to the approximate value, the sample was allowed to cool in a desiccator.

3.2. Qualitative Studies of the Melts.

3.2.1. Chemical and Physical Stability.

One of the main disadvantages of mono-divalent nitrate melts was that decomposition occurred spontaneously at any temperature when more than about 50 mole % of the divalent salt was present. The temperature at which noticeable decomposition occurred decreased slightly with increasing content of the divalent salt but all the values lay between 360°C. and 420°C. Since the decomposition evolved gas, it

was readily detected but none was noted, even over long periods of time below 360°C. in any system. All the experiments were carried out with fresh melts so that the residence time of the melt in the apparatus was limited to two to three days in each case. There was no appreciable difference in the physical measurements with time even in the case of the highly supercooled melts described in 3.2.2., which were kept in the apparatus for periods of two to three weeks.

All the nitrate melts used should be completely clear and miscible but in the case of certain melts, some opacity was found, probably as a result of a small percentage of calcium oxide in one batch of calcium nitrate. The opaque melts were reduced to as low a temperature as possible and some nitric acid introduced below the surface. After drying, the treated melts became clear, and no difference was detected in the measurements between these and normal melts. Similar problems were encountered in preliminary investigations of trivalent nitrate melt mixtures but the formation of oxide persisted in this case and the runs were abandoned.

3.2.2. Possible Glass Formation.

Glass formation in certain compositions of the potassium nitrate-calcium nitrate melts has been reported

by Rostowski[3], Dietzel and Poegel[4] and Urnes[5] but it is not clear whether they consider a truly homogeneous glass or whether the low temperature form is partially or totally composed of translucent crystallites. The published phase diagram shows that every mixture may be crystallized and, under the carefully controlled conditions of the viscosity and conductivity experiments, all the mixtures used crystallized readily. Since a lower temperature was required for the dielectric experiments and since the nature of the low temperature form became theoretically interesting, a further investigation of the supercooled melt was carried out.

The system reported as giving maximum glass formation, that containing 62 mole % of potassium nitrate, was used. The ability of this melt to supercool depended both on sample history and the physical constraints placed on it. It is much simpler to supercool the bulk phase. In bulk phase experiments, the sample was kept at 250°C. for 5 days, the air space above the melt was heated to prevent surface crystallization and then, during cooling, the physical vibrations in the surrounding bath were minimised. With such treatment, the sample could be cooled to room temperature to give a translucent mass, the physical nature of which was further investigated using a microscope with crossed polaroids, and simple X-ray photography techniques.

PHOTOGRAPH A.

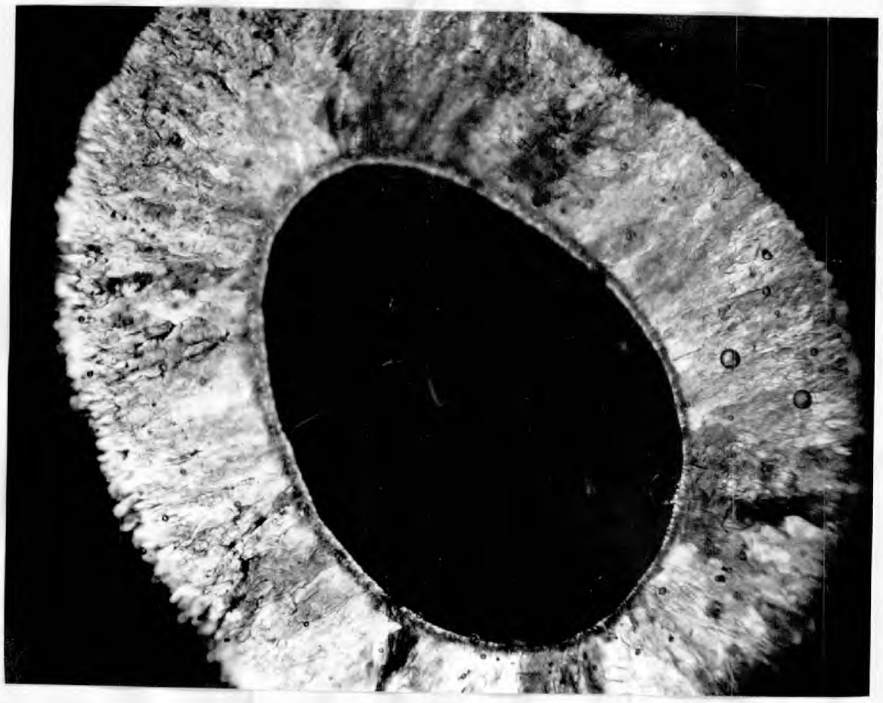

PARTIALLY CRYSTALLIZED SAMPLE OBSERVED WITH POLAROIDS CROSSED.

PHOTOGRAPH B.

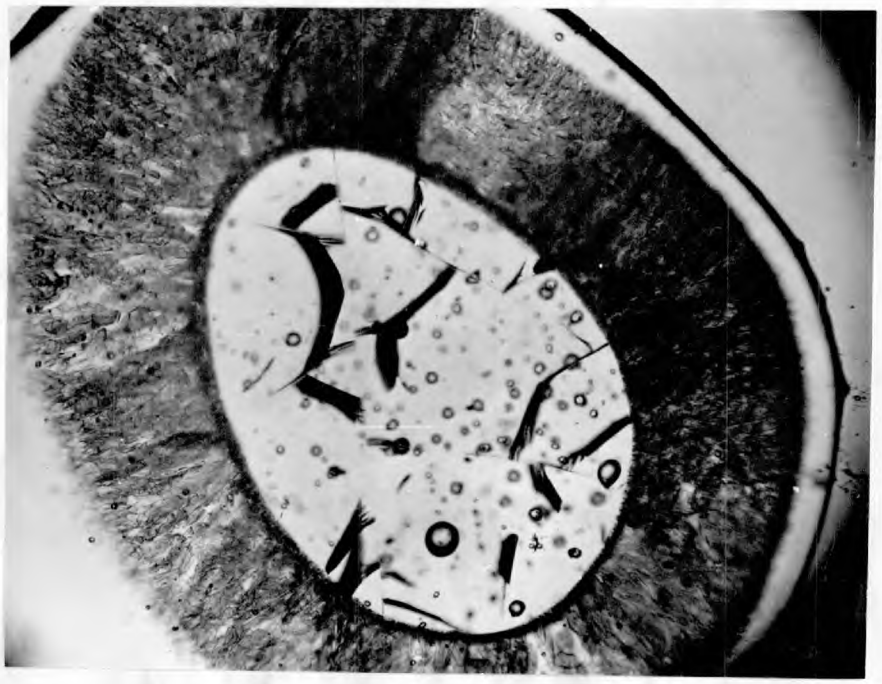

PARTIALLY CRYSTALLIZED SAMPLE OBSERVED WITH POLAROIDS UNCROSSED.

A thin film sample was observed between the crossed polaroids at various temperatures down to 25°C. The microscope hot stage consisted of a cylindrical furnace controlled by an electronic temperature controller. Both ends of the furnace were enclosed by glass cover plates and temperature measurement was by a thermocouple set in the enclosed space.

After heating the hot stage to 150°C., a drop of the melt at a higher temperature was spotted on to a cover plate held in the furnace and a second plate dropped on top to create a thin film sample. The top cover plate of the furnace was added and the assembly allowed to come to equilibrium.

The sample was observed at a series of temperatures between 150°C. and room temperature. The polaroid filters were set to give a dark field and, by rotation, a check was made for extinction. None was noted at any temperature. Any crystals, except cubic ones, would be expected to give some rotation of the polarised light and so be observed in this manner. This effect is illustrated by the photographs of a partially crystallized sample. In photograph A, the polaroid filters were at 90° to each other so that no direct transmission of light could occur. The outer crystalline ring refracted the light and, since the plane of polarisation was changed, it passed through the second filter. Thus the

disordered or cubic central region is dark, the crystalline ring is light.

In B, the filters were placed parallel so that the thermal cracks and bubbles characteristic of a disordered solid phase were visible.

To verify these observations and to finally prove that the translucent state is not a strained cubic crystal, X-ray photographs of the material were taken. Special glass capillaries with a wall thickness of 1/100 mm. and a 1 mm. bore which give no appreciable X-ray pattern were used. The liquid sample at 200°C. was drawn into the capillary, sealed with an oxygen flame at the top and allowed to cool.

Figure C shows a powder photograph taken at 45 KV. for three hours at room temperature. It shows a double diffuse ring characteristic of a disordered state. Figure D, by comparison, is a sample in which partial crystallization had been induced.

Thus, while it was more normal to achieve crystallization, this melt could be supercooled to a translucent disordered state. The structure may consist of a mass of extremely small crystallites sufficiently small to induce line broadening or be completely disordered. Since both these postulates have been used to describe standard glasses and no definite proof of the validity of either been adduced, the sample may be considered in this condition as a glass.

This conclusion is verified by the spectroscopy experiments of Chapter 4.

PHOTOGRAPH C.

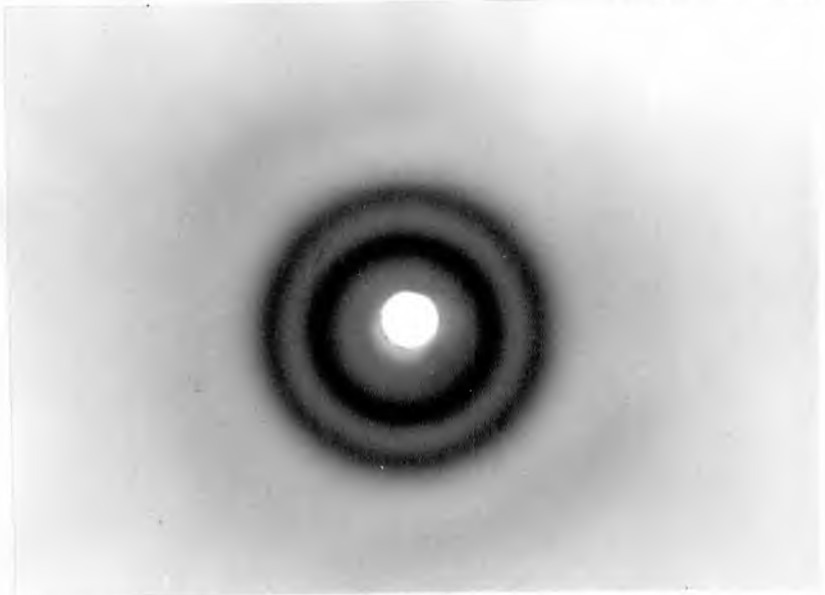

X-RAY STUDY OF THE DISORDERED STRUCTURE.

PHOTOGRAPH D.

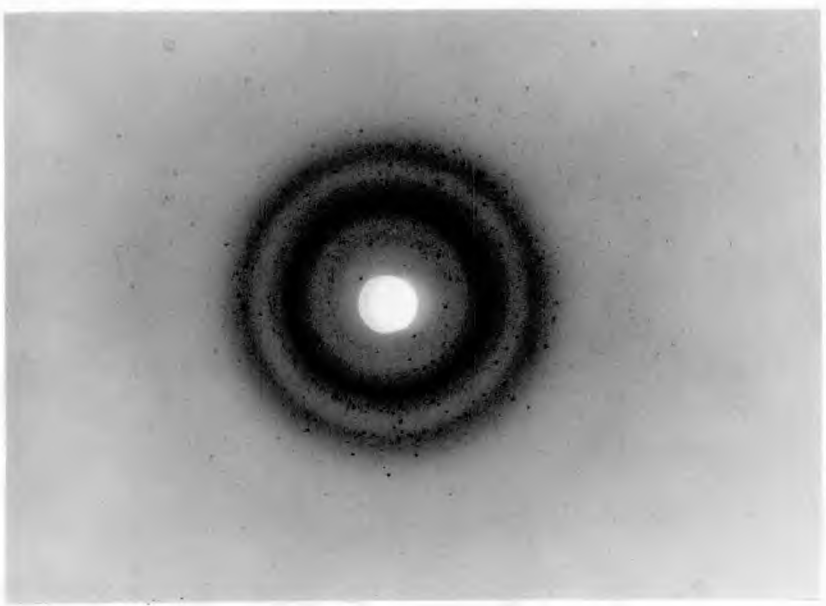

X-RAY STUDY OF PARTIALLY CRYSTALLIZED STRUCTURE.

Chapter 4.

Results of Quantitative Experiments.

This chapter deals with quantitative experiments carried out to determine the behaviour of the viscosity, conductivity and ultraviolet spectra of the melts with changing temperature and composition. The methods used were modifications of techniques previously developed by Ubbelohde and co-workers.

The results are expressed both as graphs and computed functions. The transport data is expressed as simple Arrhenius plots since these reduce the wide range of data to acceptable proportions and dislay the anomalous nature of the curves. The computed functions are polynomials calculated on the university Atlas computer, using a least squares regression analysis.

4.1. Viscosity.

4.1.1. Definition.

Normally, viscosity is defined without reference to the microscopic nature of a fluid[6]. The fluid is considered as a continuum in which the conditions of flow have impressed a velocity distribution at right angles to the direction of flow. In diagram 4.1., consider the thin segment bounded by planes A and B. When conditions of equilibrium flow exist,

LIQUID FLOW DIAG 4.1.

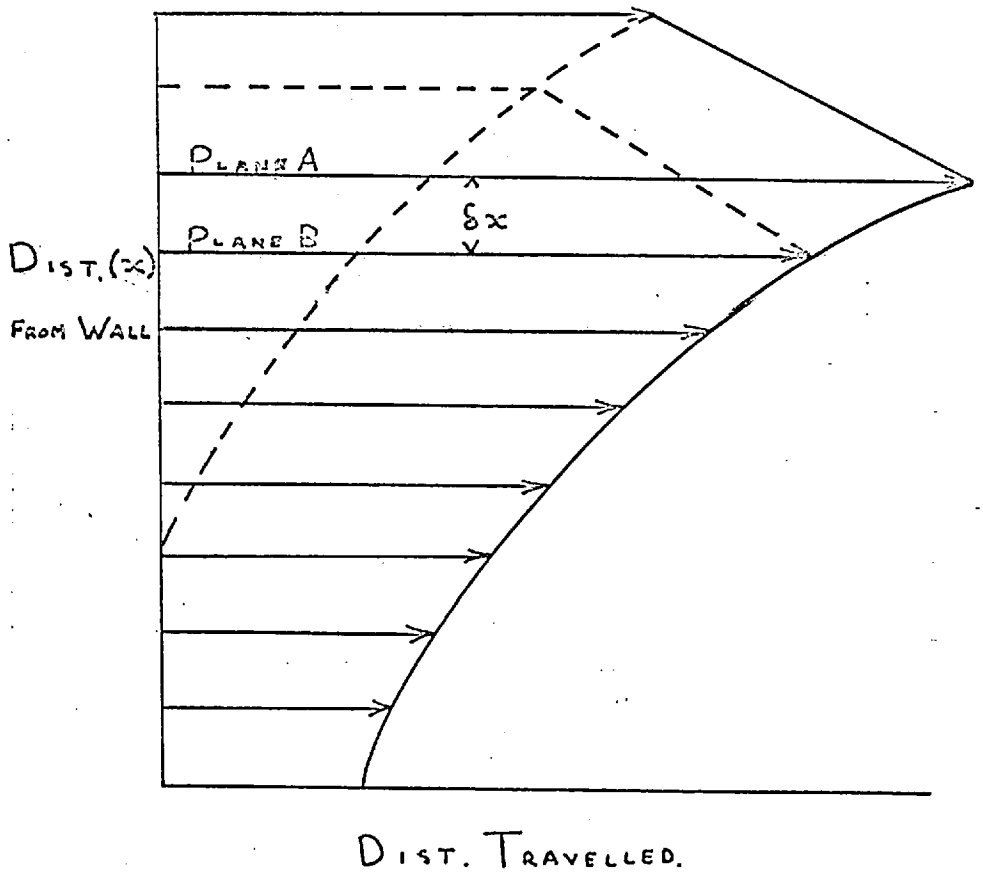

the force/unit area on plane A will equal the force per unit area on plane B. Since plane A flows faster than plane B, the force producing motion is greater in plane A than plane B. This discrepancy of forces is made good by a shearing force dependent on the properties of the material, and the difference in velocity between the planes (δv).

$$f = \eta \frac{\delta v}{\delta x}$$

As plane A approaches plane B,

$$f = \eta \frac{dv}{dx} .$$

η, a constant, is a property of the material and is called the shear viscosity coefficient.

Hagenbach[7] derived theoretically the experimental expression of Poiseuille for the streamlined flow of a liquid in a tube. The expression is,

$$v = \frac{4 p r^4 t}{8 l \eta}$$

v : volume of liquid passing through the tube in time t.

p : the pressure applied.

r : the tube radius.

l : the length of tube.

There are three main assumptions,

i) the applied pressure is employed solely in overcoming the viscous resistance of the fluid;

ii) the flow is steady throughout the entire length of the capillary and is at all times parallel to the capillary axis;

iii) there is no slip between the capillary and the wall.

The Poiseuille equation was used in the experimental determination and these assumptions define the basic conditions required.

4.1.2. Description of Apparatus.

The four main techniques used for measuring viscosity are Stoke's Law methods, vibrational, inertial and capillary techniques. Stoke's Law methods, while exceptionally simple, are difficult to refine to high accuracy. Modern vibrating crystal and vibrating wire techniques have not yet been applied to molten salts due to development difficulties. Of the other two methods, Janz[8] has obtained accurate measurements of the molten alkali carbonates using an oscillating crucible and Ubbelohde et al have developed the use of capillary techniques in the study of a wide range of molten salts including nitrates[9]. The present viscometer shown in diagram 4.2. is a modified version of that used in previous studies. It is simple, accurate and being of pyrex construction easily altered. A thorough survey of the errors and inaccuracies inherent in the technique is given later.

VISCOMETER

DIAG 4.2

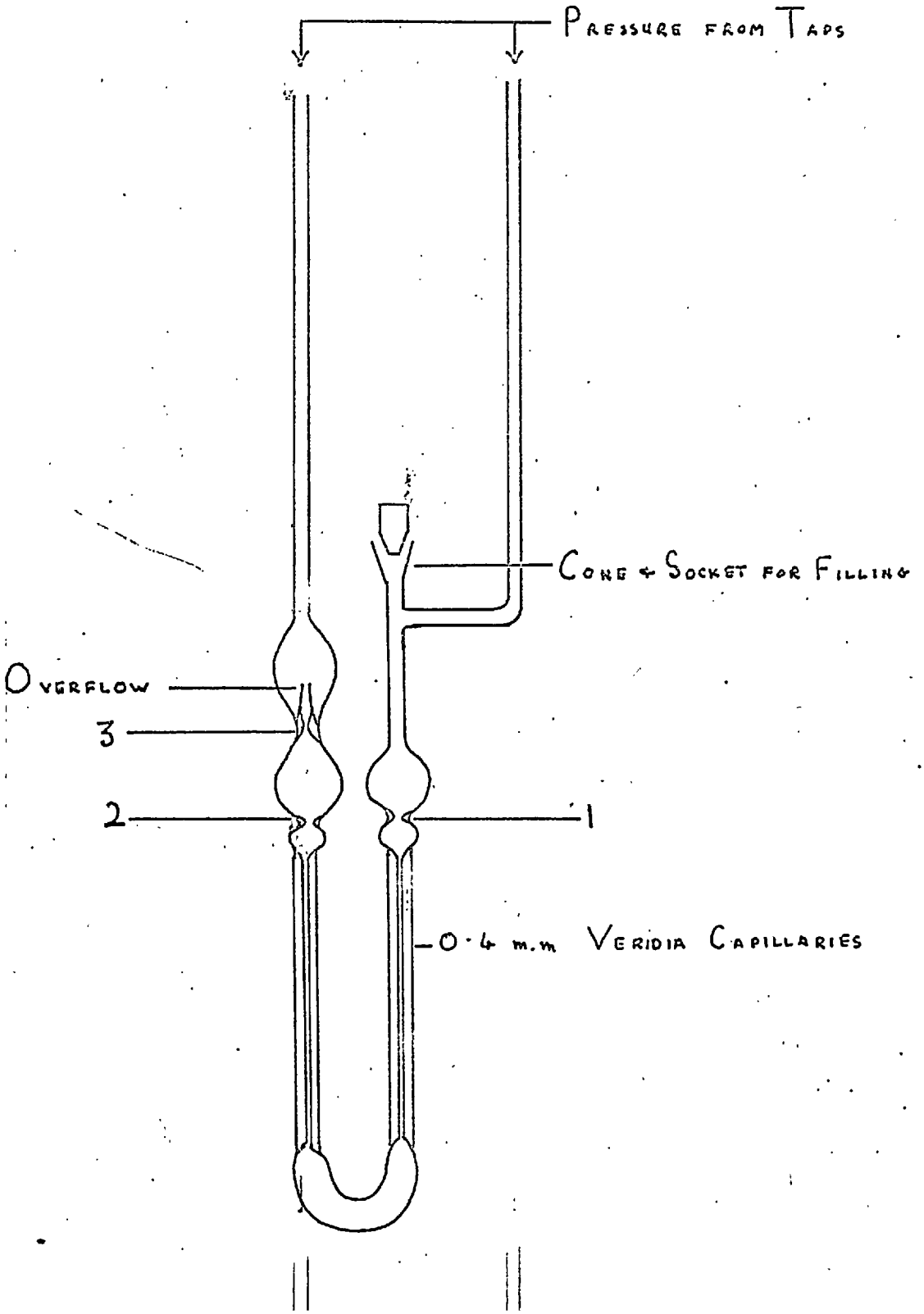

4.1.3. Description of the Method Used.

The apparatus was as shown in diagrams 4.2. and 4.3. The viscometer was placed in the thermostat and approximately filled (see 3.1.2.). Before replacing the stopper, it was smeared with a little melt which set hard and formed a leak proof joint. When correctly filled, the melt occupied the volume between level 1 and the tip of the overflow device, excess liquid having been forced over into the reservoir. After allowing the apparatus to come to equilibrium in the thermostat for one hour, a suitable pressure was applied through the contact head device and two way tap system. The time of flow from level 3 to level 2 and a similar time from 2 to 3 was measured on a stopwatch. The readings were repeated at a number of different pressures using a mercury manometer and a cathetometer.

Experimental accuracy depended mainly on the stability of the applied pressure and the precision with which it was measured. The constant head device (diagram 4.3.) gave a suitable stability. The white spot nitrogen supplied to the head was passed through a cotton wool filter, a liquid air trap and a ten litre aspirator for ballast. A lead from the aspirator was passed across the top of the head and the pressure adjusted so that a continuous flow of bubbles was exhausted at the foot of c_1. The pressure was effectively

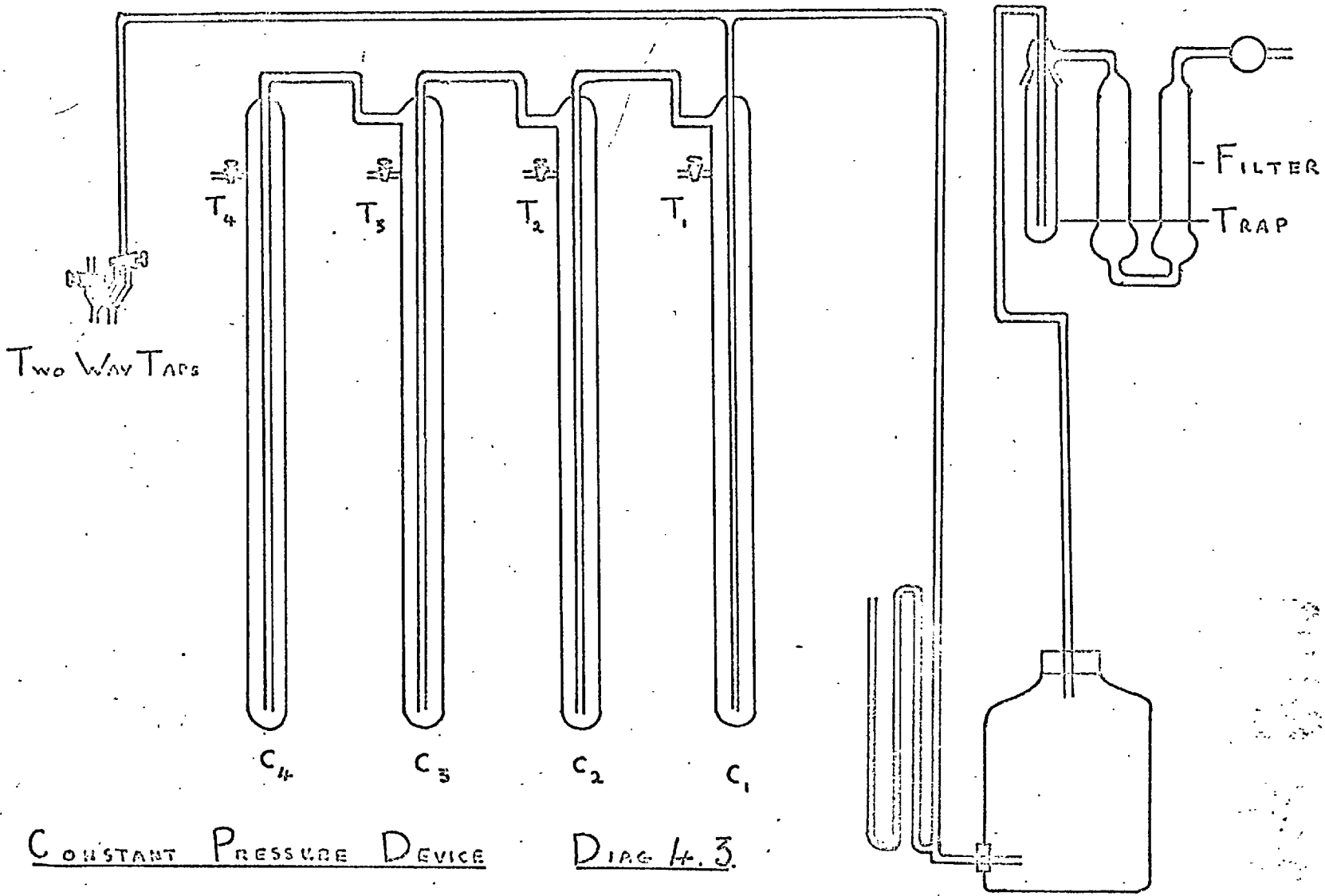

Constant Pressure Device Diag 4.3.

the head of water c_1. When a higher pressure was required, tne tap T_1 was closed, and the pressure allowed to rise until a similar equilibrium condition was reached with bubbles emitting from the foot of c_2. The pressure was then equivalent to the combined heads c_1 and c_2. Higher pressure can be obtained by closing the taps T_2 and T_3. The manometer readings were taken using a Cambridge cathecometer capable of reading to $\pm$ 0.002 cms

4.1.4. Experimental Error Analysis.

The viscometers were calibrated by measuring the pressure x time product of a 40% sucrose solution at 25°C., whose viscosity is known. For any one viscometer, the capillary dimensions are fixed, so that, from the Poiseuille equation,

$$\eta = \frac{\text{pressure x time}}{\text{constant}}$$

Thus, the value of the constant can be calculated from the sucrose results and used to obtain the molten salt viscosities. The two main sources of error were inaccuracies in preparing the calibration fluid and differences between calibrational and operational conditions. The calibration was carried out at three different temperatures in a water thermostat bath and a plot of the pressure x time product for a number of pressures at each temperature was drawn. The

linearity of these plots served as checks on the composition, accuracy and purity of the sugar solutions.

The difference in temperature between the calibration and the experimental observations is between 200 and 400°C. A simple consideration of the effects of the Poiseuille equation shows that to a first approximation, there is no expansion effect.

$$\eta = \frac{\pi\, p\, r^4}{8lv}$$

Let r_c, l_o and v_o be the values of radius, length and volume of the capillaries at low temperatures, and let α be the coefficient of expansion of the glass. Then, for a temperature rise ΔT,

$$\eta = \frac{\pi .\ p.\ r_o^4\ (1 + \alpha .\ \Delta T)^4}{8 l_o v_o (1+\alpha .\Delta T)(1+3\alpha .\Delta T)}$$

and,

$$(1+ \alpha \Delta T)^4 = 1 + 4\ \alpha .\Delta T \ldots\ldots \text{terms containing powers of } \alpha .$$

Thus for $\alpha \ll 1$,

$$(1 + \alpha \Delta T)^4 = (1 + \alpha .\ \Delta T)\ (1 + 3\ \alpha .\ \Delta T)$$

That is, the change in viscosity caused by expansion effects in the glass is fully compensated and the calibration is valid.

The time of flow was taken in each direction and the results should be identical. Any discrepancy was normally due to either a gas leakage in the line from the two way tap or to a partial blockage in the capillaries. Checks were also made to ensure that there was no leakage in the lines from the constant head device.

A number of theoretical corrections to the viscosities measured by capillary techniques have been suggested.

1) The Kinetic Energy Correction.

When a fluid is passed through a tube there is a pressure drop and a consequent change in the kinetic energy of the system. The effect of this change on viscosity has been considered by Bingham and Jackson[10] and a theoretical correction derived.

2) The Couette Correction[11].

At the entry to the capillaries, the streamlines in the fluid are not parallel but convergent so that extra resistance to motion is produced. A theoretical correction is also available for this term.

In order to give a standard condition in which the above corrections may be calculated, the ends of the tube must be ground out flat. Alternatively. the amount of the

correction is minimised by making the tubes as long as possible and "belling out" the ends. This second procedure was adopted.

A plot of viscosity against the pressure x time product will pass through the origin only if the Poiseuille law holds exactly and the correction terms are negligible. A graph (4.4.) is shown of such a plot for the calibration results, the lines pass through zero. This is in agreement with a review suggesting that such terms only become applicable if accuracies of 0.1% are required[12].

Viscosity of Sucrose (40% w/w)

Kinetic Energy Test.

Graph 4.4.

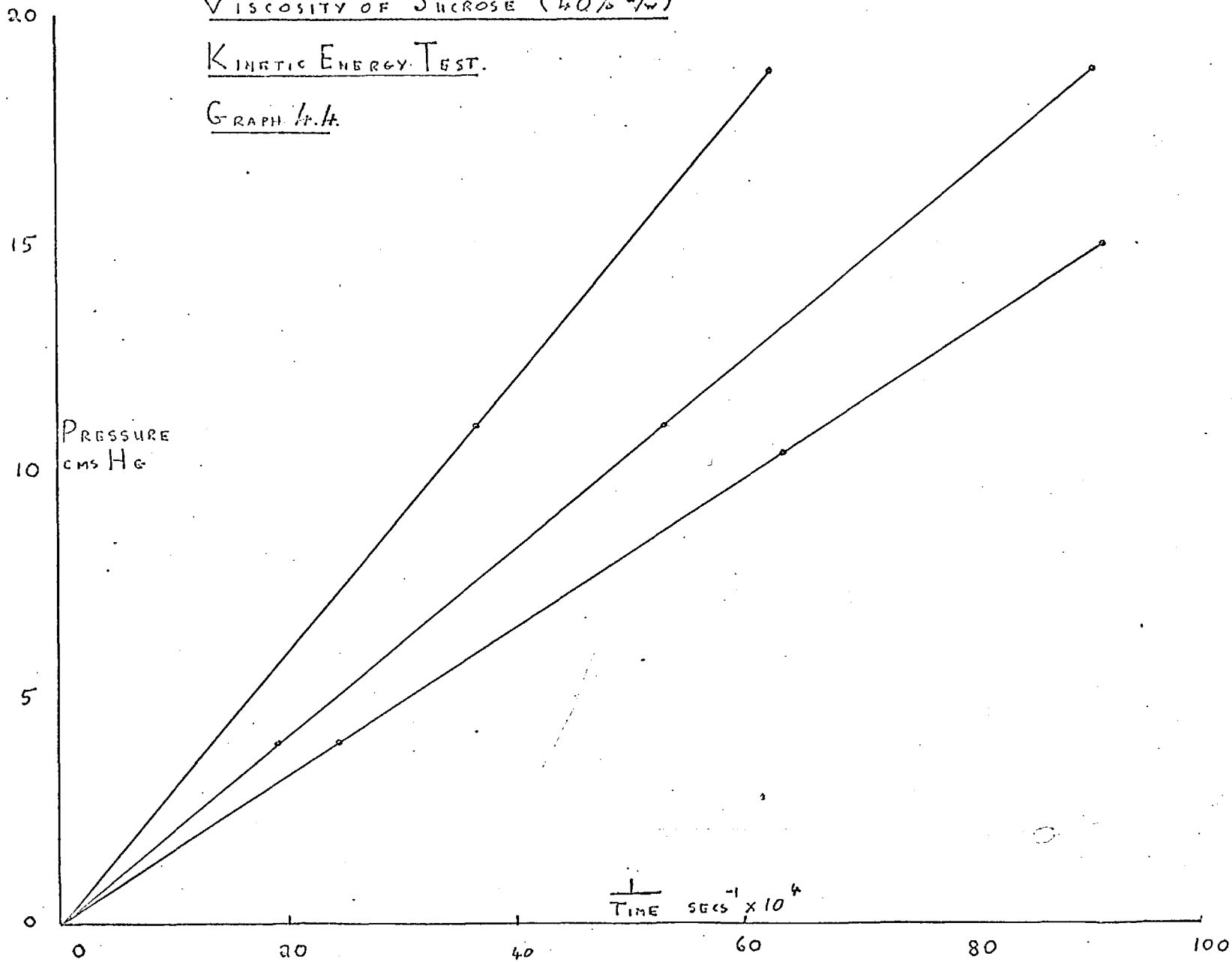

4.1.5. Accuracy.

The duration of runs was between 5 and 100 minutes, and the time taken was measured on a stopwatch to $\pm$ 0.2 secs. or less than $\pm$ 0.07%. Pressures can be read to $\pm$ 0.002 cms. of mercury and stabilities of $\pm$ 0.01% obtained. Temperature was to $\pm$ 0.02°C. or a viscosity charge of about 0.02% on average. The results were found experimentally to be accurate to $\pm$ 0.5%.

4.1.6. Results.

Graphs showing the results of viscosity experiments on binary mixtures of sodium, potassium, rubidium and caesium nitrates with calcium nitrate are given. Tables of polynomials corresponding to these graphs are given. A graph of the ternary mixture of the monovalent salts sodium potassium and rubidium nitrate is also included.

Viscosity of $NaNO_3/Ca(NO_3)_2$ System.

Mole Fraction $NaNO_3$ as Parameter

Graph 4.5

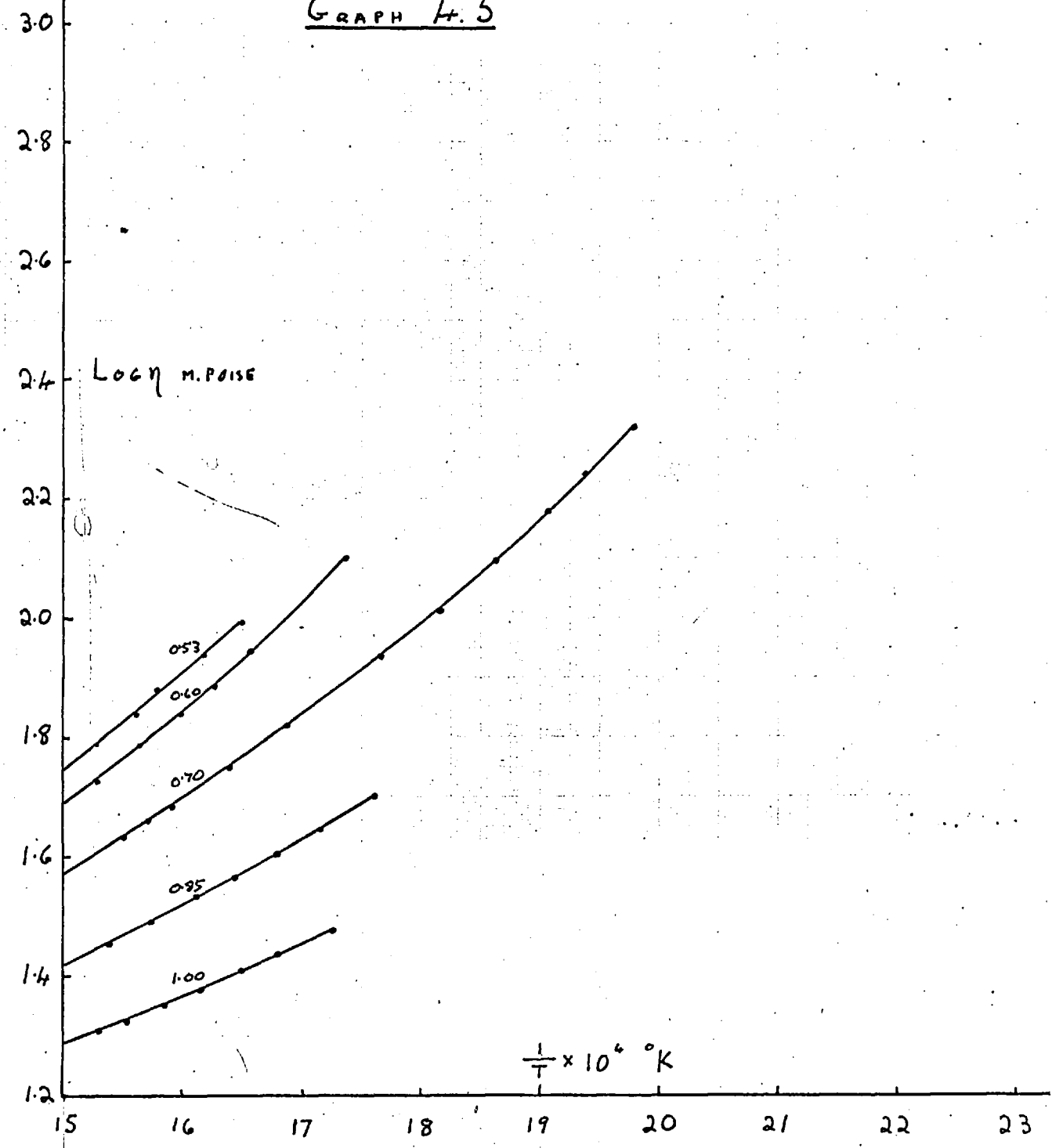

Viscosity of KNO_3 / $Ca(NO_3)_2$ System

Mole Fraction KNO_3 as Parameter

Graph 4.6.

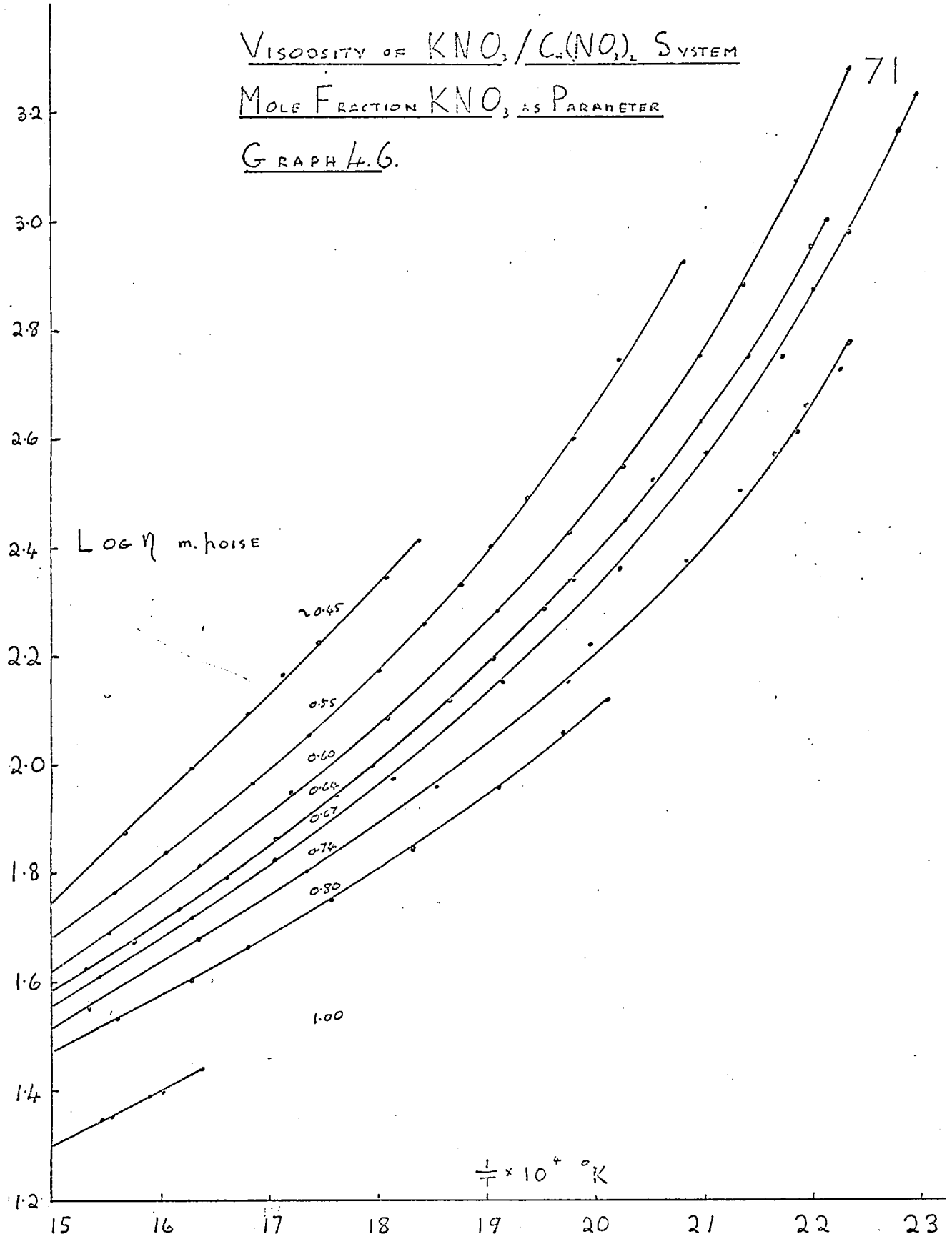

Viscosity $RbNO_3/Ca(NO_3)_2$ System

Mole Fraction $RbNO_3$ as Parameter.

Graph 4.7

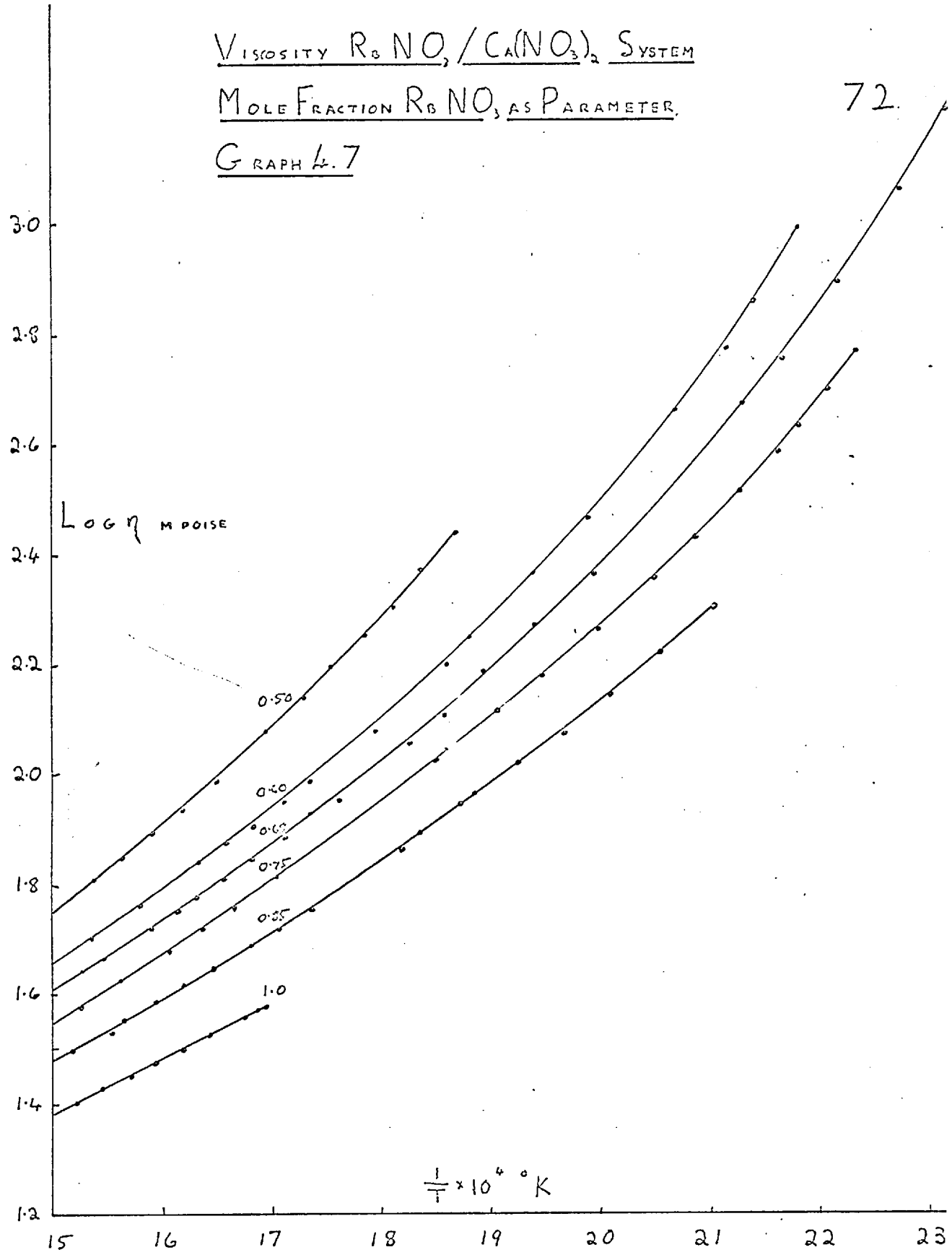

Viscosity $CsNO_3/CaNO_3$ System.

Mole Fraction $CsNO_3$ as Parameter

Graph 4.8

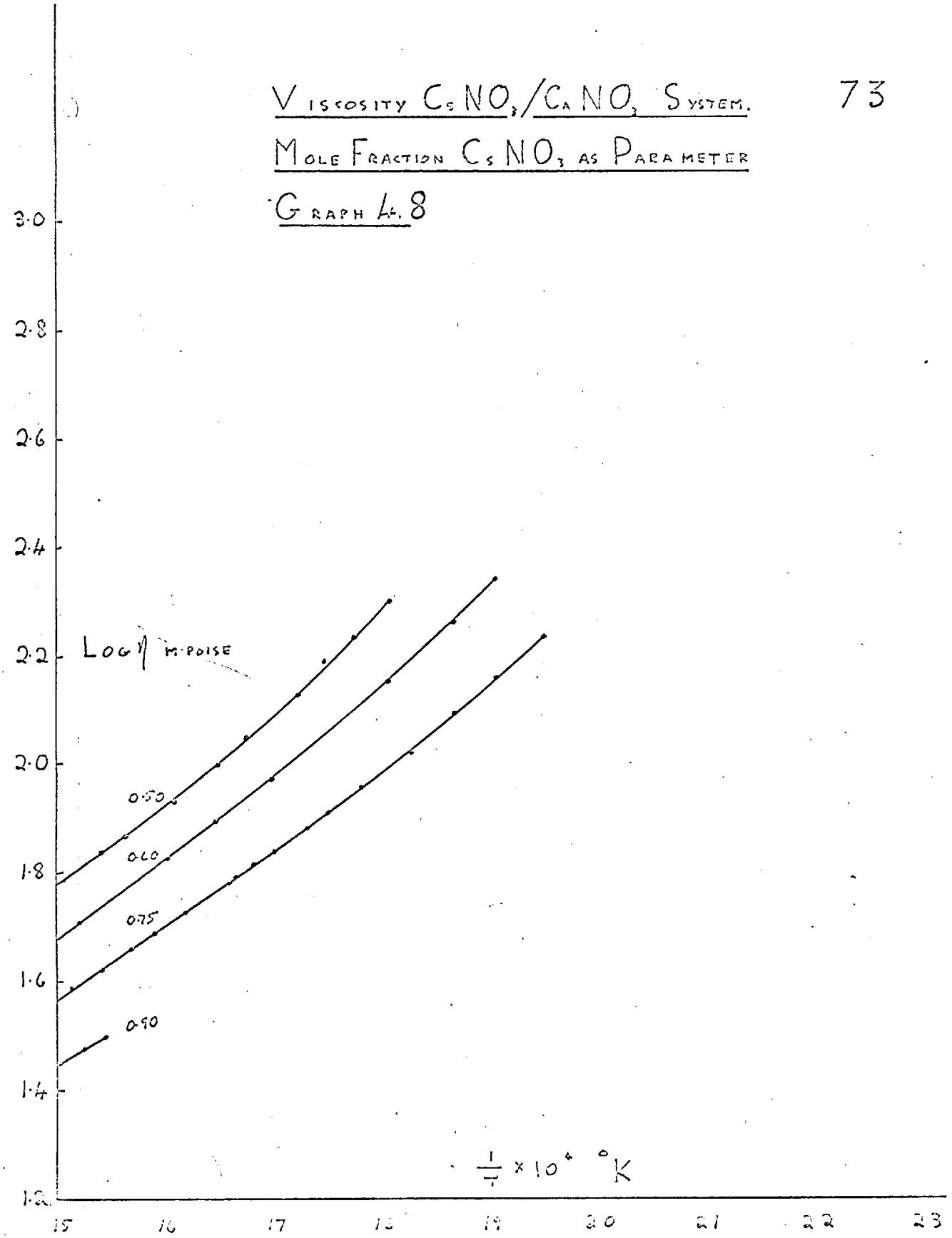

Viscosity Ternary Mixture.

x_{NaNO_3} = 37·8 x_{KNO_3} = 37·8 x_{RbNO_3} = 24·4

Graph 4.9

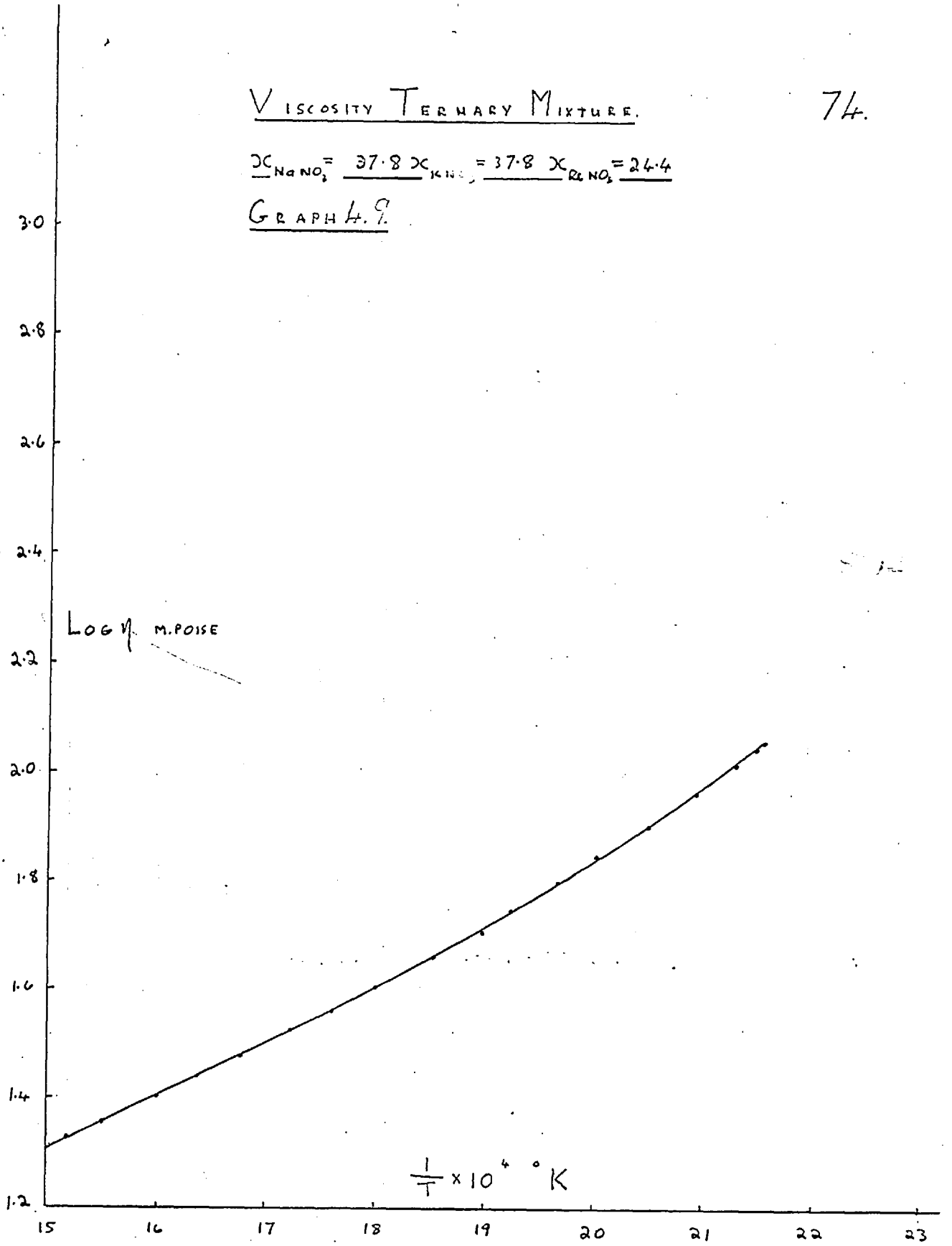

Computed Equations

Data is expressed in the form of a polynomial,

$$\log \eta = a - b\left(\frac{1}{T} \times 10^4\right) + c\left(\frac{1}{T} \times 10^4\right)^2$$

η in m.poise.

T in ^{o}A.

by a least squares method. Calculations being carried out on the Atlas and Mercury computer.

System Sodium Nitrate - Calcium Nitrate.

Compstn. moles $NaNC_3$.	a	b x 10	c x 10^2
0.55	4.7466	5.3427	2.2382
0.60	6.4252	7.4931	2.8971
0.70	0.2424	-0.3578	0.3522
0.85	1.4120	0.8911	0.6034
1.00	0.8966	0.2672	0.3521

System Potassium Nitrate - Calcium Nitrate.

Compstn. moles KNO_3	a	b x 10	c x 10^2
0.55	4.9175	5.1518	2.0182
0.60	5.3221	5.4829	2.0404
0.64	4.9700	5.0042	1.8654
0.67	5.1649	5.2060	1.8976
0.74	2.6364	2.3765	1.0890
0.80	1.3986	0.8695	0.6026
1.00	-0.1849	-1.0134	-

System Rubidium Nitrate - Calcium Nitrate.

Compstn. moles $RbNO_3$.	a	b x 10	c x 10^2
0.50	2.6286	2.5298	1.3021
0.60	2.5312	2.2776	1.1331
0.68	3.1306	2.8741	1.2527
0.75	2.4199	2.0379	0.9842
0.85	2.5567	2 2060	1.0049
1.00	-0.1184	1.0025	-

System Caesium Nitrate - Calcium Nitrate.

Compstn. moles $CsNO_3$.	a	b x 10	c x 10^2
0.50	1.9404	1.6484	1.0229
0.60	2.3220	2.0183	1.0648
0.75	1.7860	1.4169	0.8507
0.90	3.7136	4.0933	1.7230

4.2. Conductivity.

The A.C. conductivity of the potassium nitrate calcium nitrate melt was measured to give a second transport parameter for correlation with the viscosity. A Wayne Kerr B.221 bridge operating on the transformer ratio arm principle was used to measure the resistance of a simple dipping type capillary cell. The principle, operation and precautions taken in using this bridge are described in Chapter 5. In this case, since only simple conductivity results at one frequency were required, the internal oscillator of the bridge was used as a source. The frequency supplied is 1,592 cycles/sec.

The conductivity cell design is shown in diagram 4.10. The electrodes were made of platinum, the foot one being a wire ring secured to the glass and the top one a flat plate. The cell leads were unshielded, but since capacitance effects are displayed on a separate dial, the effect of stray capacitance can be ignored.

Conductivity Cell

Diag. 4.10

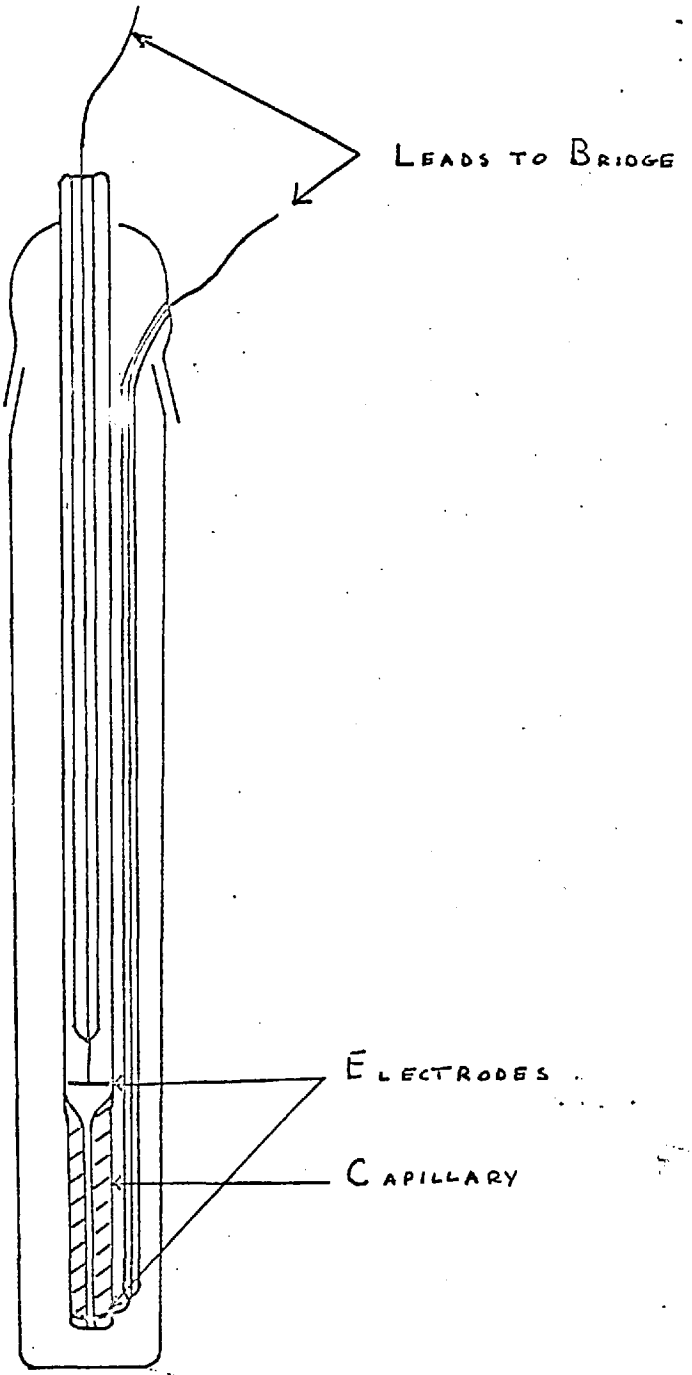

The cell was calibrated using a standard solution of $\frac{N}{10}$ potassium chloride, whose conductivity is known accurately, in a water thermostat bath at 25°C. The difference in temperature between the calibration and actual measurement conditions caused a slight error, of the order of 0.1% due to the expansion of the capillary. Errors can also occur in the preparation of the standard solutions and an overall accuracy of ± 1% was estimated for the results.

Errors can arise if any part of the electric flux through the capillary is cut off by the outer glass container. The actual distance separating the foot electrode from the container was investigated to discover the distance at which this effect became appreciable. It was found that as long as the capillary was 2 cms. away from the foot and 1.5 cms. away from the walls of the containing vessel, any effects of this nature were negligible.

Results were taken using the same melt mixtures in the same temperature controlled bath, at the same time as the viscosity, and are displayed in a similar manner. Only the binary potassium nitrate calcium nitrate was studied.

Conductivity of $KNO_3/Ca(NO_3)_2$ System

Mole Fraction KNO_3 as Parameter

Graph 4.11.

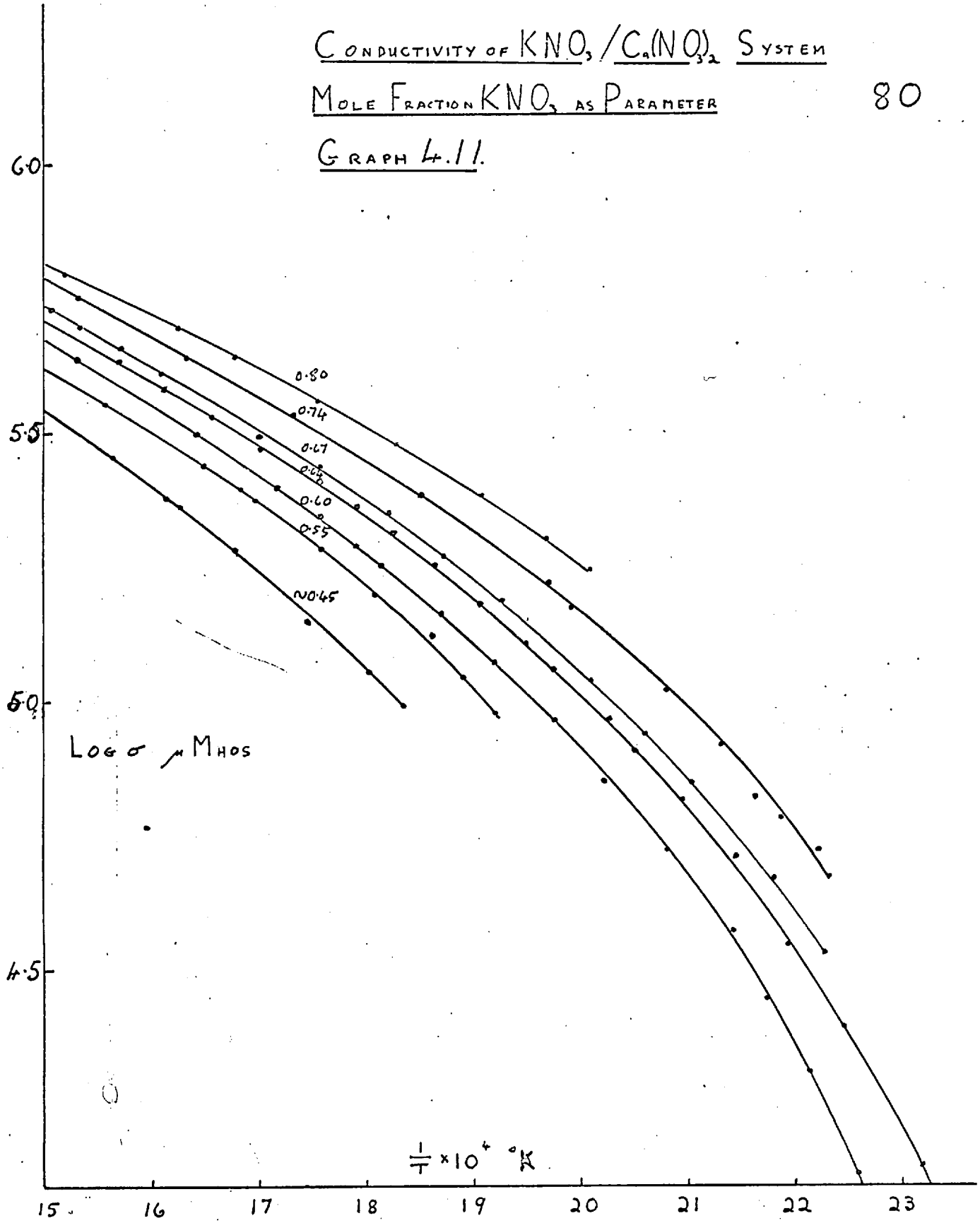

Computed Equations.

Results, calculated using the Atlas and Mercury computer are expressed as a polynomial of the form,

$$\log\sigma = f + g\,\frac{10^4}{T} - 1\left(\frac{10^4}{T}\right)^2 .$$

σ in mho's

T in ^{o}A.

System Potassium Nitrate, Calcium Nitrate.

Composition mole fraction of KNO_3.	f	10g.	$10^2$1.
*0.55	+12.454	-4.3319	-
0.60	1.8807	5.3420	1.9270
0.64	3.5145	3.4694	1.3728
0.67	3.7586	3.2305	1.3049
0.74	8.2629	7.9829	2.4700
0.80	5.8137	0.7559	0.5265
*1.00	+7.1188	-0.8056	-

* These results are more accurately fitted using only the f and g terms.

4.3. Additions of Chlorides and Bromides to the mixed melts.

For theoretical reasons, the effect of additions of bromides and chlorides to the melts was studied. The size of additions was limited by crystallization effects occurring in the temperature range of measurement. The compositions were chosen so that the total cation charge per anion remained the same as that for the anomalous potassium nitrate calcium nitrate mixture with a mole fraction potassium nitrate of 0.64.

In the case of the potassium bromide melt, crystallization occurred in the range of study but its results do not differ appreciably from the potassium chloride run as shown. The effect of the same concentration of both potassium salts and sodium chloride is very similar for the viscosity plot, but the sodium chloride addition markedly alters the conductivity of the solution. The results are presented in graphs 4.12. and 4.13.

Viscosity of Additives

Graph 4.12

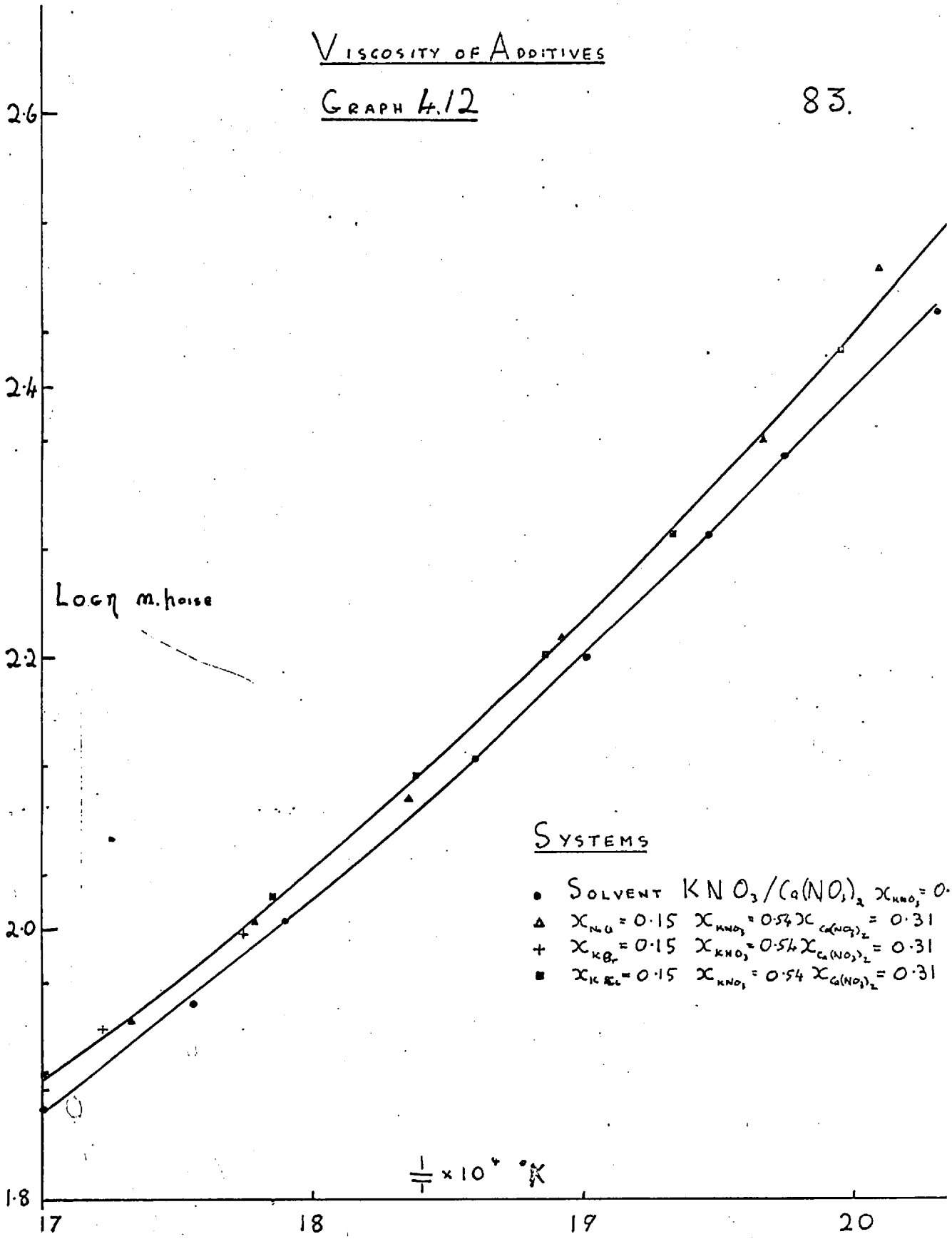

Conductivity of Additives.

Graph 4.13

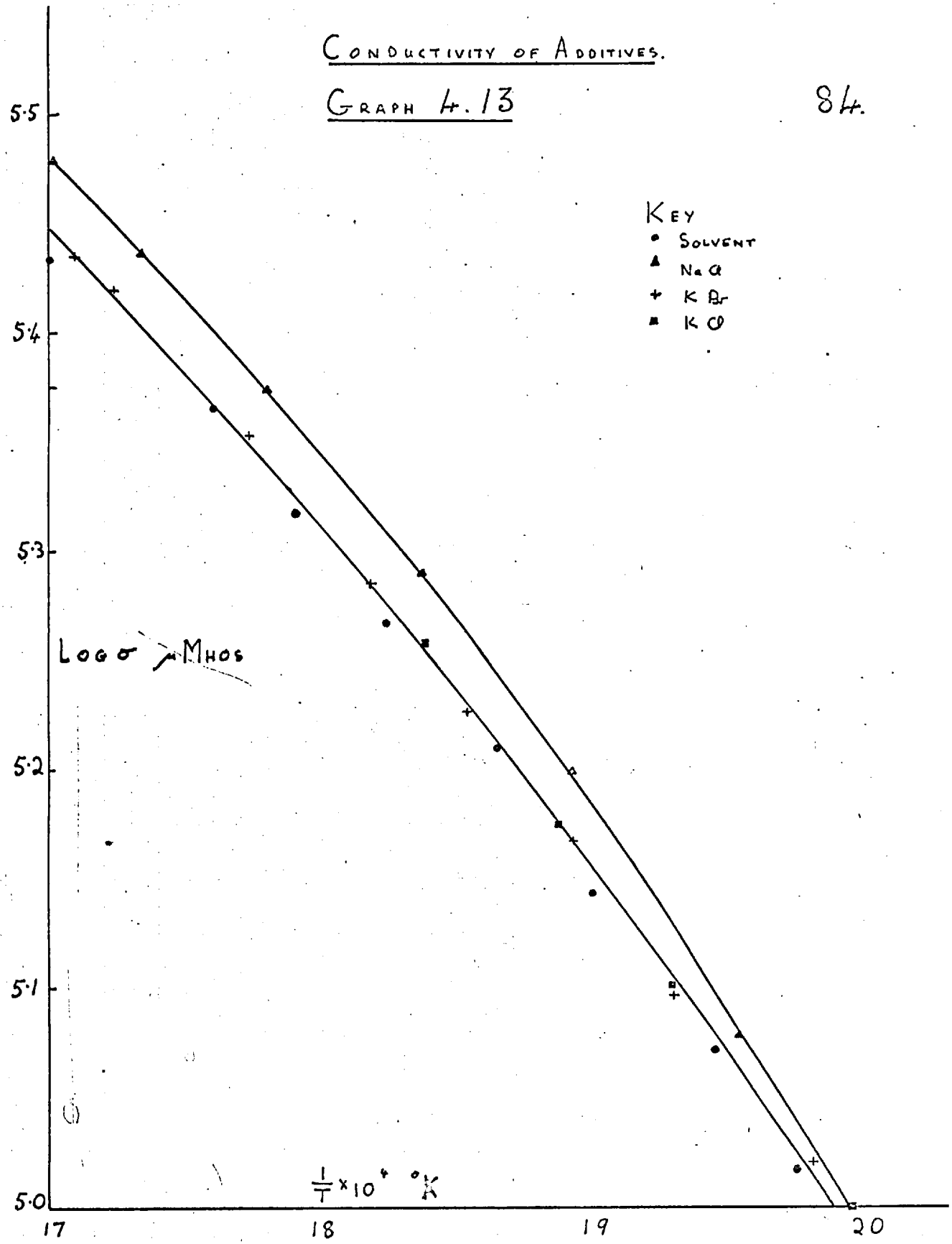

4.4. Ultraviolet Spectroscopy Measurements.

The position of theweak band in the ultraviolet spectra of the nitrate ion is sensitive to its environment. Investigations of this energy shift in molten salts have been carried out by Cleaver, Rhodes and Ubbelohde and by Smith and Boston and an explanation advanced in terms of the basic structure of the melt. (See 2.1.2.). The apparatus described here is essentially that developed by Cleaver, Rhodes and Ubbelohde.[13]

A standard Cambridge S.P.700 double beam ultraviolet spectrometer was used with the cell compartment modified to take a heated temperature controlled block. Only the cell compartment was altered, the instrument, after rebalancing to match the new compartment is operated in the conventional manner.

The cell compartment must comply with quite vigorous specifications. A constant sample temperature with a minimum temperature gradient across it must be maintained and the temperature outside the block must be below 30°C. to prevent heating the photomultiplier tube used as a detector. There must be no direct emission of radiation from the heaters in the direction of the beam or the results may be affected. Optically, the beam should not be chopped, deflected or

scattered in any way, although some allowance can be made for this at reduced precision.

The ultimate design of Cleaver, Rhodes and Ubbelohde which satisfies these criteria well is shown in diagram 4.14. The windows of quartz at A and C were required to prevent convection currents. The outer cooling jacket ensured that the photomultiplier tube was not overheated. Cleaver used a probe thermocouple to investigate the temperature gradient across the sample at 300°C. and found a temperature difference of 0.5°C. across it, quite adequate for the present experiments. Temperature measurement was by a thermocouple and control was provided by an electronic controller using a platinum resistance thermometer as a sensing element.

Since molten nitrates have very high extinction coefficients, very thin samples were required. The method of preparing a film of salt of the approximate thickness between two quartz plates has been described. (See 3.1.2.). The sample was then mounted in a metal frame which locates in the sample compartment. The peak of the weak band should show 40-60% transmission when the sample is melted in the heated block. Final adjustments to thickness can be made at this stage by adjusting the screws clamping the sample into the frame.

Thermostat Cell Compartment Diag 4.14

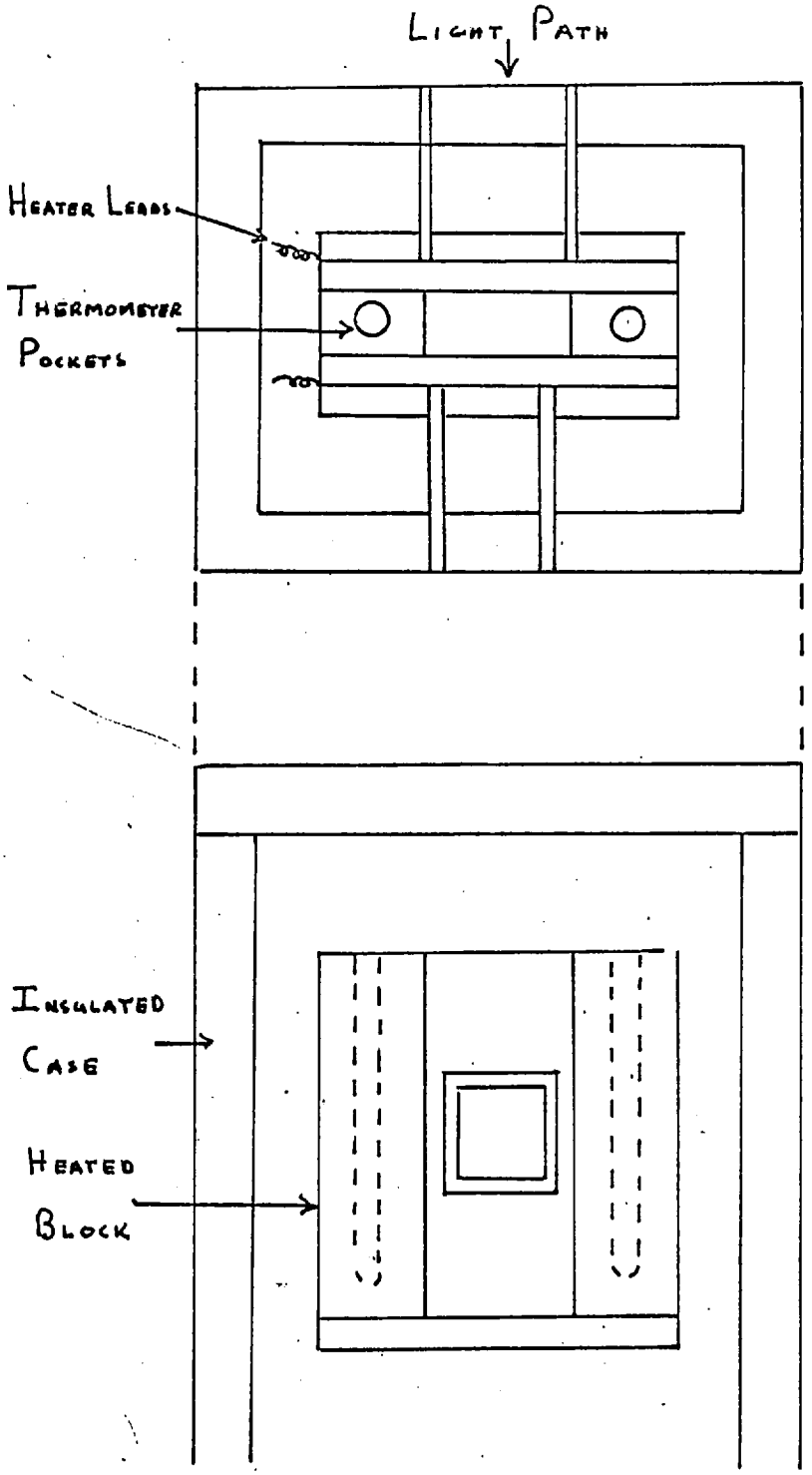

The samples have a long liquid temperature range and the films remain complete mainly because of the high surface tension and viscosity of the mixed melts. Some difficulty was occasionally encountered, particularly with monovalent melts at high temperatures but, provided they were sufficiently thin, all the systems investigated gave complete films up to 350°C. Decomposition was easily observed, since bubbles of gas quickly formed in the sample causing frequency independent transmission and, similarly, crystallization was detected by frequency independent absorption.

The instrument scanned the frequency range automatically, using hydrogen and deuterium sources, and plotted percentage transmission against frequency in wave numbers. A typical plot is shown in diagram 4.15. Since the main peak overlapped to a small extent the weak band, this was slightly skewed. To obtain the true position of the peak, the mid-points of a series of chords, taken at various heights on the band, were joined as shown. A simple construction of similar triangles gave an accurate measure of peak position.

Spectra. Method of Measurment of Peak Position

Graph 4.15

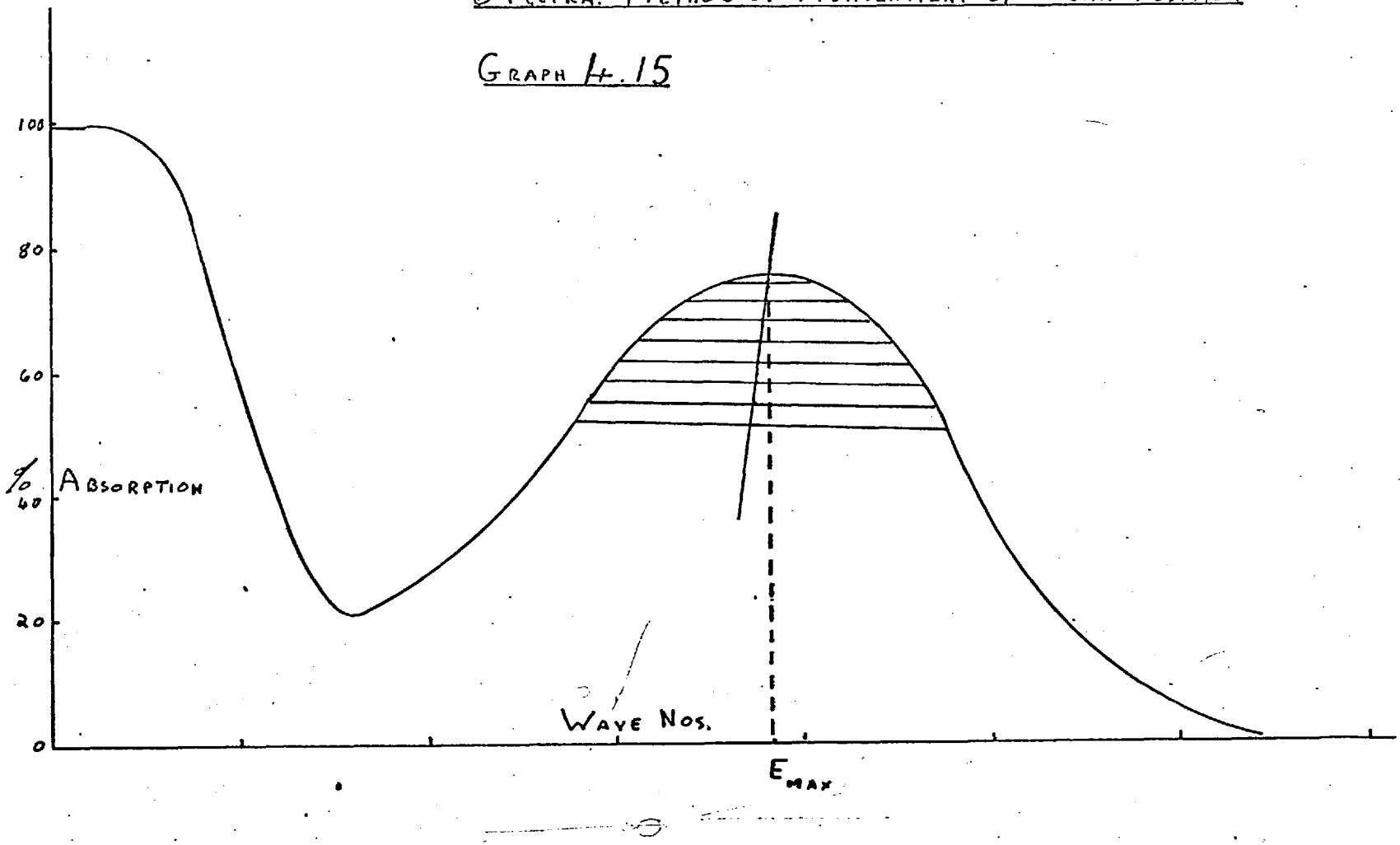

The frequency values were calibrated by adjusting the instrument cams till the value of the hydrogen line was correct at 15,237 cms^{-1}. Cleaver investigated the accuracy of this method of calibration in the region of the nitrate spectra and discovered it to be 80 cms^{-1} in error[14]. This correction has been added to all results.

A graph of peak position against temperature is shown for various mixtures of potassium and calcium nitrates. The graph of the highest calcium containing mixture is curved. In order to establish the normal behaviour of nitrate melts in this temperature region, the spectra of the equimolar mixture of sodium nitrate and potassium nitrate was also measured. A considerable degree of supercooling down to 100°C. was obtained probably due to the use of thin films.

Plots of peak position against temperature for the weak band are given. The system sodium nitrate potassium nitrate shows no departure from linearity but the deviation in the potassium nitrate-calcium nitrate melt (mole fraction KNO_3 = 0.64) is very marked. This latter curve was repeated several times with two separately prepared samples.

PEAK POSITION VS. TEMPERATURE

GRAPH 4.16

SYSTEMS

A $x_{KNO_3} = 0.64$ $x_{Ca(NO_3)_2} = 0.36$

B $x_{KNO_3} = 0.80$ $x_{Ca(NO_3)_2} = 0.20$

C $x_{KNO_3} = 1.0$

D $x_{KNO_3} = 0.5$ $x_{NaNO_3} = 0.5$

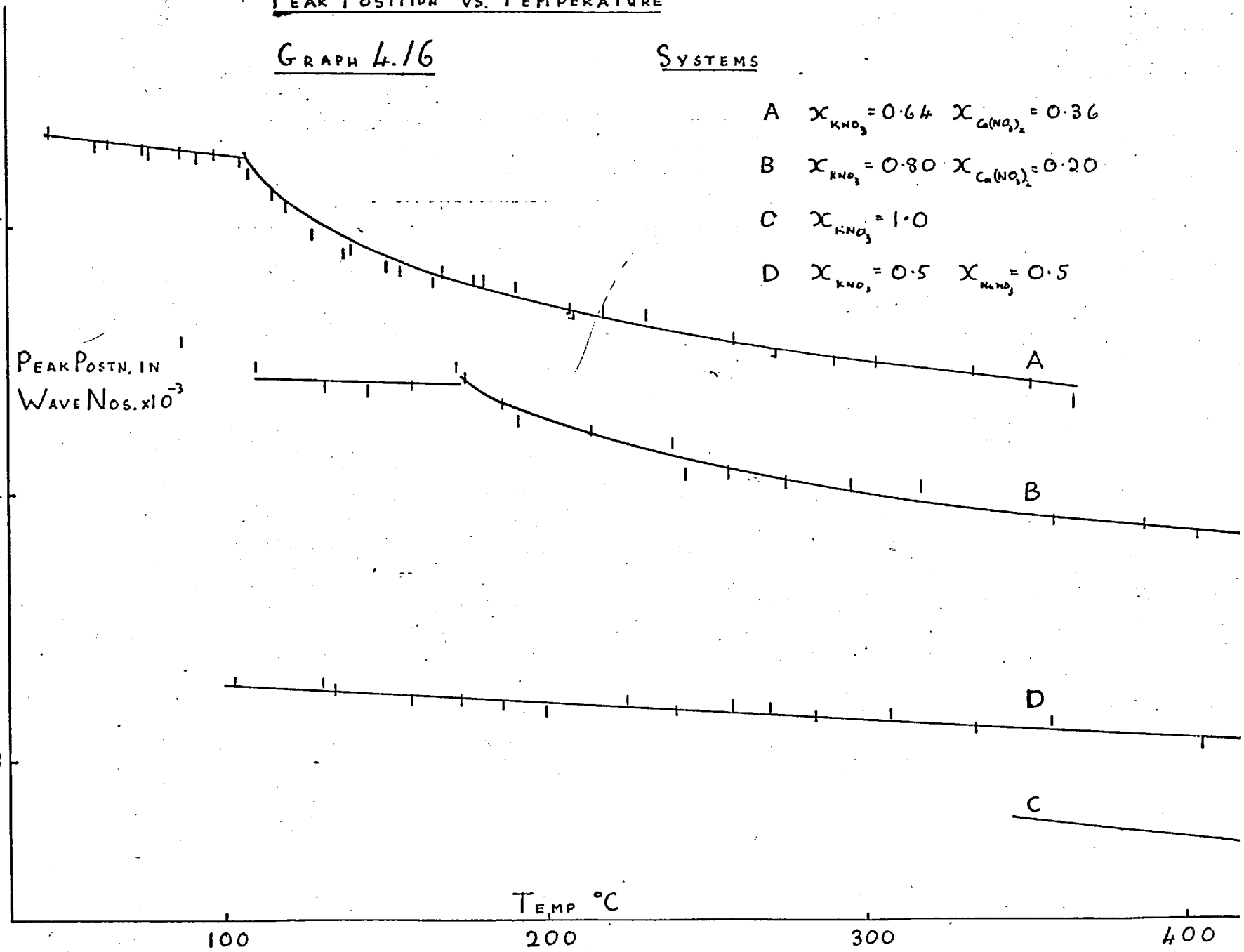

Chapter 5.

Experimental Studies of the dielectric behaviour of the supercooled melt.

In good conductors such as molten salts (about 0.1 mhos cm^{-1}) the measurement of dielectric behaviour is made extremely difficult by the magnitude of the resistive component. Supercooled mixtures of the anomalous potassium nitrate calcium nitrate melt have extremely low conductivities (about 10^{-4} to 10^{-5} mhos cm^{-1}) and, in this region, it is possible to discriminate between simple conductivity and anomalous capacity and loss effects. The theoretical reasons underlying this study are considered in the discussion and the methods used to prepare the supercooled melts are described in 3.1. The present chapter is in two main parts, a description of the cell and bridge measurement circuits including possible errors inherent in them and the presentation of the results in terms of the standard constants.

5.1. Methods of Measurement.

5.1.1. Cell Design.

The cell design used is shown in diagram 5.1. The cell plates were two pieces of heavy platinum sheet approximately 2 cms. by 1 cm. in area and 1.5 cm. apart. It was

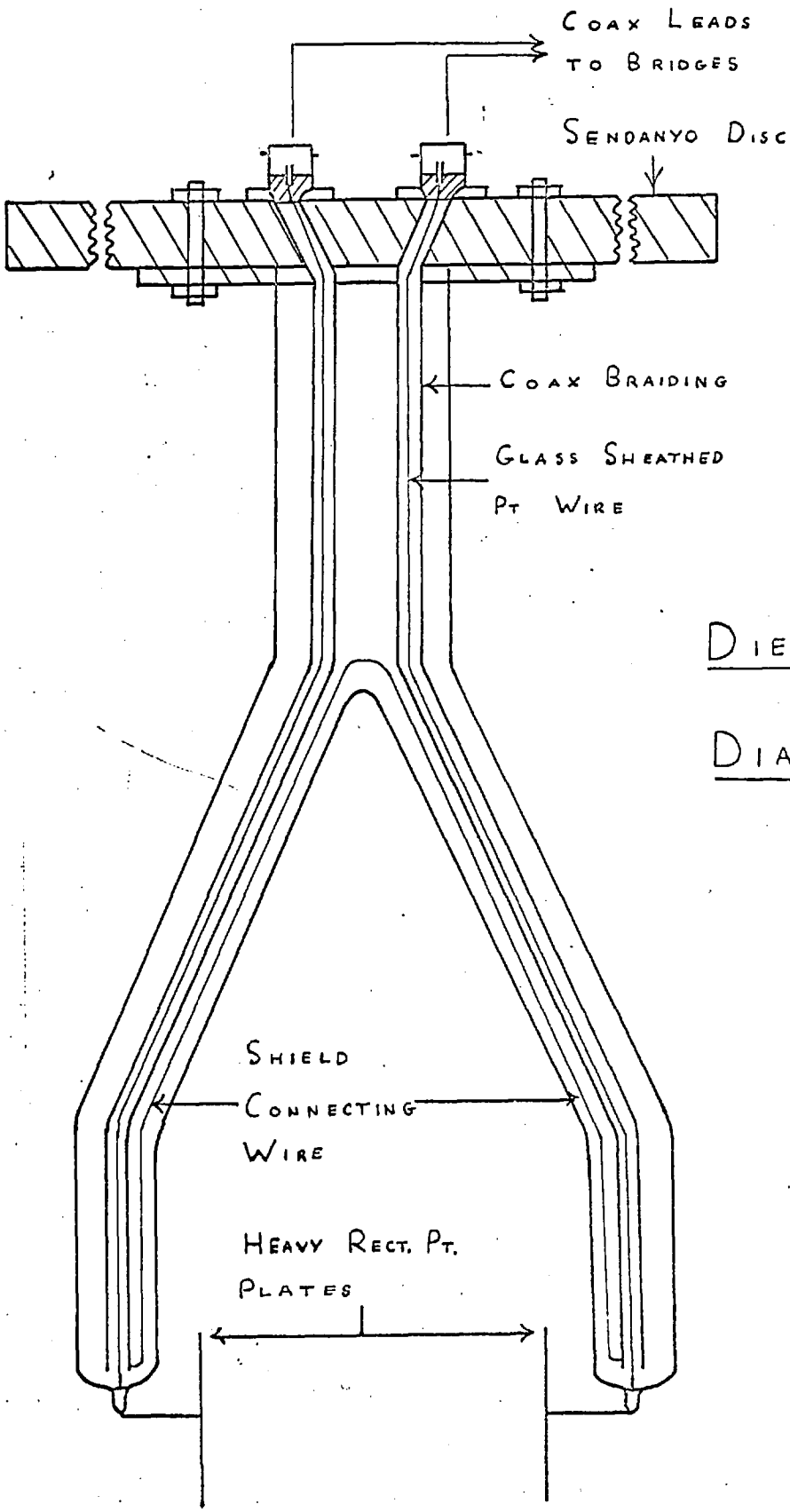

Dielectric Cell

Diag 5.I

impossible to seal the heavy leads required to support the plates to the pyrex sheath. The thinner leads used inside the sheath were sealed through the pyrex and the heavy leads welded to them. This join and part of the heavy leads was covered in pyrex to keep the assembly rigid.

The leads inside the sheath were covered in glass and electrical shielding was provided by slipping standard coaxbraiding over them. The braids were joined by a wire connection at the ends near the plates to conform to the wiring arrangements of the B.221 neutral circuit.

The cell top was a round "Sendanyo" (an asbestos composition) disc split through the middle. The top of the leads were packed with additional insulation between the braiding and the central wire. They were passed through two angled channels in the Sendanyo and connected to the BNC sockets on the top in the normal way. The two halves of the disc were bolted together through the metal flanges on the sockets and the assembled disc bolted to the flanged top of the glass sheath. In this position the packed lead tops were squeezed into the channels in the Sendanyo, effectively preventing the central wire being pushed down when the BNC sockets were connected. The leads from the cell to the bridge were of standard 75 Ω co-axial cable.

The Sendanyi disc rested on the glass flange top of the vessel containing the salt.

Using this construction, the leads were shielded to as near the plate electrodes as possible and were kept short and simple, thus reducing the possibility of complex lead effects at high frequency. The plates were made as large as was mechanically practicable and a suitable separation distance chosen to give a good balance between resistive and reactive components in the salt.

The plates were coated with platinum black using the method of Janz[15]. This reduces the possibility of interference from plate to melt impedance terms by increasing the surface area and so decreasing the resistive component. While the effectiveness of platinum blacked surfaces in molten salts is open to question, the results obtained are only affected below about 2 kilo.c/sec. There was very little change in the shade of the platinum black for periods of up to about one week. Small but noticeable changes occurred over longer periods suggesting some poisoning of the surface.

5.1.2. Transformer Ratio Arm Bridge Circuits.

The bridges used were the Wayne Kerr B.221 and B.601 bridges. Compared with conventional bridge circuits, the

Bridge Circuits

Diag 5.2

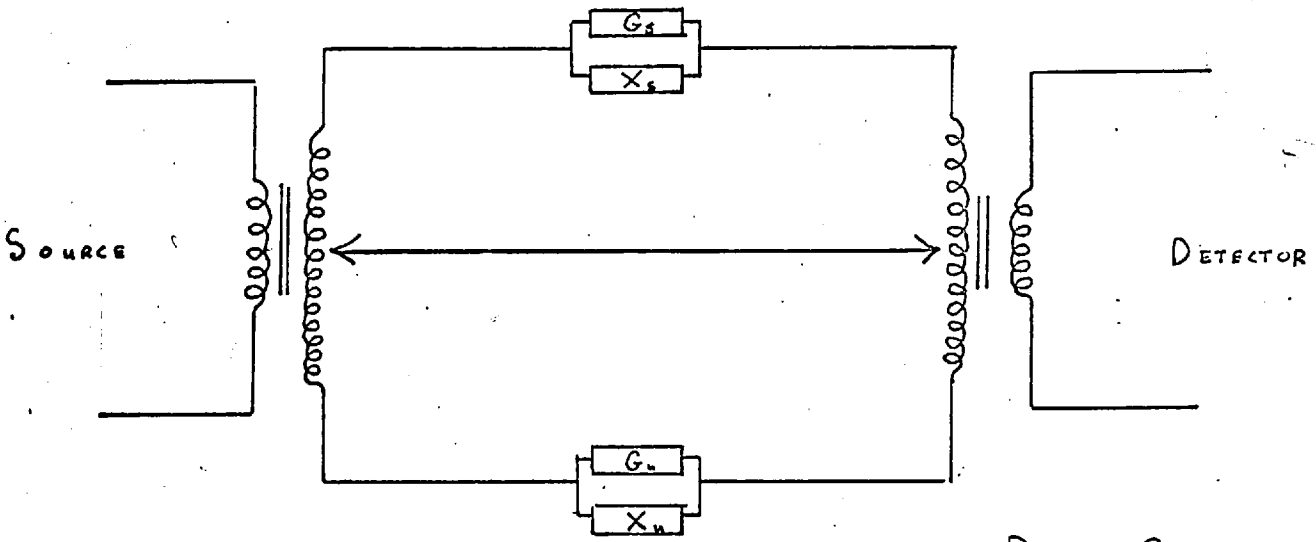

Basic Circuit

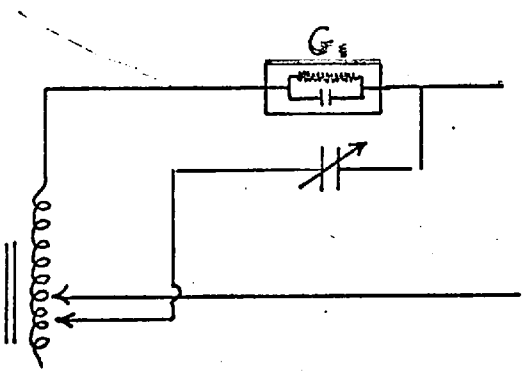

Trimming Standards

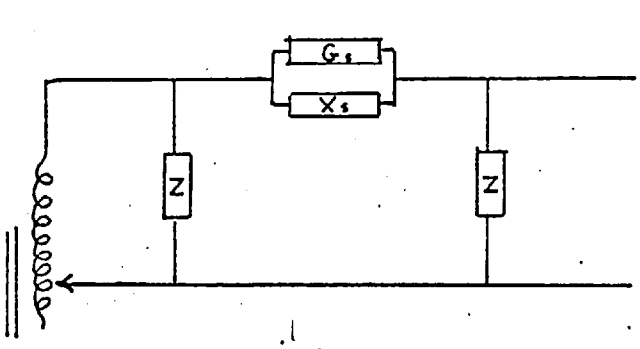

Elimination of Stray Impedance

transformer ratio arm bridge principle considerably extends the range of measurement, reduces the number and purity of the standards required and largely eliminates earthing problems[16]. The system being measured is considered as an equivalent parallel circuit and the results expressed directly as a resistive and capacitive component.

The basic bridge circuit is as shown in diagram 5.2. G_S and X_S represent suitable conductance and reactance standards G_N and X_N an unknown impedance. To balance the bridge the standard side is adjusted until there is no current in the secondary winding of transformer B. This adjustment can be carried out either by altering the number and value of the standards or by altering the tappings on the bridge transformers. This latter method greatly extends the range of the bridge measurements. For example, if 1000 turns are used on the unknown side of transformer A and only 10 turns on the standard side, the unknown will be 100 times larger than the balancing standard.

Relatively less pure standards can be used since the stray component can be trimmed out. An example is given in diagram 5.2. for an impure resistance standard. A variable capacitor is inserted in the opposite sense to the standard

and trimmed to remove any stray reactance. This system is particularly useful because it allows the bridge to read resistance and capacitance directly whereas most comparable systems require the subtraction of two impedances.

Stray impedance effects are eliminated by connecting one end of the stray component to the neutral of the bridge, so as to shunt the component across the transformer. For example, the outer sheathing of the wax leads in the cell were connected to the bridge neutral, thus eliminating lead errors as shown in diagram 5.2.

The B.221 bridge measures resistances to 0.1% and capacitances to 1% or better up to 20 kilo.c/sec. The B.601 bridge measures resistances to 1% and capacitances to 2% between 15 kilo.c./sec. and 10 Meg.c/sec. There is some diminution in accuracy above 5 Meg.c/sec.

5.1.3. The Complete Bridge Measuring Circuit.

A block diagram 5.3. of the equipment is given. The power source was a Marconi wide band oscillator accurate to 3% over its entire range of 10 c/sec. to 10 Meg.c/sec. The output frequency is continuously variable.

Below 1 Meg.c/sec., the out of balance signal from the bridges was amplified and displayed on a Telequipment

MEASURING CIRCUIT

ALL LEADS SCREENED

DIAG 5.3.

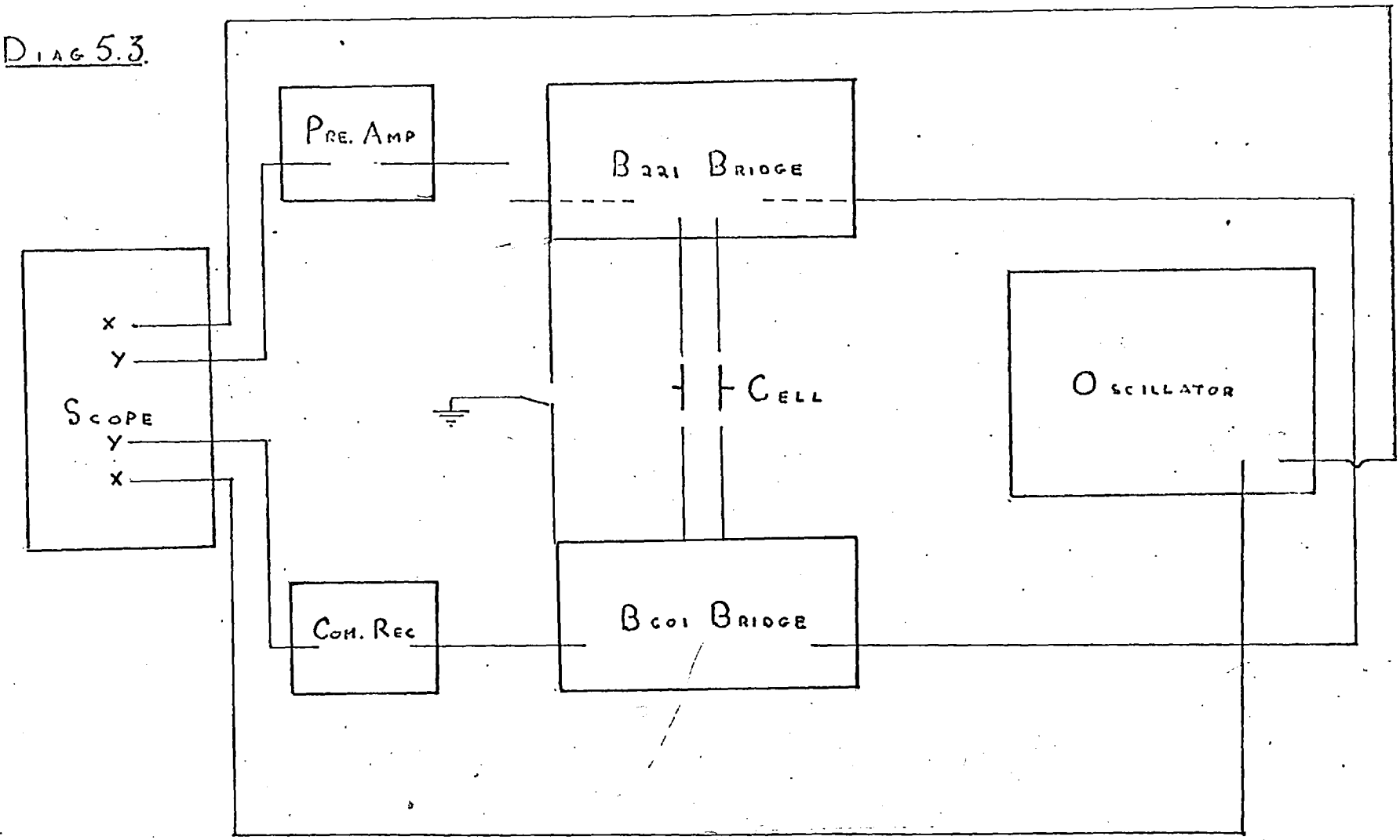

oscilloscope, but above this frequency, the possible amplification markedly decreased and some phase shift was caused in the signal. Between 600 kilo.c/sec. and 10 Meg.c/sec., the signal was fed to an Eddistone EC.10 communications receiver which acted as a tuned amplifier. A constant frequency output (456 kilo.c/sec.) from the intermediate stage amplifier was fed to the scope. In each case the bridge controls were adjusted to give the point of minimum signal, at which point the bridges were in balance.

5.1.4. Equipment checks.

Using a series of resistances and capacitances the performance of the bridges was tested. It was found that with small resistances of values from 10-30 Ω lead effects were very important, particularly at high frequencies. Directly coupled components gave the correct answers but two ft. leads, shielded or unshielded, gave readings in error up to 60%.

Above 100 Ω, no appreciable difference in value was noted between directly and indirectly coupled components and the results were in agreement with the values of the standards. Thus, as long as the bridges were used with resistances above 1 kilo Ω, the lead effects can be ignored. Capacity values

were not affected by leads when used in conjunction with the higher resistances. The capacity values varied slightly between the two bridges at 20 kilo.c/sec., by amounts of up to 1 p.F. An example is shown in Table 5.5. for benzene and air capacities in the cell. Nevertheless both bridges give the same dielectric constant.

5.2. Presentation of Results.

The bridges measured the resistance and capacitance values of the material in the cell directly. To express the large number of observations taken at various temperatures on the salt the results have been fitted to polynomials of the form,

$$\frac{1}{f.R.} = a - bf + cf^2$$

f : frequency in c/sec.

R : resistance K.Ω.

~~and~~

~~$c = d - gf + hf^2$.~~ ~~c : capacitance p.F.~~

where a, b, c, ~~d, g and h~~ are constants. The results are given in Table 5.4. For theoretical reasons it is more informative to express the results in terms of the dielectric constant ϵ' and the loss term ϵ''. The methods used to obtain these terms are analysed and the measurement techniques verified by reference to standard solutions.

Table 5.4.

Temp. °C.	Results for $\frac{1}{f R.} \times 10^{+7}$ mhos secs/K.cs. vs. f in K.cs/sec. a	b x 10^{3}	c x 10^{7}	Results for C f in K.cs/sec. d	g x 10^{3}	pF vs. f x 10^{7}
84.6	8.7245	5.796	6.492	~~10.04~~	~~1.782~~	~~1.701~~
86.0	20.394	14.211	16.13	~~10.80~~	~~1.768~~	~~1.631~~
88.8	45.596	30.522	34.24	~~15.02~~	~~3.598~~	~~3.517~~
93.1	70.276	49.56	57.01	~~14.93~~	~~2.905~~	~~2.700~~
94.6	139.68	84.09	93.29	~~14.88~~	~~2.075~~	~~1.843~~
95.8	131.85	87.93	99.03	~~16.60~~	~~2.806~~	~~2.464~~
99.4	370.30	265.51	304.46	~~16.87~~	~~2.338~~	~~1.999~~
100.6	616.78	413.45	463.78	~~17.59~~	~~1.706~~	~~1.183~~

5.2.1. Measurements of the dielectric constant.

The dielectric constant of a material held between two parallel plates is defined as,

$$\epsilon' = \frac{\text{Capacity of the plates when the space between them is filled with the material}}{\text{Capacity of the plates in vaccuo.}}$$

Air has a dielectric constant of about 1 and so by measuring the capacity of the cell in air and in the test liquid the dielectric constant can be calculated.

Before measuring the molten salt values, but using electrodes which had been immersed in the liquid salt for one week, measurements were taken using benzene and 0.5×10^{4}N potassium chloride solution over the entire frequency range. The dielectric constant of benzene is well known, the best value in this frequency range appears to be 2.35[17]. For the dilute aqueous solution, it is well known that the dielectric properties do not differ markedly from the values for pure water of about 80[18]. A table of the results is given. (5.5.).

At high frequencies, the low dielectric constant of the air makes the cell extremely dependent on its surroundings to distances of 10 cms. or more. In consequence the value used . is taken as a constant 0.60, from the lower frequency results.

Table 5.5.

Frequency kilo cycles/sec.	Cell Cap. in Air. (Co)pF.	Cell Cap. in Benzene pF.	ϵ' for Benzene.	ϵ' for 0.5×10^{-4}N KCl.
7,800	0.45	1.40	2.34	91.6
5,850	0.53	1.46	2.44	85.0
3,950	0.56	1.50	2.50	83.4
2,970	0.59	1.53	2.55	80
1,980	0.59	1.53	2.55	80
1,000	0.60	1.54	2.57	80
800	0.60	1.55	2.58	80.8
600	0.59	1.54	2.57	80.8
20	† 0.369	†0.944	2.54	80
10	† 0.371	†0.948	2.55	
6	† 0.372	†0.946	2.55	
4	† 0.371	†0.945	2.54	

† These values measured on B.221 bridge.

These results verify that the bridges can reproduce standard results with moderate accuracy. Higher precision than 5% is not expected with this technique. The difference in absolute values between the capacity readings on the two bridges has already been noted and presumed to be due to calibration errors. The identical values for the dielectric constant of benzene verify this. Owing to the higher conductivity of the aqueous solution, the more accurate but less flexible B.221 bridge cannot measure the small reactive term correctly.

5.2.2. Dielectric Loss Measurements.

The analysis of dielectric loss phenomena in an ionic conductor inovlves basic postulates concerning the melt structure and is analysed in the discussion. A simple analysis of the behaviour without reference to structure is made here to allow the derivation of the dielectric parameters.

In a pure capacitor, the admittance,

$$Y = j\omega c = j\omega C_o \epsilon$$

where $j = \sqrt{-1}$, ω is the angular frequency, c is the capacity of the capacitor filled with the dielectric of dielectric constant ϵ and C_o is the capacity of the capacitor on vaccuo. If there is any anomalous adsorption

the admittance will also have a real component. This is best expressed by re-defining the dielectric constant as,

$$\epsilon = \epsilon' - j\epsilon''.$$

ϵ' : dielectric constant

ϵ'' : dielectric loss term.

So that.

$$Y = \omega C_o \, '' + j\omega C_o \epsilon'$$

However, in parallel with the dielectric effect, a molten salt also has a pure conduction term $\left(\frac{1}{R}\right)$, which will be shown later to be invariant with frequency.

The bridge measures the total real component as a single resistance R_m.

$$\therefore \quad \frac{1}{R_m} = \frac{1}{R_c} + C_o \epsilon''$$

or,

$$\epsilon'' = \frac{1}{\omega C_o} \quad \frac{1}{R_m} - \frac{1}{R_c}$$

Theoretically, the term R_c should be the D.C. conductivity but this is not available and low frequency A.C. measurements are affected by polarisation effects. The value of R_c is therefore taken at 60 K.cycles/sec. throughout.

Since this value lies above the low frequency polarisation and on the B.601 bridge it is the nearest value to the D.C. one which can be accurately obtained, a plot $\frac{1}{f.R.}$

is given for the molten salt and for the aqueous solution. Deviations from straight line behaviour denote some form of loss effect. The straight line behaviour of the aqueous solution to much higher frequencies verifies that the loss effect is not due to spurious instrumental effects. (graphs 5.6. and 5.7.).

Values of ε' and ε'' have been computed for a number of systems. Their behaviour with frequency and temperature is displayed in plots 5.8. and 5.9. and Tables 5.10. and 5.11. The values of ε' follow a typical loss curve with considerable dispersion. The ε'' values are not sufficiently defined for the shape of the curve to be assessed.

Frequency Dependence $KNO_3/Ca(NO_3)$ System

$x_{KNO_3} = 0.62$ $T = 93\,^{\circ}C$

Graph 5.6.

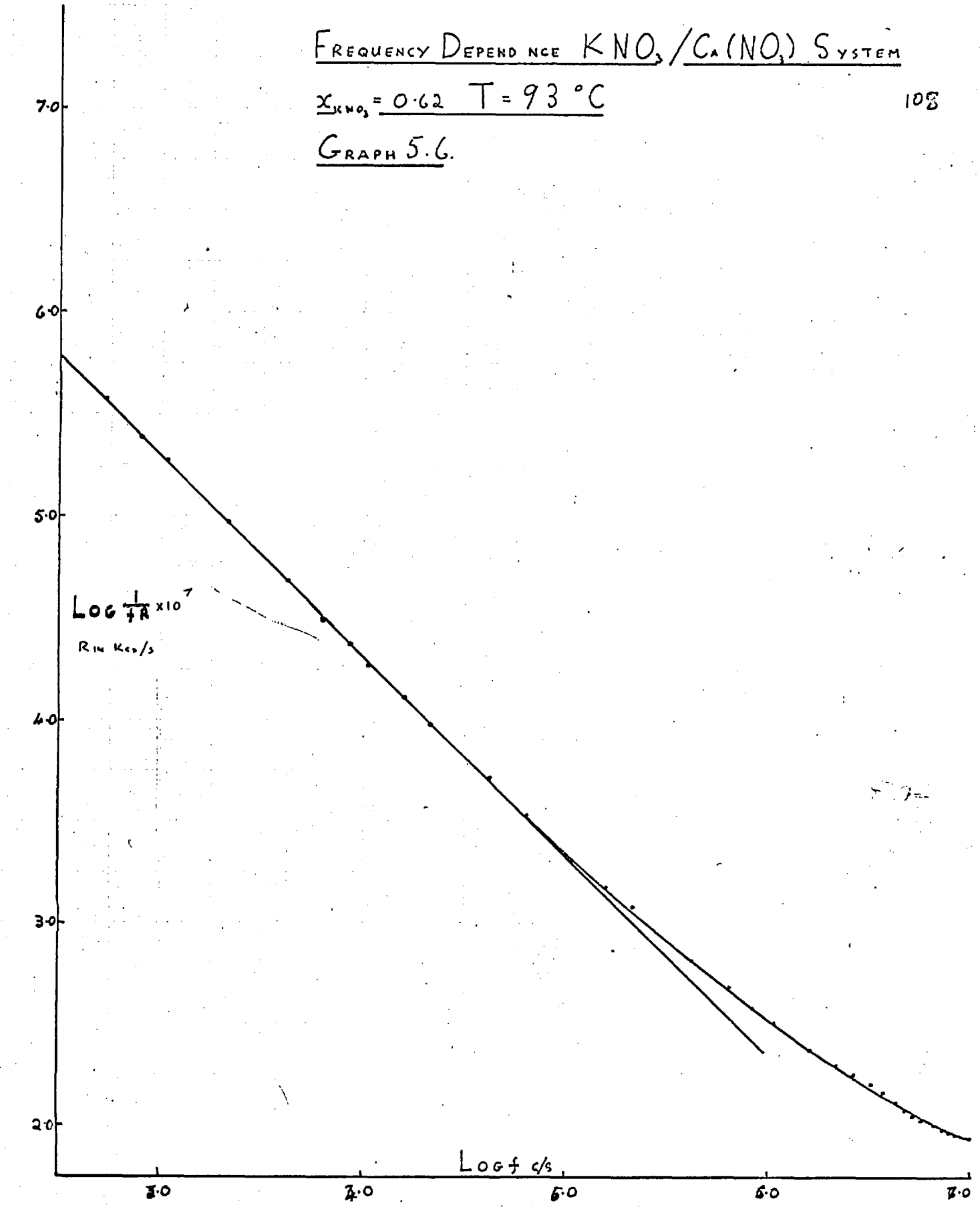

Frequency Dependance $\frac{N}{20,000}$ KCl Soln.

Graph 5.7

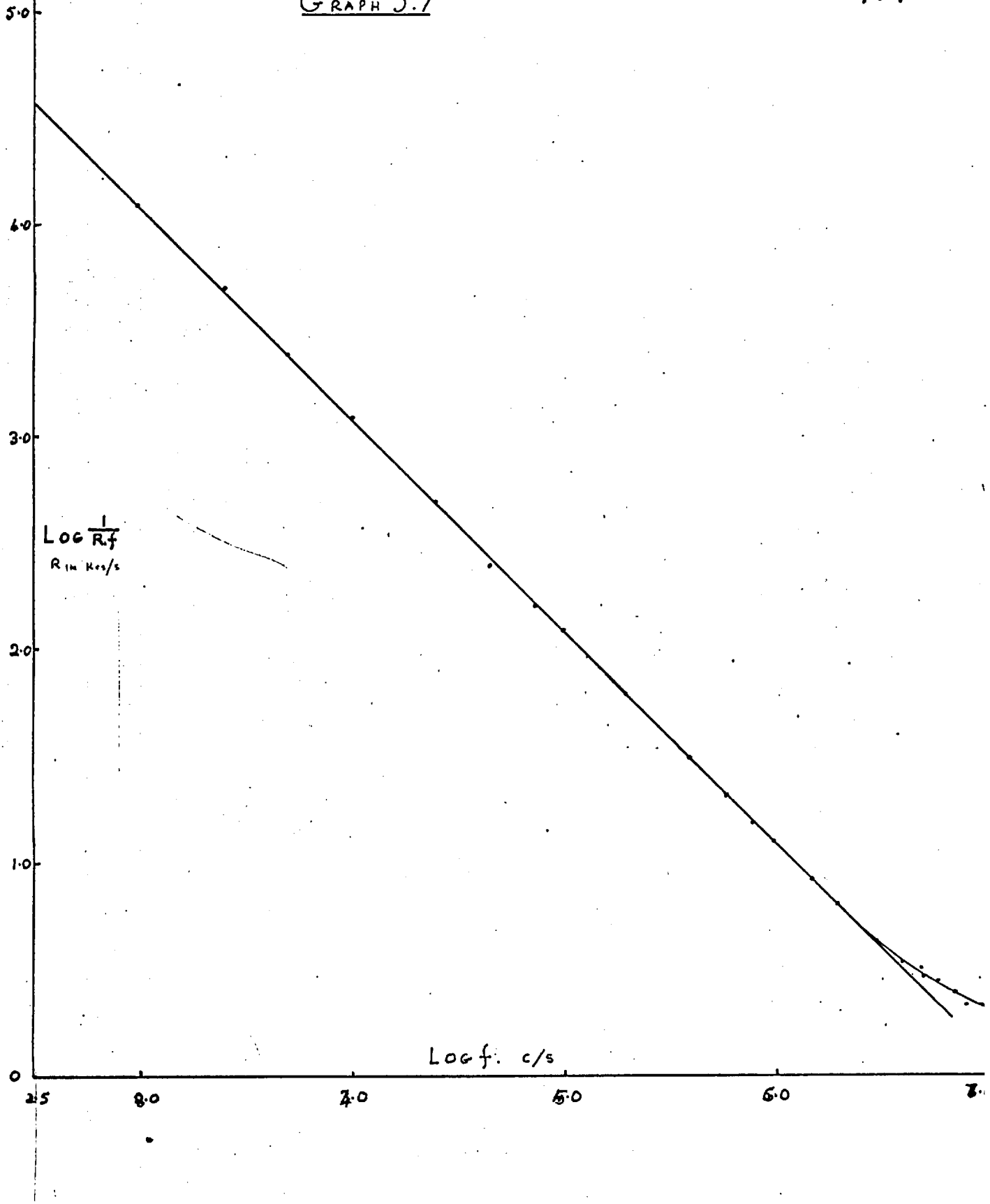

Table 5.10.

Log f	T = 84.6 °C.		T = 88.8°C.		T = 95.8°C.	
	ϵ'	ϵ''	ϵ'	ϵ''	ϵ'	ϵ''
6.892	10.0	0.77	12.0	2.01	15.0	3.98
6.767	10.0	0.99	12.3	2.31	15.7	4.31
6.597	10.4	1.28	12.8	2.70	16.9	4.47
6.470	11.3	1.53	13.8	3.04	18.4	4.84
6.297	11.9	1.68	14.8	3.24	19.8	5.00
6.000	12.4	2.23	16.3	3.92	21.5	5.65
5.903	12.7	2.45	16.6	3.71	21.8	5.92
5.845	13.0	2.54	17.2	-	22.8	5.33
5.778	13.2	3.04	17.8	3.92	23.5	5.08
5.602	14.5	2.43	19.5	4.02	25.3	2.91
5.301	16.2	2.46	21.2	3.31	26.2	
5.000	17.7	1.66	23.3	2.41	27.4	
4.903	17.8	1.25	24.8	1.19	30.0	
4.778			25.7			
4.601			26.4			
4.301			27.0			
4.000			29.2			

Table 5.11.

Temperature $^{o}C.$	ϵ'	ϵ''
81.4	10.80	1.15
84.6	11.30	1.53
86.0	12.50	2.23
88.8	13.80	3.04
93.1	15.50	4.54
94.6	17.30	-
95.8	18.30	4.84
99.4	20.20	4.38
100.6	22.9	6.9
103.0	22.8	-

FREQUENCY DEPENDENCE OF ϵ' AND ϵ''

$KNO_3 / Ca(NO_3)_2$ $x_c = 0.62$

T AS PARAMETER GRAPH 5.8

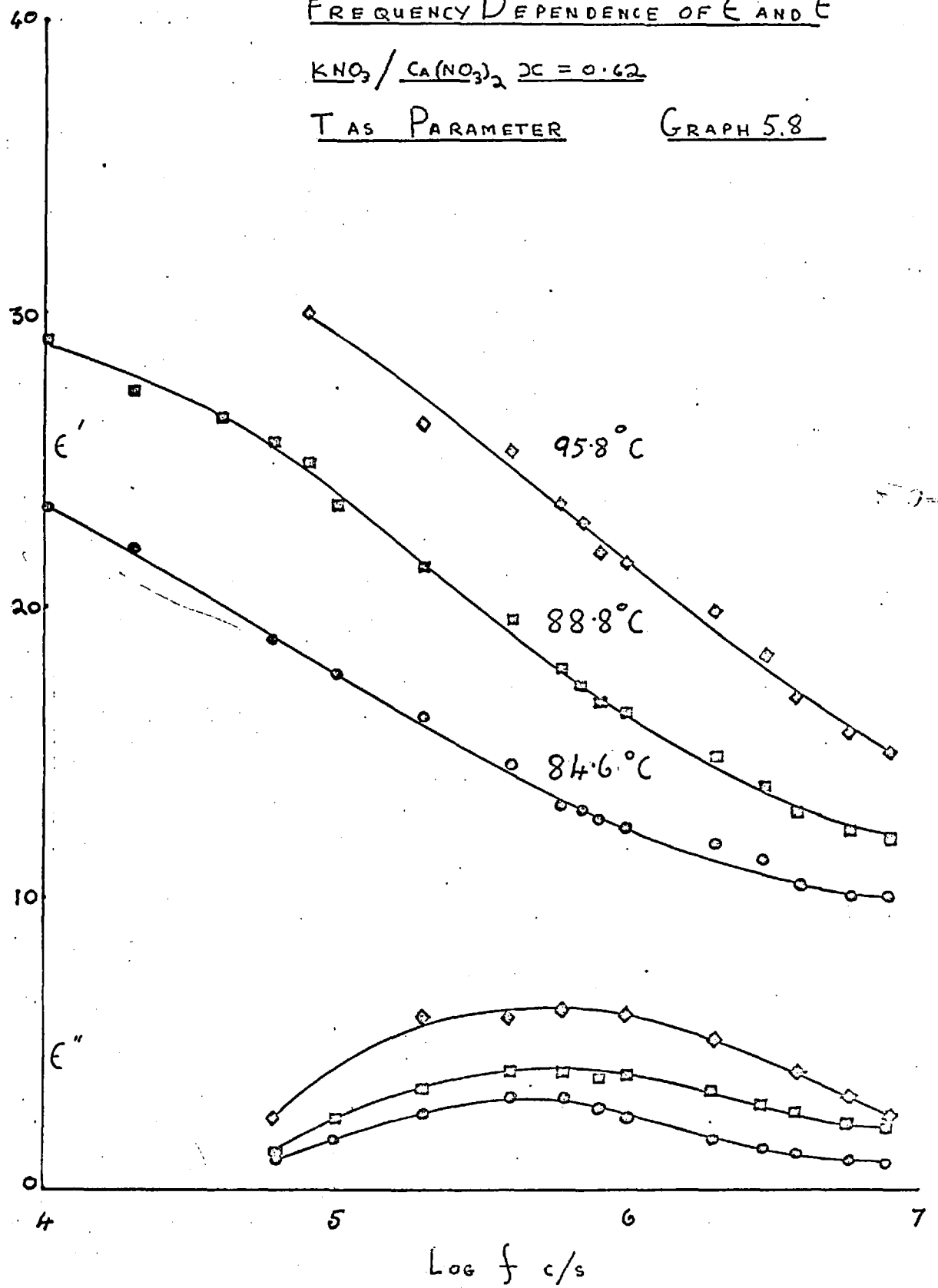

T DEPENDENCE OF ϵ' AND ϵ'' GRAPH 5.9

$KNO_3 / Ca(NO_3)_2$ $x = 0.62$

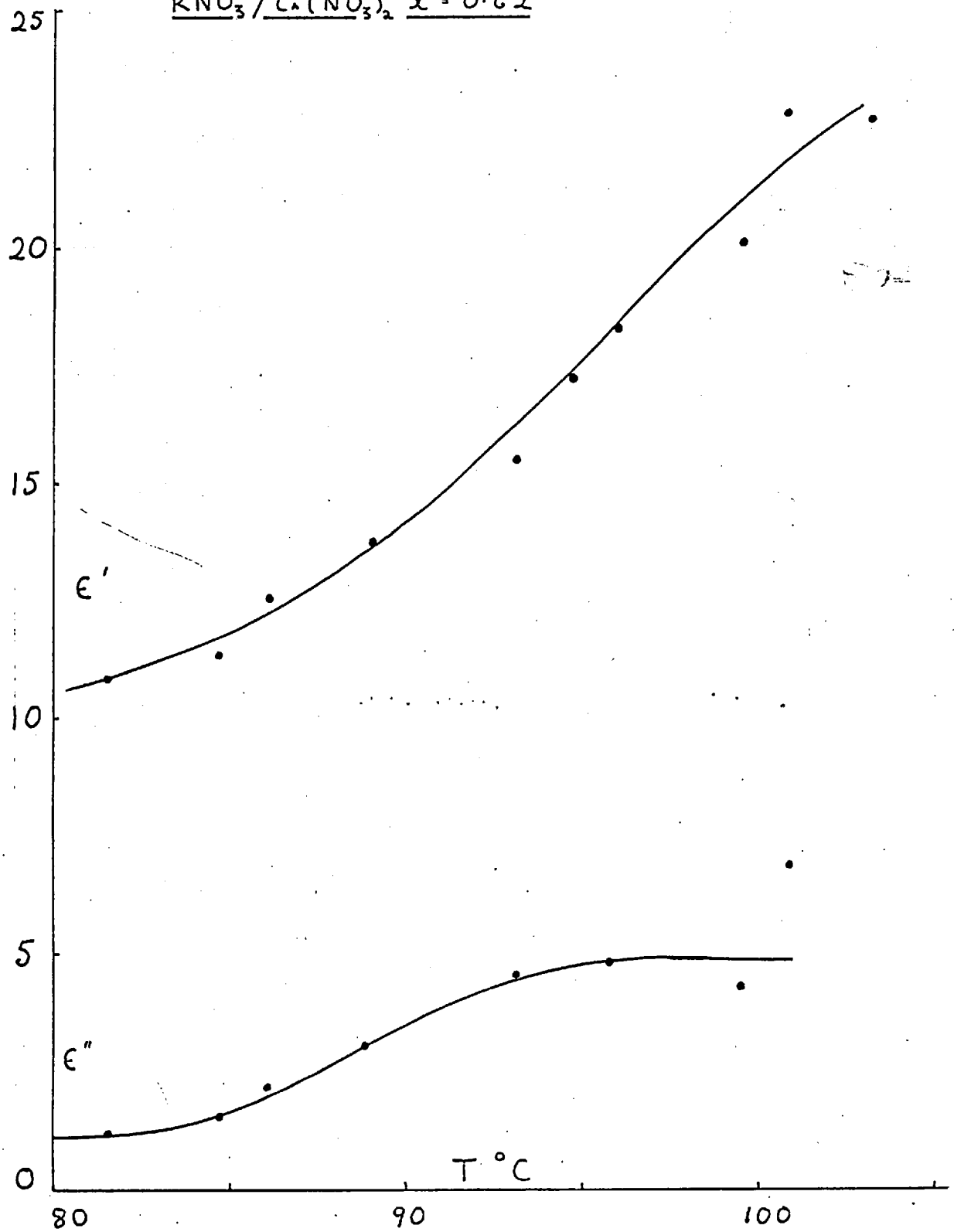

SECTION III.

In Chapter 6, the experimental behaviour is analysed in terms of simple molecular models and various semi-empirical correlations of the varied measurements made. The simple theory of dielectrics and the experimental data obtained is described in Chapter 7. Comparisons are made with more standard systems. Finally, in this chapter a model for the low temperature liquid, compatible with the conclusions of Chapter 6, and which could explain the nature of the dielectric behaviour is proposed.

Chapter 6.

Explanation of the results in terms of a simple liquid model.

In Chapter 1, general liquid state theory was discussed and the concepts underlying simple cell theories described. The high alternating coulombic charges in a molten salt further suggest that such systems are most likely to conform to these models. Temkin[1] has used a model based on two interpenetrating lattices of charge to describe, with some success, the thermodynamic properties of a wide range of molten salts. The simple volume model described in Chapter 2 is also essentially a lattice or cell structure

Essentially the disadvantage of all these theories is the fact that to calculate the macroscopic parameters, a regular infinite three-dimensional pattern of cells characteristic of an ordered state must be assumed. The X-ray studies of liquids (2.1.1.) show that it is just such long range order which does not exist. The introduction of disorder by such methods as the formation of holes represents a disordered modification of an ordered state, not an inherently disordered one.

In liquids the extremely high packing density ensures that some form of local ordering exists. The X-ray results

of potassium chloride[2] give a good example of the nature of a simple molten salt, containing only spherical ions. The average separation distance of cations and anions is 3.10 Å and the average co-ordination number suggested by the radial distribution function is 3.6. The total separation distance of the centres of the potassium and chlorine ions is, calculated from the Pauling repulsion radii for the solid state, 3.14 A. The liquid state packing is thus very close and the co-ordination number reasonably high so that a considerable degree of local ordering is ensured but there is no guarantee it is either time stable, or of the same form for each ion taken as reference. The results do not give any indication of the time stability of local packing arrangements, nor of their size, shape or relative orientation.

A simple liquid consisting of spherical ions can but be considered as a statistical distribution of local structures of differing form and co-ordination number. Part at least of the 20% excess volume of melting is then taken up by the miss-match between such local regions. A concept of this type is qualitatively in direct agreement with the X-ray results outlined in Chapter 2, which suggest some degree of ordering out to the third and fourth

co-ordination shells. On this basis certain simple properties concerned only with nearest neighbour properties, such as U.V. spectra, will be explicable on the basis of simple lattice models, assumed to be equivalent to the most common form of packing in the liquid distribution.

For nitrates, the shape of the nitrate ion is a complexing feature. The simple quasi-crystalline model examined by McAuley, Rhodes and Ubbelohde to explain the volume results has been outlined in Chapter 2. While it describes certain properties of the nitrate surprisingly well, the model is open to a number of criticisms.

1) The concept of a freely rotating nitrate ion leaves no room whatsoever for free volume of the type found in the chloride melts (2.1.4.). This suggests a form of ordering as tight or tighter than a normal crystal and is not typical of general liquid state results. Furthermore, the energy uptake required to make the nitrates freely rotating, as they are not in the solid state, would be high and yet the enthalpy of melting is low compared to the chlorides. (2.1.3.).

2) As has been described (2.1.3.) ., the Janz radius is not necessarily correct, there must be some doubt about the exact value which should be taken. If the larger

value suggested by X-ray data is used the results are badly in error compared to experiment.

3) The ionic radius of sodium and calcium are approximately the same. The theory therefore predicts that sodium ions will fit into the nitrate lattice cube centres and will give no excess volume of mixing. There should be sufficient sites to accommodate the larger number of sodium ions. Kleppa et al[3] find an excess volume of mixing for the system potassium nitrate sodium nitrate, a result corroborated (O'Leary and Minns - unpublished) using the equipment of McAuley.

The structure of molten nitrates is more complex than suggested by the simple volume model. In this discussion the nitrates are regarded as vibrating discs, thus allowing more positional freedom in the melt. The attractive forces are assumed to be predominantly coulombic in character and the repulsive forces to be due to hard sphere repulsion envelopes of the ions and vibrational and translational energy terms. Since the melts are assumed to contain distributions of local packing structures, properties relating solely to nearest neighbour effects can be analysed on a quasi-crystalline model. The essentially

predictable and normal nature of the high temperature liquid form of monodivalent nitrate mixtures is first demonstrated and then analysis of the curvature of certain properties of these systems with falling temperature made.

In Chapter 3, a qualitative analysis is described which verifies the reported conclusion of earlier workers (2.2.1.) that it is possible to supercool certain compositions of the binary potassium nitrate-calcium nitrate liquid to a glass. The more comprehensive quantitative data of Chapter 4 will now be analysed. The high temperature behaviour of the various properties is first used to establish some concept of the nature of the intermolecular forces and then the behaviour of the systems as the temperature drops considered. The theory presented in previous sections will be applied wherever it appears necessary and a final conceptual solution to the problem suggested. The methods of reasoning are not rigorous, but the lack of knowledge of even the most fundamental liquid parameters precludes a more basic approach.

The most significant feature of the high temperature liquid behaviour is the overall thermodynamically perfect behaviour of the volume-composition plots measured by McAuley (2.2.3.). There is no excess volume of mixing in any of

the systems measured at 300°C. To obtain this linearity, it is necessary to specify that the volumes will be calculated as the volume per gm. ion of nitrate and the compositions in equivalent fractions. Other parameters, such as mole fractions, do not give this behaviour.

The behaviour of the ultraviolet spectroscopy of a large range of mixtures of molten salts at 360°C. was correlated by Smith (2.1.2.) in terms of a simple charge parameter. The behaviour of the spectra of the potassium nitrate-calcium nitrate system at 360° agrees with this plot. For any one system, the charge parameter bears a constant relation to equivalent fraction, so that for the one system of mixtures a plot of the volume per gm. ion of nitrate against the Smith charge parameter is a straight line. This plot is shown for the potassium-calcium nitrate system (graph 6.1.). Thus both volume and spectra results appear dependent on the cationic potential of the melt.

Smith Potnl. Function vs Molar Volume Graph 6.1.

$KNO_3 / Ca(NO_3)_2$

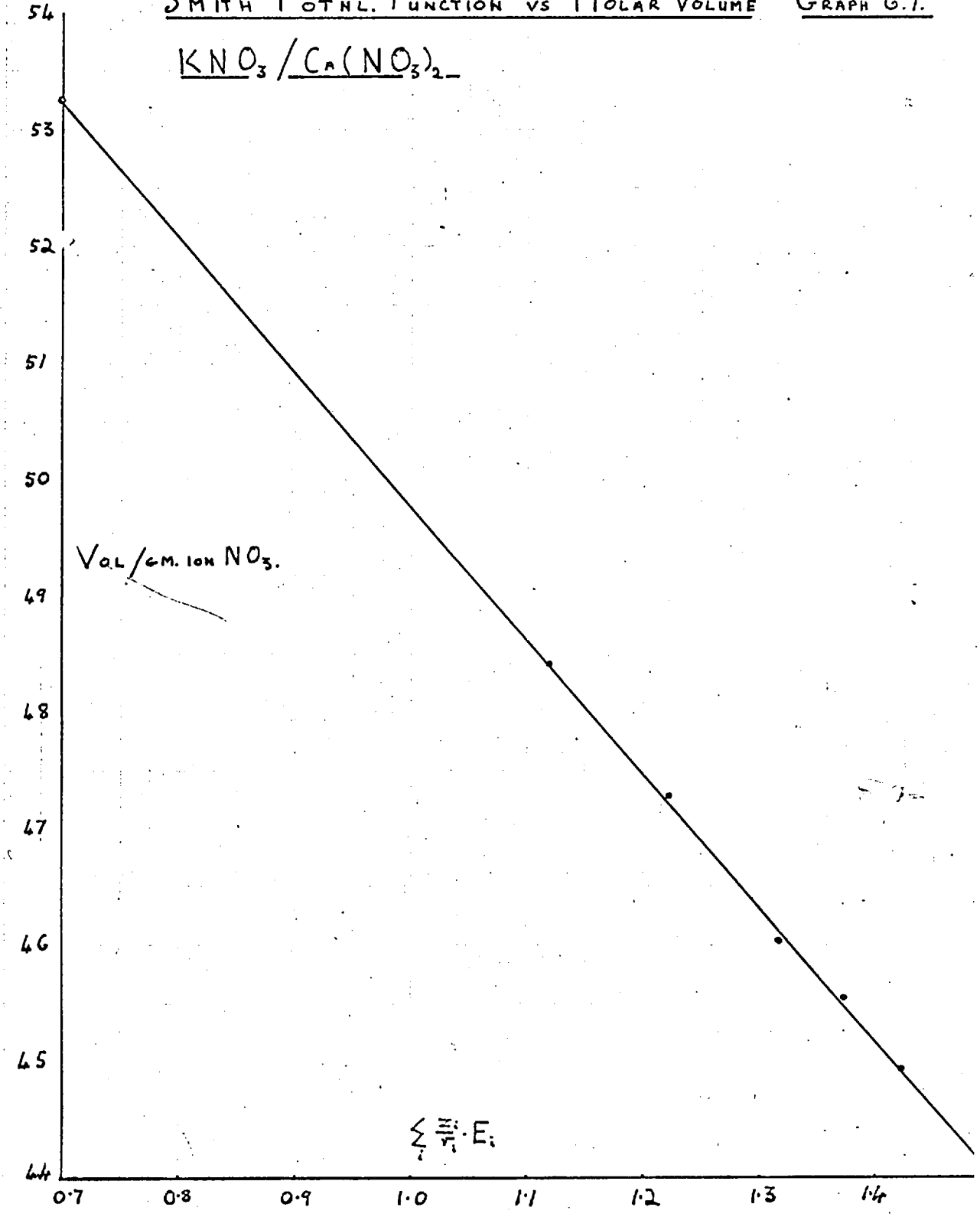

A similar correlation of the viscosity data is also possible, dependent more on the number and distribution of charges and the weights of the particles. In this case, mole fractions were used since this keeps the total number of charges considered, not the number of ions, a constant and the weight per charge added to the expression to compensate for inertial effects. The expression used is of the form,

$$\sum_i \frac{z_i x_i m_i}{r_i}$$

z_i is the charge per ion, x_i the cation mole fraction, m_i the weight per charge and r_i the Pauling radius of the species i. Linear dependence of this parameter when plotted against the viscosity Arhenius activation energies has been found (graph 6.2.) for all systems measured at 352°C.

Thus, one of the main features of high temperature behaviour is the apparent over-riding importance of coulombic effects. In order that the volume behaviour be directly related to charge, both the attractive and repulsive forces must contain some terms related to charge. Such terms must be due either to kinetic or steric considerations. These arguments are developed more specifically later.

Cation. Potnl Function vs E_η Graph 6.2

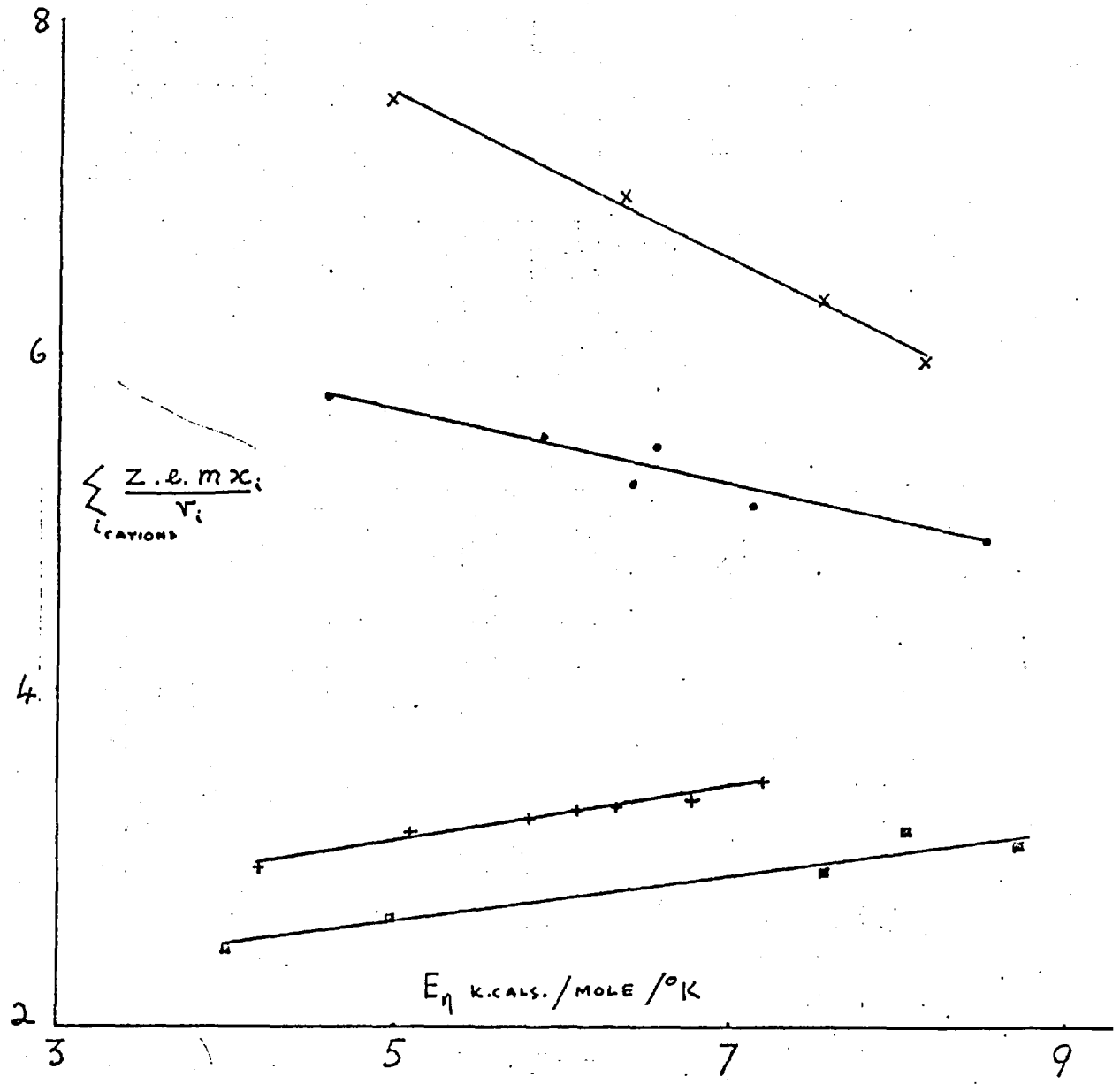

As the temperature decreases, plots of coulombic parameters become of little use since the range of compositions in which the salt mixtures remain liquid becomes very limited. An Arrhenius plot (graph 6.3.) is shown of the temperature behaviour of the viscosities of one composition of all four systems measured. Both the viscosity and the degree of curvature of the high temperature region are very similar in each case. Two of the systems, sodium and caesium, freeze, the other two show a continuation of a similar curvature trend to that observed by all four at the higher temperatures.

In the high temperature region, the amount of curvature is sufficiently slight to allow it to be approximated by a straight line on the Arrhenius plot. The best straight line for this region was computed and extrapolated into the anomalous region. From this and the actual values of viscosity, a series of excess functions at selected temperatures for the system potassium-nitrate calcium nitrate were calculated. A graph of these is shown against composition (graph 6.4.). The essential straight line behaviour of the plot insofar as it can be ascertained further demonstrates the dependence of the anomalous mixtures on the same trends as affect the remaining melts.

Log Viscosity vs $\frac{1}{T}$. $x = 0.60$ Graph 6.3

Systems Na, K, Rb and $CsNO_3$ with $Ca(NO_3)_2$

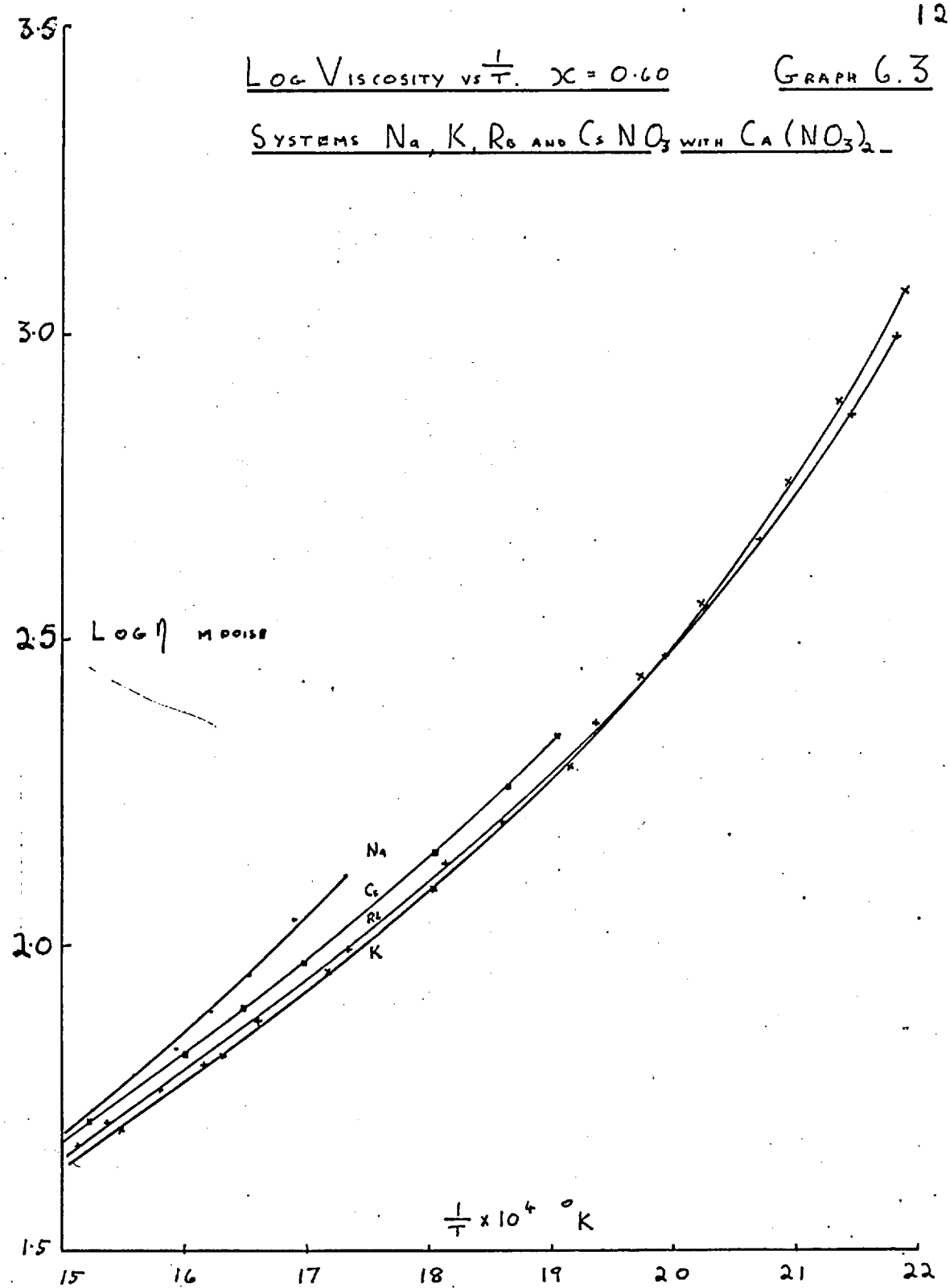

Excess Viscosity vs Composition. Graph 6.4

$KNO_3 / Ca(NO_3)_2$

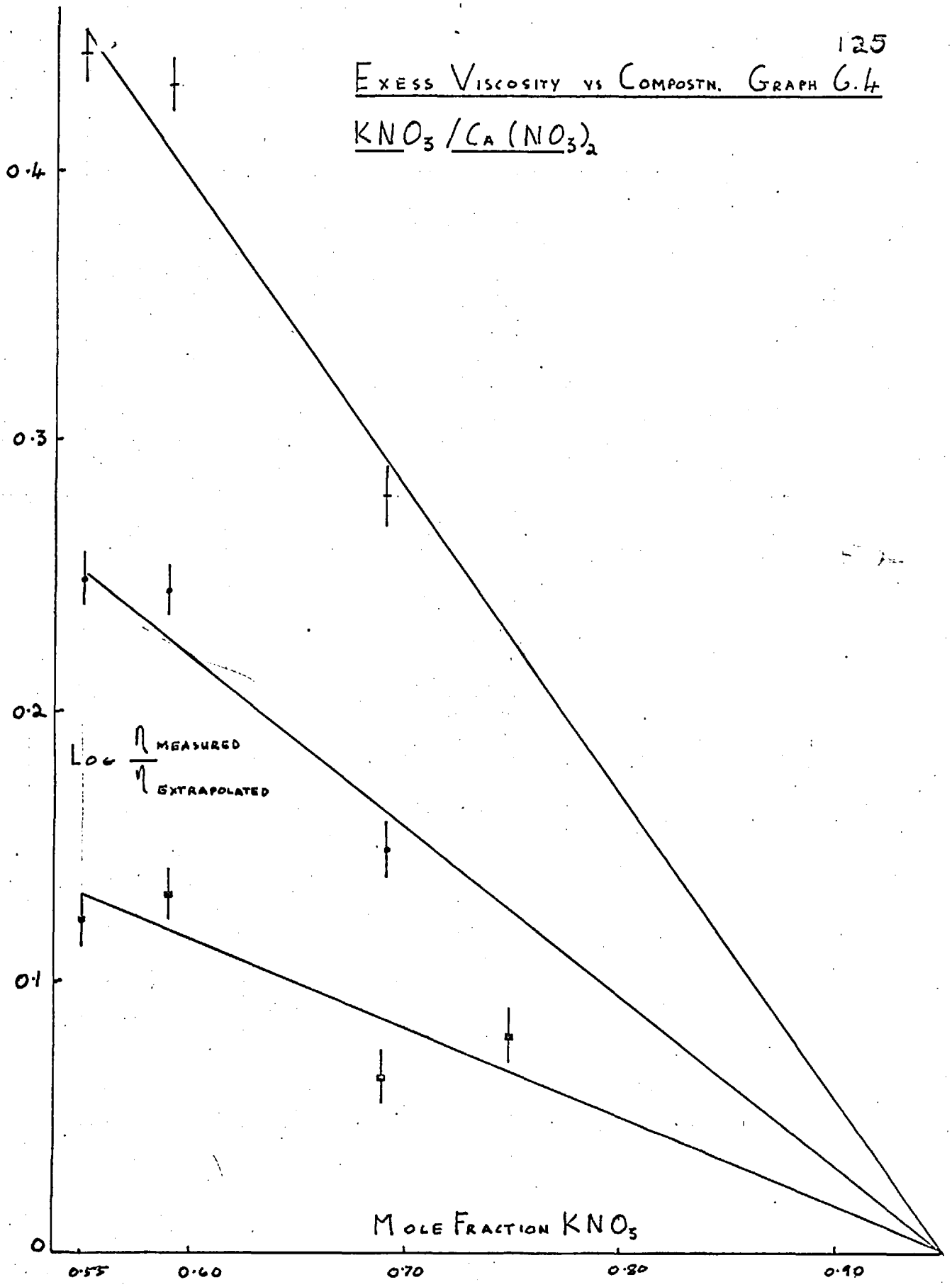

To ascertain the degree of departure from ideal Arrhenius behaviour which might be anticipated in monovalent nitrate melts over the range of temperatures used, a ternary system of sodium, potassium and rubidium nitrate was measured (graph 4.9.). While the deviation from ideal behaviour is quite marked, it is not as great as in the monodivalent melts, but neither is the initial temperature dependence.

At high temperatures, therefore, the degree of curvature in the binary mixtures, though marked is not in itself specifically abnormal, nor is there any evidence of differing behaviour in the glass forming systems.

The most fully investigated system with regard to temperature is the potassium nitrate-calcium nitrate mixture containing a mole fraction of potassium nitrate of 0.64. The viscosity, conductivity, and U.V. spectra have all been investigated to a temperature of 160°C. or below and the volume behaviour was measured by McAuley to this temperature. McAuley found that the volume was a linear function of temperature over the entire range. The dependence on temperature of the other properties is markedly non-linear.

A most interesting feature of the results is the comparison between the linear behaviour of the volume plot and the curved U.V. spectra results (graph 4.16.). A similar spectra run on the entirely monovalent system potassium nitrate-sodium nitrate over the same temperature range was completely linear.

The difference between the two parameters is that while volume takes account of long range packing effects in the melt, the spectroscopic results are normally regarded as average nearest neighbour effects over the entire melt. Regions of miss-match between local packing structures will thus affect spectra far less than volume results.

In order to explain the apparent over-riding importance of charge at high temperatures and this difference between spectra and volume, a simple model is proposed which leads to a possible correlation between spectra and viscosity.

The melt is known to be approximately charge ordered (2.1.1.) and consequently at the surface, each ion will be surrounded by charges of unlike nature on three sides but not towards the vapour. These charges will therefore constrict the melt and tend to produce the minimum steric

volume possible. In the volume model, the nitrate minimum volume was assumed to be a close packed structure and a suitable two-dimensional representation of this is given in diagram 6.5. This structure does not represent the position of minimum charge in a monodivalent melt. Thus, charge considerations in the bulk phase will tend to produce structures in the melt, which lie closer to the minimum coulombic potential position and which are likely to produce less dense packing arrangements. On such considerations, charge effects control both the effective repulsive and attractive forces in the melt, so that the overall dependence of high temperature behaviour on charge is explained.

Simple Lattice Model Diag. 6.5

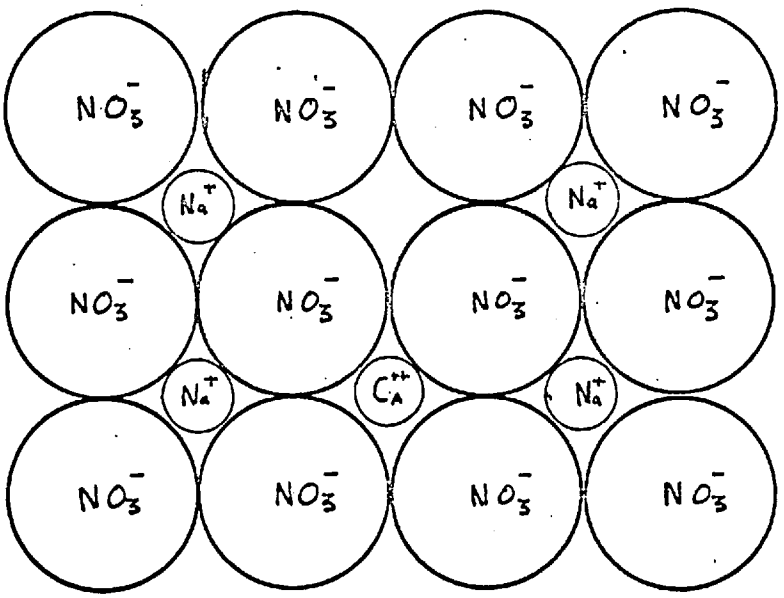

Approx. Min. Volume Position

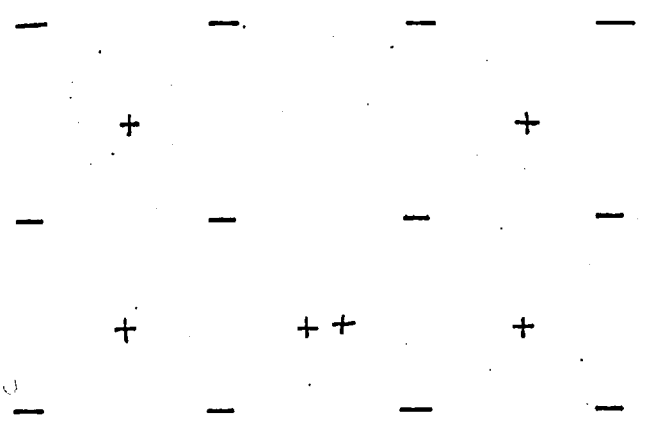

Corresp. Charge Position (Not Min.).

The curved nature of the U.V. spectra temperature dependence can also be explained by similar arguments. Three main considerations affect repulsive forces,

(1) steric terms due to the shape and size of the ions

(2) kinetic energy terms

(3) charge terms which affect the geometry.

The attractive forces are presumably coulombic, both due to charge interactions at the surface and in the bulk of the material.

As the temperature is reduced, the coulombic terms are not affected, but the kinetic energy term falls commensurately. This will alter the balance between repulsive and attractive forces and so change the geometry of the local packings. Since only the kinetic energy changes, the change in volume would be expected to be linear.

U.V. spectra, on the other hand, is well known to be very sensitive to geometrical changes and is used to investigate solid state transitions[4]. Since it is also presumed to be a nearest neighbour effect, compensating terms such as greater miss-match between packing arrangements will not be effective. The plot therefore curves.

Such arguments lead also to a correlation between viscosity and spectra. The degree of curvature of the spectroscopy plot on the above analysis should be indicative of the increase in local ordering of the structure. The Smith expression reduces for one set of mixtures to an expression of the form,

$$E_{max} = K\ Eq. + L.$$

Eq is the equivalent fraction of one species.

The term K contains the expression relating the radii of the cations and their charges to E_{max}. So that, at a different temperature when a different local order is established, it will be the term K.Eq which will be affected. By extrapolating the linear high temperature behaviour into the low temperature region, the anomalous change in the term K.Eq was calculated (K') as a ratio of the ideal and experimental values.

If absolute reaction rate theory is used for viscosity, an entropy term directly related to ordering effects is available.

$$\eta = \text{const.}\ e^{\frac{\Delta S}{R}}\ e^{\frac{E}{RT}}$$

E, the activation energy is assumed to be constant, so that ΔS may be evaluated. It is assumed to indicate the degree

Spectra Viscosity Relation Graph 6.6.

KNO_3 / $Ca(NO_3)_2$

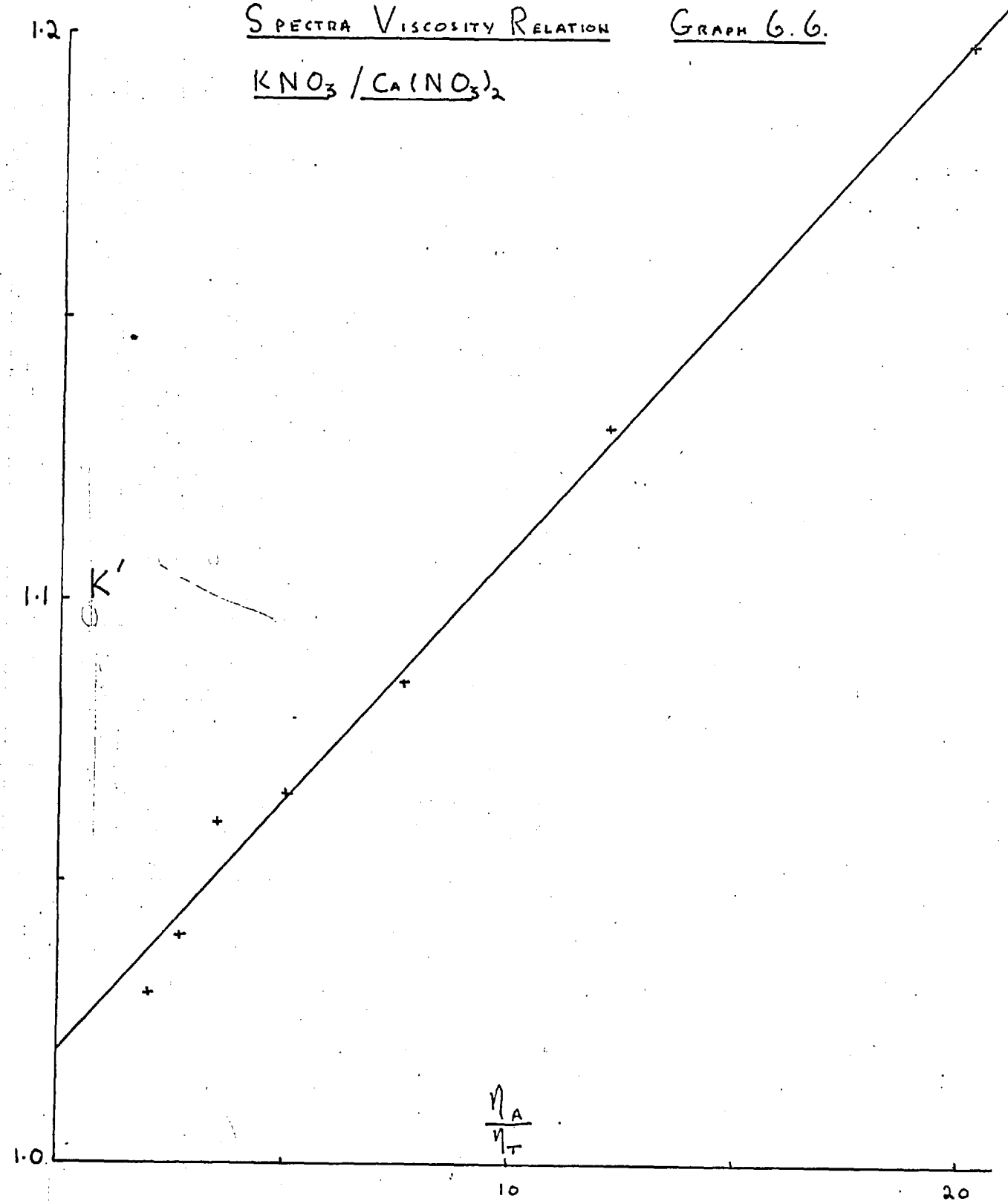

of order possible in the system.

If no ordering takes place as the temperature falls,

$$\log \eta_{Theoretical} = \frac{\Delta S_1}{R} + \frac{E}{RT} + \text{const.}$$

and if it does,

$$\log \eta_{Actual} = \frac{\Delta S_2}{R} + \frac{E}{RT} + \text{const.}$$

$$\therefore \log \frac{\eta_{Actual}}{\eta_{Theoretical}} = \frac{\Delta S_2 - \Delta S_1}{R}$$

By extrapolating the high temperature approximately linear part of the viscosity plot into the low temperature region, values of $\frac{\eta_A}{\eta_T}$ could be calculated. When this term was plotted against K' it was found to be linear (graph 6.6.) or,

$$K' = \text{const } e^{\frac{\Delta S_2 - \Delta S_1}{R}}$$

The term K' is related to changing local order in the melts, that is it is effectively a measure of the change in the statistical distribution of local structures in the melt. The form of the expression is the same as the standard result of statistical mechanics,

$$S = k \ln W$$

where W is the number of possible configurations permitted to a given system.

The concept of the nitrate melt as consisting of a statistical distribution of local structures with the nature of the distribution ordered by charge parameters seems to give a good explanation of the equilibrium behaviour and of the high temperature transport behaviour. In order to discover why some systems form a disordered solid or "glassy" state while others crystallize, a more detailed analysis of the transport data is required.

There is no completely successful structural theory for transport; the outline of various viscosity theories given in Chapter 1 is good evidence of this. Essentially, any molecular theory of transport attempts to link some type of microscopic friction coefficient with the macroscopic properties, but so little is known about the number and nature of moving species in the melt, that no well defined structural model can be achieved.

The Eyring absolute reaction rate theory is used as a basis here. While the elementary model from which it was derived is too simple, provided the number of each transporting species and its nature does not change, similar arguments could be used for far more complex transport mechanisms without altering the nature of the equations. The theory also introduces an order dependent

term in a fundamental manner.

Results of measurements on both the conductivity and viscosity of the potassium nitrate calcium nitrate melt are given in Chapter 4, in the form of Arhenius plots. To express the relationship between the two more directly, the conductivity results were converted using the volume data to equivalent conductivities and both viscosity and conductivity plotted on a large scale. In any local region of temperature, the plots may be regarded as approximately linear and E_η and E_Λ values calculated. This was carried out by taking tangents at various temperatures by a graphical construction. The results are shown in Table 6.7.

Temp. °C. / Comp. Mole % KNO_3	352	315	283	253	227	203	181	
	6.03	6.20	6.93	8.22	9.67	11.76	15.38	
	5.80	5.80	5.95	7.13	8.81	10.49	12.39	$E\eta$
0.67	5.80	5.80	5.95	7.13	8.81	10.49	12.39	$E\wedge$
	1.04	1.07	1.17	1.15	1.10	1.12	1.24	$E\eta / E\wedge$
	6.26	6.70	7.25	8.91	10.71	12.64	17.25	$E\eta$
0.64	5.84	5.87	6.52	7.78	9.15	12.47	17.43	$E\wedge$
	1.07	1.14	1.11	1.15	1.17	1.01	0.99	$E\eta / E\wedge$
	6.77	6.98	7.72	9.14	11.38	14.03	17.71	$E\eta$
0.60	6.41	6.37	6.80	8.09	10.11	12.55	17.24	$E\wedge$
	1.06	1.10	1.12	1.11	1.13	1.12	1.03	$E\eta / E\wedge$

Table 6.7. ACTIVATION ENERGIES $KNO_3/Ca(NO_3)_2$ SYSTEM.

The ratio of E_η to E_Λ is approximately unity over the entire range of temperature. A possible reason for the slight discrepancies is given later, but that such unity is unusual for molten salts is shown in Table 2.3.

Two main viscosity theories are possible;

1) That groups of ions form into "clusters" or non-crystalline packings in the melt and move through it as single species, thus causing an enhancement of viscosity in a manner analagous to colloidal suspensions[5]. Such theories inevitably assume some form of segregation between various regions of the melt, but the clusters need not be time stable, provided that they have a finite existence appreciably longer than the time for a single viscous relaxation.

2) On a more uniform theory, viscous shear may require that each ionic link in the melt is overcome. Thus, whereas the liquid may consist of a complete distribution of statistical local packings, all of those packings must be sheared or distorted for movement to occur.

While it is difficult to distinguish between the two types of theory, especially since neither is well defined, the ratio of the activation energies for the system

suggests that whichever mechanism is preferred for viscosity, a similar one must be applicable to conductivity. Since conductivity is generally assumed to be carried by single ion charge carriers, a uniform theory in which restriction to motion is applied over the entire melt would seem more likely.

If the Nernst-Einstein relation held for salt systems, then the argument would be strengthened greatly by diffusion data. Unfortunately, this relationship has been widely studied for molten salts and does not hold exactly[6, 7, 8]. C.A. Angell[9] recently measured diffusion coefficients in the potassium nitrate-calcium nitrate system and postulated that the deviations from ideality observed were more indicative of mutual ion interference than paired vacancy diffusion mechanisms.

A single mechanism capable of explaining the transport behaviour will be postulated as a result of the relaxation data in Chapter 7.

A series of experiments on the 0.64 mole percent potassium nitrate-calcium nitrate mixture to which small additions of chlorides and bromides of sodium and potassium were made in such a way as to replace a single potassium

nitrate molecule in the solvent melt (graphs4.12, 13) The results do not show very marked changes so that their interpretation is limited. The effect of equal additions of sodium and potassium chloride produces a similar slight rise in viscosity. The effect of sodium chloride raises the conductivity markedly in the high temperature condition but this enhancement is partly frozen out at low temperatures. The potassium chloride does not appreciably affect the conductivity. The volumes of the melts are not known so that equivalent conductivities cannot be obtained, but it would appear that at low temperatures, the more labile sodium ions become constricted. This suggests that at low temperatures, there is little motion of one ionic species relative to another and hence that some single mechanism controls the transport in this region.

Urnes (2.2.1.) has measured the conductivity of one binary mixture between 160°C. and 120°C., i.e. at lower temperatures and discovered that the slope of the curves for viscosity and conductivity do tend to unity, verifying the results obtained here.

The slight rise in the ratio of E_η to E_Λ at

intermediate temperatures is difficult to explain but, presumably when the coulombic asymmetric forces first begin to affect the melt structure, the larger particles are restricted first. Thus the lighter cations become relatively more labile and decrease the slope of the conductivity plot. At sufficiently low temperatures these particles are more tightly held and the conductivity plot assumes the same slope as viscosity.

Thus, the anomalous glass-forming mixtures are considered as normal molten nitrates. They contain a very high, locally asymmetric coulombic field due to the cations which are set in a disordered assembly of vibrating nitrate discs, comprising the bulk of the melt volume. The volume of the melt is very low and there will consequently be considerable interaction between the nitrates. The average structural geometry of local groupings in the melt will alter as the temperature is lowered.

The transport data suggests, although the argument is not rigorous, that particularly at low temperatures the movement of one ion species relative to another in the melt is restricted. Hence, the internal mobility and the consequent facility for forming crystal nucleii will be reduced.

The probable reason for this is a combination of steric and charge effects due to the size and shape of the constituent ions and the high coulombic charge. Thus supercooling and eventual glass formation will be more favourable in these systems.

Chapter 7.

Discussion of the Dielectric Results.

The problem of measuring dielectric loss effects in good conductors is made extremely difficult by the relative magnitude of the pure conductance term. A.C. bridges measure resistance and capacitance in terms of a complex impedance and, in order to differentiate between the reactive and resistive components of impedance, the two terms must be of similar size, i.e. the phase angle must be between about 20^{o} and 80^{o}. In molten salts the phase angle is normally lower, and so the minor reactive term cannot be discriminated.

The salts used here differ. In Chapter 6 the anomalous nature of certain potassium-calcium nitrate melts was assessed and it was suggested that they remained liquid at low temperatures due to a combination of steric and charge effects. The systems in the low temperature state have sufficiently low conductivities (about 1.0×10^{-4} mho's cm^{-1}) to allow moderately accurate measurement of the reactive component. This anomalous mixture represents, therefore, one of the few cases in which a liquid consisting purely of simple charged particles can be analysed using dielectric techniques.

Since this phenomena has not been observed before in molten salts, consideration was paid in Chapter 5 to the elimination of possible spurious effects in the electrical system. The analysis that follows is a first attempt to relate the results to basic molecular theory. The model finally proposed may not be a unique solution but it appears to be compatible with the conclusions of the previous chapter and to explain effectively the dielectric effects.

7.1. The Standard Interpretation of Polarisation phenomena in terms of Molecular Structure[10].

In a simple parallel plate condenser in vacuo, the amount of electric charge it can retain depends on the geometry of the plates (free charge). If a material is then introduced, the amount of charge or capacity increases by a quantity dependent on the nature of the material. This effect is due to charged species in the material which align in the electric field and effectively bind extra charges to the plate surfaces(bound charges). Since this effect depends on the nature and number of the charged species, it is a property of the material. Expressed in vector terms,

$$\chi = \frac{P}{\epsilon_o E} = \frac{\text{bound charge density}}{\text{free charge density}}$$

P is called the polarisation, E is the field strength and χ the electric susceptibility.

In an electrically neutral material the only charges which can contribute are dipoles or higher terms. P may also be regarded as the dipole moment/unit volume. It is this term which is normally related to structure. The standard mechanisms used to explain polarisation in a material are,

(1) electronic polarisation

(2) atomic polarisation

(3) orientation polarisation

(4) space charge polarisation.

Electronic contributions are due to a drift of the electrons of an atom in the applied field causing a distortion of the electron cloud round the central nucleus which produces a nett dipole. Atomic polarisation is caused by a displacement of one atom relative to another in a molecule causing a change in the dipolar effect between them. Orientational effects are due to the tendency of molecules containing permanent dipole moments to align in the direction of the field. Space charge polarisation is caused by free charge carriers accumulating

either at an interface or in the bulk of the material, causing a distortion of the charge density.

The most informative method of distinguishing between these mechanisms is to consider the frequency region in which they may cause anomalous behaviour. The present discussion concerns a loss mechanism at low frequency so that mechanisms one and two can probably be eliminated. They would not be expected to give such low frequency loss effects.

A "loss" effect[10,11] is some mechanism causing anomalous absorption of energy in the material. When pure conduction occurs in a dielectric, the conducting species produce heat according to the simple Ohms law relation. If the time in which field reversal occurs is long compared with the acceleration time of the particles, i.e. the time required for the species to reach their equilibrium drift velocities, the Ohms law relation holds and the effect of conduction will be invariant with frequency. Rotating or vibrating species in the material attempt to align with an alternating field and the energy absorption caused in overcoming the internal friction coefficient depends on the characteristic frequency of

the species and the frequency of the applied field. The effect will be a maximum when these two frequencies are equal. The standard mathematical development of these terms is given by Murphy and Morgan[12].

The form of the ϵ' and ϵ'' curves against frequency are well understood for systems which can be described in terms of a single rotating or vibrating species. In diagram 7.1. these results are given for a typical system, methyl alcohol[13]. Many actual systems show much more gradual relaxation curves (e.g. Transformer oil[14]) and this is normally assumed to be due to a spread of relaxation times. Cole and Cole[14] predicted that, for a single relaxation process, a plot of ϵ' against ϵ'' would be a semi-circle with its centre on the X-axis. While this holds for systems such as methyl alcohol, for less standard systems such as transformer oil, the curve becomes an arc of a circle with its centre below the axis due to dispersion. Ideally the semi-circles of the Cole-Cole plot should move along the axis away from the origin as the temperature rises without increasing the radius of the semi-circle. The results of the plot for the molten salt at three temperatures is given (graph 7.2.) and is anomalous.

Frequency Dependence

Graph 7.1.

Methyl Alcohol Results

T = 20 °C

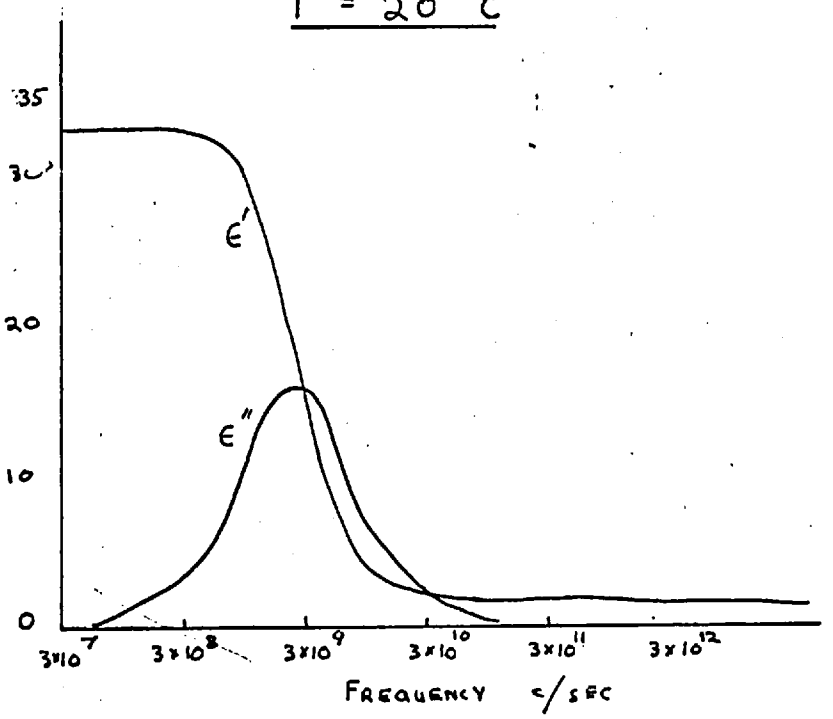

Cole Cole Plot

Transformer Oil

T = 0 °C

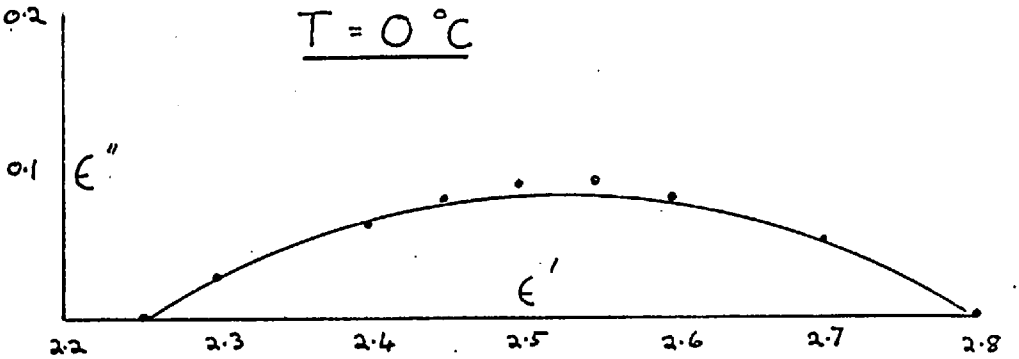

Cole Cole Plot for Molten $KNO_3/Ca(NO_3)_2$

T. as Parameter

Graph 7.

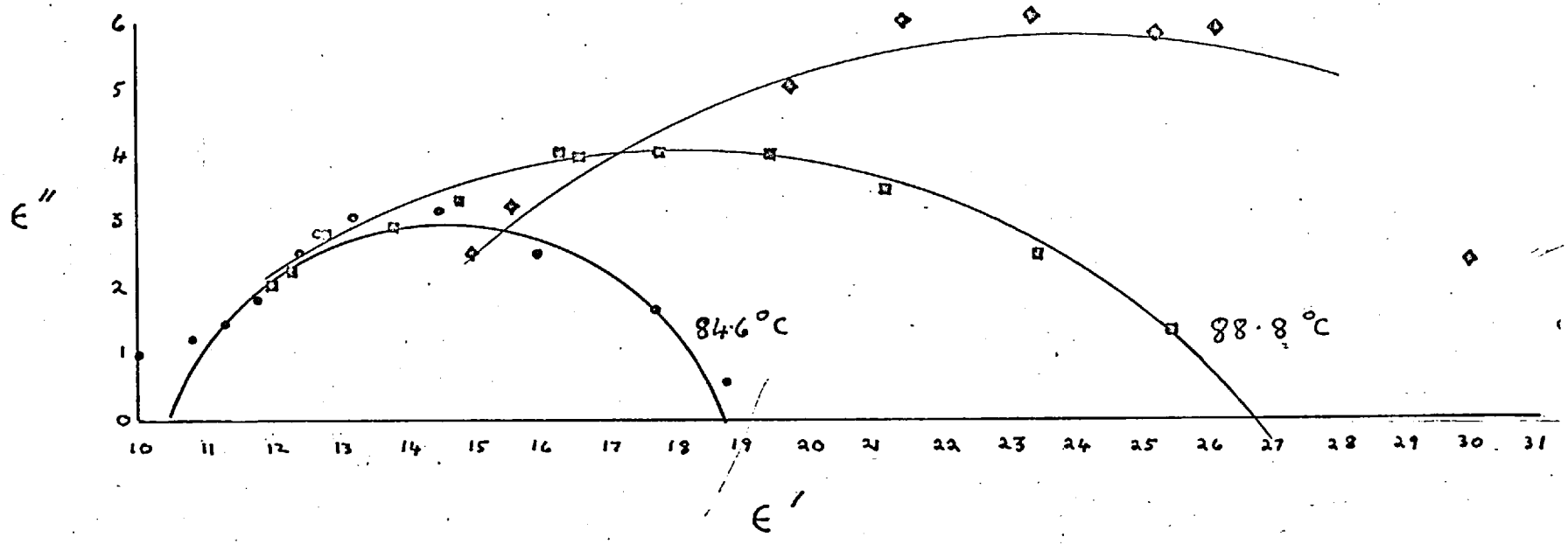

Space charge polarisation effects all ionic conductors to some extent. Results of the conductivity studies below 2 K.cycles/sec. tended to be high and not very reproducible, so that quantitative studies in the low frequency region were abandoned. This effect is due to the build up of charges at the plate to melt interface and is common in conductivity measurements of molten salts.

7.2. The Experimental Behaviour.

The temperatures at which relaxation phenomena are observed lie well below the lowest values measured for viscosity in the present study. From the results of Urnes, (2.2.1.) the viscosity is given as about 2×10^2 poise in this region. Such a figure is well below the normal glass point at 10^{13} poise claimed by Dietzel and Poegel as 56°C. (2.2.1.). There is no evidence of glass formation at these temperatures and the system is considered as a liquid.

An analysis of the temperature dependence is complex and, since the low temperature results are both better defined and approximate more closely to ideal behaviour, an analysis of these results is given first.

At low temperatures, the Cole-Cole plot (graph 7.2.) is a circular arc but not a semi-circle, indicating that a single relaxation mechanism is present in the melt at these frequencies and that there is some spread of relaxation times. The mean value of the spread corresponds to a time of about 4×10^{-7} secs. which is extremely slow.

A relaxation time of the same order is given by glycerol at about -22°C.[15], at which temperature the viscosity is about 2.2×10^{3} poise[16]. For the molten salt, the viscosity estimated from the results of Dietzel and Poegel (2.2.1.) is about 2×10^{2} poise. The relaxation phenomena is therefore of a similar magnitude to that in the heavily hydrogen bonded liquid.

Due to space charge polarisation effects, the static dielectric constant cannot be measured exactly but it may be estimated from the Cole-Cole plot, as between 18 and 20, the value rapidly rising with increasing temperature. This low frequency constant compared with the results for benzene 2.35, methyl alcohol 33, glycerol 55 and water 80, lies at an intermediate value. The static dielectric constants of methyl alcohol, glycerol and water are very high, normal liquids have values between about 2 and 6.

Thus, at the low temperature, the dielectric phenomena are characteristics of a single Debye relaxation process in a very viscous liquid. The magnitude of the dielectric term is rather similar to but more diffuse in form than for methyl alcohol.

As the temperature rises, the dielectric effects become more diffuse and more difficult to define. As is shown in the Cole-Cole plot, the maximum value of ϵ'' increases as the temperature rises causing an increase in the area under the curve.

Part of this rise could be due to an assumption used in the derivation of ϵ''. The D.C. conductivity was not known and the value of A.C. conductivity at 60 K.cycles/sec. was used as the best approximation. As the conductivity rises, the difference between the two resistance terms in the expression derived in 5.2.2., becomes very small and possible errors in the value of the D.C. conductivity more important. It seems unlikely that this effect alone could account for the anomalous rise. A structural explanation can be postulated to explain the behaviour.

Since dielectric effects of this nature have not previously been measured in molten salts, there is no directly comparable evidence to aid in interpreting the results. A qualitative explanation which is by no means unique but appears to be compatible with the previous chapter will be outlined.

The lowest temperature of measurement is well within the liquid range with a viscosity of about 2×10^2 poise. The relaxation time in the liquid, 4×10^{-7} secs., is extremely slow. Loss effects in this frequency range are unlikely to be explicable in terms of simple orientation effects of single molecules, since even in inorganic glasses, the cations are assumed to have equilibrium vibration times of about 10^{-12} secs. A more likely explanation would be in terms of the relaxation of groups of ions in the melt.

Since only a single Cole-Cole arc is obtained, only one relaxation time is present in the melt, not the complete spectrum which would be expected from the diverse nature of the contributing species. This also suggests that the relaxation is due to multimolecular groupings in the melt.

In Chapter 6, it was suggested that a liquid could be considered as a distribution of molecular scale close packed assemblies of differing geometry which may not be time stable. As the temperature is reduced, the internal energy of the melt falls and the range of possible structures in the distribution will gradually be reduced until the lowest energy forms of packing predominate.

In normal liquids, when the energy is sufficiently low, crystallization takes place, but presumably in these liquids the high locally asymmetric coulombic charge produces a more dense form of packing which is incapable of long range three-dimensional order.

That the behaviour of the U.V. spectra data with falling temperature is explicable on the basis of a gradual, charge determined increase in local ordering has already been demonstrated. Janz[17] in explaining the splitting of the Raman Spectra 10°C. above the melting point in monodivalent melts postulates that the cations reside at preferred positions on the nitrate anion thus introducing a concept of local order from a different but compatible standpoint.

The segregation of the melt into local packing arrangements joined by regions of miss-match leads to a fluctuation in the potential energy of local regions between the clustered regions and the regions of miss-match. To minimise this, the packings presumably form and dissipate with a time characteristic of the liquid at that temperature. Since the packings do not have three-dimensional order, the orientation of the anions alter with the same periodicity as for the packing formation.

If an alternating field is applied to the melt the local asymmetric cation potential will distort in response to the field causing a re-orientation of the nitrates. When the periodicity of the field and the formation time of the clusters are the same, relaxation will occur.

These concepts are comparable to the flickering cluster model for water of Frank and Wenn[18] and Nementhy and Sheraga[19]. The latter authors consider a model for water in terms of groups of water molecules joined by hydrogen bonds in a manner analagous to quartz structures. The groupings which are not presumed to be time stable, consist of 25 to 91 molecules. The dielectric constant of water is higher than for the salts but methyl alcohol,

which has a comparative dielectric constant of glycerol with a comparative viscosity could be expected to give similar models.

When the temperature drops sufficiently low for only one form of predominant packing to occur, the cations which establish this form will be interlocked with the nitrate discs. Thus, both conductivity and viscosity will depend on the relaxation of the packings for movement to occur.

In the case of viscosity, during the time of formation or dissipation, the interlocked nitrates will become more labile and, if a shearing force is applied, flow will occur preferntially here. For conductivity, similarly, the less rigid packing during formation will allow the relative moment of anions and cations at lower energies. Thus, both processes are dependent on the relaxation time and will tend to have similar slopes at low temperature.

The temperature dependence can also be explained on this basis. The amount of local ordering present is entirely dependent on the kinetic energy of the system and consequently the gradual broadening of the dispersion as

the temperature rises is due to the formation of larger numbers of packing arrangements in the melt. The increase in size of ϵ'' is probably due to free conduction effects associated with the reduced ordering forces.

The standard mechanisms postulated to explain dielectric effects in inorganic glasses[11, 20, 21] are somewhat different to those suggested above. In this case the covalently bonded anions trap the metal cations in holes in the structure, where they vibrate with a periodicity of about 10^{-12} to 10^{-14} secs. When a field is applied, the equilibrium position of the cation changes due to a distortion of the anion network. In an alternating field the continuous change of equilibrium position gives rise to a dielectric effect. As in the present case, the temperature dependence is anomalous due to conductivity effects.

REFERENCES.

SECTION I.

(1) Rowlinson, J.S. — Liquids and Liquid mixtures 1959 Butterworth, 263.

(2) Kirkwood, J.G. and Boggs, E.M. — J. Chem. Phys. 1942, 10, 394.

(3) McLellan, A.G. — Proc. Roy. Soc. 1952, A 210, 509.

(4) Rodriguez, A.E. — Proc. Roy. Soc. 1957, A 239, 373.

(5) Barker, J.A. — Lattice Theories of the Liquid State 1963, Pergammon, 263.

(6) Lennard-Jones, J.E. & Devonshire, A.F. — Proc. Roy. Soc. 1937, A 163, 53.

(7) Lennard-Jones, J.E. & Devonshire, A.F. — Proc. Roy. Soc. 1938, A 165, 1.

(8) Corner, J. and Lennard-Jones, J.E. — Proc. Roy. Soc. 1941, A 178, 401.

(9) Barker, J.A. — Lattice theories of the liquid state Chapter 6, Pergammon, 1963.

(10) Rowlinson, J.S.and Curtiss, C.F. — J. Chem. Phys. 1951, 19, 1519.

(11) McLaughlin, E. — Quarterly Revs., 1960, 14, 238.

(12) Longuet-Higgins, H.C. and Valleau, J.P. — Mol. Phys. 1958, 1, 284.

(13) Kirkwood, J.G. — J.Chem.Phys. 1946, 14, 180, 347.

(14) Green, H.S. — Handbuch Der.Physik 1960, 10, 1.

(15) Frenkel, J. — Kinetic Theories of Liquids Clarendon, 1946.

(16) Andrade,E.N. da C. — Phil. Mag. VII 1934, 17, 497, 698.

(References - contd.).

(17) Lindemann, F.A. Phys. Z. 1910, 11, 609.

(18) Glasstone, S., Laidler, K.J. and Eyring, H. Theory of Rate Processes 1941, McGraw-Hill.

(19) Batchinski, A.J. Z. Phys. Chem. 1913, 84, 643.

(20) Eyring, H. and Marchi, R.P. J. Chem. Ed. 1963, 40, 562.

(21) Cohen, M.H. and Turnbull, D. J. Chem. Phys. 1959, 31, 1164.

(22) Cohen, M.H. and Turnbull, D. J. Chem. Phys. 1961, 34, 120.

(23) Fox, T.G. and Flory, P.J. J. App. Phys. 1950, 21, 581.

(24) Doolittle, A.K. J. Appl. Phys. 1951, 22, 1471.

(25) Levy, H.A. and Danford, M.D. Molten Salts, Ed. Blander, M. 1964 Wiley.

(26) Furukawa, K. Disc. F. Soc. 1959, 32, 53.

(27) Levy, H.A., Agron, P.A., Bredig, M.A. and Danford, M.D. Ann. N.Y. Acad. Sci. 1960, 79, 762.

(28) Smith, G.P. Molten Salts. Ed. Blander. 1964. Wiley.

(29) Smith, G.P. and Boston, C.R. J. Chem. Phys. 1961, 34, 1396.

(30) Cleaver, B., Rhodes, E. and Ubbelohde, A.R. Proc. Roy. Soc. 1963, A 276, 437, 453.

(31) Janz, G.J. and James, D.W. J. Chem. Phys. 1961, 35, 739.

(32) Janz, G.J. and Kozlowski, T.R. J. Chem. Phys. 1964, 40, 1699.

(References - contd.).

(33) Sauerwald, F. and Shinke, H. — Z. Anorg. Chem. 1960, 304, 25.

(34) Blander, M. — Molten Salts. Ed. Blander. 1964 Wiley.

(35) Frame, J., Rhodes,E. and Ubbelohde, A.R. — Trans. F. Soc., 1959, 55, 2039.

(36) Present Thesis. Chapter IV.

(37) Rostowski, A.P. — Z. Russ. Fiz.Chim. Obscht, 1930, 62 , 2055.

(38) Stevels, J.M. — Phillips Tech. Rev. 1952, 13, 293.

(39) Bergmann, A. — C.R., Acad. Sci. URSS 1939, 38, 304.

(40) Jones, J.O. — Glass. Methuen 1956.

(41) Dietzel, A. and Poegel, H.J. — Atti.III Intern. Glass Cong. Venice 1953, 214.

(42) Urnes, S.U. — Glass technische Berichte 1961, 34, 213.

(43) Gross, E.F. and Kolesowa, V.A. — Acad.Nauk SSSR Pamyati S.T. Vavilova 1952, 231.

(44) Kroger, C. and Janetzko, W. — Z. Anorg. & Allegem Chem. 1956, 287, 28.

(45) Katz, L.J., Powers,B.F. and Kleppa, O.J. — J. Phys. Chem., 1961, 35, 765.

(46) McAuley, W.,Rhodes,E. and Ubbelohde, A.R. — Proc. Roy. Soc. 1965 (in publication).

(47) Angell,C.A. — J.Phys. Chem., 1964, 68, 218.

(48) Al Mahadi, A.A.K. — J. Appl. Chem. 1964, 14, 269.

(49) Husband, L.J.B. — J. Sci. Inst., 1958, 35, 300.

(50) Leary and Minns — unpublished observations.

(References - contd.).

(51) Wells, A.F. Structural Inorganic Chemistry Clarendon 1962.

(52) Sass, R.L., Vidale,R., & Donohue, J. Acta. Cryst., Camb., 1957, 10567.

(53) Janz, G.J. and James,D.W. Electrochim Acta 1962, 7, 427.

(54) Wilmshurst, J.K. and Senderoff, S. J. Chem. Phys. 1961, 35, 1078.

SECTION II.

(1) Smith, F.E. Phil. Mag., 1912, 24, 541.

(2) Frame, J. Ph.D. Thesis.

(3) Rostowski, A.F. Z. Russ. Fiz. Chim Obscht. 1930, 62, 2055.

(4) Dietzel, A. and Poegel, H.J. Atti III Intern. Glass Cong. Venice, 1953, 214.

(5) Urnes, S.U. Glasstechnische Berichte 1960, 33, 52.

(6) Starling, S.G. The Properties of Matter 1957 MacMillan.

(7) Hagenbach, E. Pogg. Ann., 1860, 109, 385.

(8) Janz, G.J. and Saegusa, J. Electrochem Soc., 1963, 110, 452.

(9) Frame, J., Rhodes,E. and Ubbelohde, A.R. Trans. F. Soc., 1959, 55, 2039.

(10) Bingham, E.C. Fluidity and Plasticity 1922 McGraw-Hill.

(11) Couette, M. Ann. Chem. Phys. 1890, 21, 433.

(12) Stross, F.H. and Porter, P.E. Encyclopedia of Chem. Tech. 1955, 14, 764.

(13) Cleaver, B., Rhodes,E. and Ubbelohde, A.R. Disc. F. Soc., 1962, 32, 22.

(14) Cleaver, B. Ph.D. Thesis.

(References - contd.).

(15) Ives, D.J.G. and Janz, G.J. — Reference Electrodes 1961 Academic Press, 106.

(16) Calvert, R. — The Transformer Ratio Arm Bridge Wayne Kerr Monograph No.1.

(17) Maryott, A.A. and Smith, E.R. — Nat. Bur. Stand. Circ. 1951, 514.

(18) Drake, F.H., Pierce, D.W. and Daw, M.T. — Phys. Revs., 1930, 35, 613.

SECTION III.

(1) Førland, T. — Thermodynamic Props. of Fused Salts. Publication from the Institute of Inorganic Chemistry, The Technical University of Norway, Trondeim.

(2) Levy, H.A., Agron, P.A. Bredig, M.A. and Danford, M.D. — Ann. N.Y. Acad. Sci., 1960, 79, 762.

(3) Katz, L.J., Powers, B.F. and Kleppa, O.J. — J. Chem. Phys. 1961, 35, 765.

(4) Hazlewood, F.J., Rhodes, E. and Ubbelohde, A.R. — Trans. F. Soc. 1963, 59, 2612.

(5) McLaughlin, E. and Ubbelohde, A.R. — Trans. F. Soc., 1958, 54, 1804.

(6) Bloom, H. and Bockris, T.O'M. — Fused Salts. Ed. Sundheim 1964 McGraw-Hill.

(7) Nanis, L. and Bockris, T.O'M. — J. Phys. Chem., 1963, 67, 2865.

(8) Tricklebank, S.B., Nanis, L. and Bockris, T.O'M. — J. Phys. Chem. 1964, 68, 58.

(References - contd.).

(9) Angell, C.A. J. Phys. Chem. 1965, 69, 399.

(10) Von Hippel, A. Dielectrics and Waves 1954 Wiley.

(11) Smythe, C.P. Dielectric Behaviour and Structure 1955, McGraw-Hill.

(12) Murphy, E.T. and Morgan, S.O. Bell System Tech. J., 18, 502, 1939.

(13) Dalbert, M., Magat, M. and Surdut, A. Bull. Soc. Chim. France 1949, 435.

(14) Cole, K.S. and Cole, R.H. J. Chem. Phys. 1941, 9, 341.

(15) Morgan, S.O. Trans. Am. Electrochem. Soc., 1934, 65, 109.

(16) Tamman, G. and Hess,W. Anorg.Allegem Chem., 1926, 156, 245.

(17) Janz, G.J. and Kozlowski, T.R. J. Chem. Phys. 1964, 40, 1699.

(18) Frank, H.S. and Wen, W.Y. 1957, 24, 133.

(19) Nementhy, G.E. and Sheraga, H.A. J. Chem. Phys. 1962, 36, 3382.

(20) Stevels, J.M. Progress in the Theory of the Physical Properties of Glass. 1948. Elsevier Chapter 4.

(21) Gevers, M. due Pré,F.K. Philips Tech. Revs., 1947, 9, 91.

****

Reprinted without change of pagination from the
Proceedings of the Royal Society, A, *volume* 285, *pp.* 263–274, 1965

Melting and crystal structure: association in nitrate melts

By Elizabeth Rhodes, W. E. Smith and A. R. Ubbelohde, F.R.S.
Department of Chemical Engineering and Chemical Technology, Imperial College, London, S.W. 7

(*Received* 22 *July* 1964)

By using various mixtures, properties of molten nitrates can be studied at temperatures well below the freezing points of any pure nitrates of alkalis or alkaline earths. Molar volumes, viscosities, electrical conductivities and ultra-violet absorption spectra have been investigated in this way for mixed nitrate melts down to 140 °C. For a typical pair of uni-univalent cations, such as potassium and sodium, each of these properties shows practically linear variation for all mixtures down to the lowest temperatures studied. On the other hand, cations such as calcium with a higher polarizing power cause marked deviations from linearity in transport properties and absorption spectra in certain mixtures. However, even in such mixtures no excess volume is found, and temperature variation of the molar volume remains linear. Effects observed are discussed in terms of the closest approach between cations and the nitrate anions in these melts. As the temperature falls, there appears to be progressive formation of regions of increased packing density in the melt and corresponding irregular voids. These more densely packed regions may be termed 'clusters' or 'associated' groups of ions. Although probably smaller, such transient clusters have analogies with 'flickering clusters' proposed in some models for water near its freezing point.

Introduction

Non-spherical repulsion envelopes of polyatomic anions have been given as a reason for the anomalously low melting points of ionic crystals such as nitrates (Davis, Rogers & Ubbelohde 1953). Other properties of pure nitrate melts, such as the small volume changes on fusion (Ubbelohde 1960) and the shift towards higher frequency of ultra-violet absorption spectra on passing from crystal to melt (Rhodes & Ubbelohde 1959; Cleaver, Rhodes & Ubbelohde 1961*a*, 1963) likewise accord with the hypothesis that approach between cation and anion can be considerably closer in these melts than in the crystals. However, properties of melts of pure alkali nitrates so far as they have been studied do not suggest association of the ions into any very large clusters, or 'regions' with density above the average. For example, viscosities and electrical conductivities follow a simple Arrhenius type dependence upon temperature reasonably well, right down to the freezing points of the pure nitrate melts. If any appreciable volume fraction of the melt were to be occupied by such regions or clusters as the temperature falls, anomalous increases in viscosity and probably of electrical resistance should become apparent (Ubbelohde 1964).

Although melts of the pure salts do not show any marked anomalies of this kind, it has been reported that binary mixtures of univalent nitrates with divalent cations such as Mg^{2+} or Ca^{2+} solidify into 'glasses' (Stevels 1952; Dietzel & Poegel 1953). Similar statements have also been made about ternary mixtures containing divalent cations as one component (Bergmann 1939). Glass formation in melts can now be given quite specific characterization involving rise of viscosity to about

10^{13} P and a freezing-in of configurational entropy leading to the change from liquid to glass (Jones 1956). Unfortunately, earlier reports do not make it clear if a glass in this precise sense occurs in any mixed nitrate melts. Methods of measurement previously described (Dietzel & Poegel 1953) are particularly confusing in relation to the above criteria applied to mixed nitrate melts. In a completely different approach, glass formation in such mixed melts has been attributed to distortion of the nitrate ion by divalent cations, though distortion is not apparent in infra-red spectra (Borgen, Grjotheim & Urnes 1960) or Raman spectra (Gross & Kolesova 1952).

Although no viscosities of the order 10^{13} P have been detected, it seemed possible, as a working hypothesis, that the moderately high viscosities for certain mixed nitrate melts might be due to incipient increases of the size of associated groups of ions, already postulated in pure molten nitrates. Such growth might be favoured:

(1) By the fact that measurements on mixed nitrate melts can be pushed to much lower temperatures than with any pure nitrate melts; this would favour exothermic processes of association; a lowering of the kinetic energy of the ions likewise enhances the role of any transient association groups or clusters.

(2) By the enhanced electrostriction arising from the presence of divalent cations for which the electrostatic potential ze/r_+ at the contact radius r_+ is considerably larger than in the pure melts hitherto examined. Such effects might even be enhanced if the distribution of divalent cations is not random throughout the mixture.

The present research aimed at elucidating whether any structural anomalies, for example ion association into 'clusters' eventually terminating in glass formation, could be established from appropriate measurements on mixed nitrate melts. Previous studies lend support to the view that when ions or molecules in a melt interlock into groups or 'clusters', identified by the fact that they are compelled to move together in fluid flow, this must enhance the viscosity. To characterize the anomaly, viscosities of a range of mixed melts were studied down to the lowest possible temperatures. Molar volumes of mixtures, though likely to be much less sensitive to any interlocking, have recently been measured for similar mixtures; this particular property of the melts in fact remains quite normal (Al Mahdi 1964; McAuley, Rhodes & Ubbelohde 1965).

Ultra-violet absorption spectra of nitrate melts and electrical conductances have also been measured, to obtain a variety of information about ion interactions in these melts for any given composition. As is discussed below, it is confirmed that mixed melts containing divalent cations show considerable anomalies in the pre-freezing region. However, in our experiments, these anomalies did not become sufficiently extensive to prevent normal crystallization. No true glasses could be found; though some of the chilled melts have a 'glassy' appearance, their structure probably remains microcrystalline.

Experimental

Salts used were $NaNO_3$ (Judactan WABA 99·99 %), KNO_3 (Judactan WABA 99·97 %) and $Ca(NO_3)_2$ (B.D.H. laboratory reagent anhydrous 98 %). Sodium and potassium nitrates were dried by heating at 250 °C for at least 12 h under vacuum followed by three cycles of shock drying (Rhodes & Ubbelohde 1959). Calcium nitrate was dried by heating for not less than 24 h in an open dish at 200 °C. The mixed melts were further dried at 300 °C by passing through them a stream of nitrogen ($O_2 < 6/10^6$) previously dried by using a liquid air trap. Earlier investigations (Frame, Rhodes & Ubbelohde 1961) showed that water was removed to below detectable limits ($< 10^{-4}$ mole fraction) by these operations.

Considerable care was necessary to obtain mixtures of accurately known composition when these included calcium ions, in view of the hygroscopic nature of calcium nitrate. After testing various procedures, calcium nitrate was weighed directly in sealed tubes, and was introduced into a mixing vessel. Potassium nitrate was then added in amounts determined by direct weighing (to 0·2 mg). Mixed melts after further drying by nitrogen, as above, were then transferred directly into the measuring apparatus, a positive pressure of nitrogen and a closed system being used. Mixtures of sodium and potassium nitrate were prepared by conventional procedures. Possible decomposition of the melts at the higher temperatures during prolonged experimentation was carefully investigated in all cases. Melts of pure KNO_3 showed no detectable decomposition at least up to 420 °C over the 100 h of experimentation with any one melt. As more $Ca(NO_3)_2$ was progressively added, thermal stability decreased. For example, in a mixed melt with mole fraction 0·6 of KNO_3, slight decomposition could be observed above 380 °C, whereas pure $Ca(NO_3)_2$ decomposes so rapidly in its melt that no accurate melting point has yet been determined directly.

For determinations of viscosities, electrical conductivities, and molar volumes, thermostats containing mixed melts were used, whose temperature was electronically controlled to $\pm 0{\cdot}05$ degC. Temperature measurements were made to $\pm 0{\cdot}02$ degC by means of Pallador thermocouples, calibrated by direct comparison with a platinum resistance thermometer standardized to 0·001 degC (at the N.P.L.). Apparatus for viscosity measurements and determinations of molar volumes were as previously described (Frame, Rhodes & Ubbelohde 1959; Cleaver, Rhodes & Ubbelohde 1961*b*). Independent tests showed that viscosity data were obtained with an accuracy of 0·5 % without the need to apply end-corrections. Conductance measurements of somewhat lower precision (± 1 %) were made on the same mixtures, by means of an a.c. bridge (Wayne–Kerr operating at 1592 c/s) and a simple capillary type cell, calibrated with N/10 KCl solution. Determinations of ultra-violet absorption spectra of mixed nitrate melts refer to the peak of the weak (E_2) band, which was measured at various temperatures using methods elaborated for pure nitrates (Cleaver *et al.* 1963).

As a general rule, measurements were carried out both with rising and falling temperatures, sometimes extending a series over several days. Results were in good agreement and no hysteresis was perceptible at any stage.

Results

Figures 1 and 2 illustrate viscosity and conductivity data by logarithmic plots. To record the large number of observations in permanent form, curves were fitted by computer to least squares polynomials of the form

$$\log_{10}\eta = a - b(10^4/T) + c(10^4/T)^2,$$

$$\log_{10}\sigma = f + g(10^4/T) \mp l(10^4/T)^2.$$

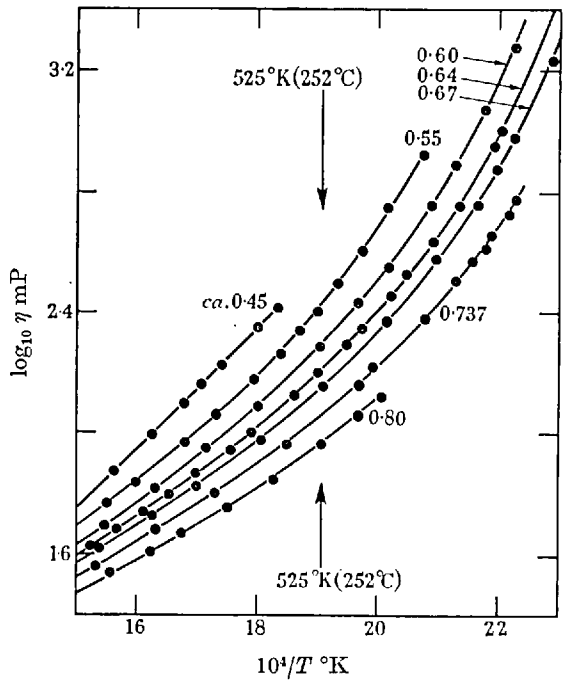

Figure 1. Viscosity of $KNO_3 + Ca(NO_3)_2$ mixtures. Mole fraction KNO_3 as parameter.

Values of the computed coefficients for the various mixtures are recorded in table 1 (viscosity data), and table 2 (conductivity data). Tests showed that although these polynomials were satisfactory for interpolation below 525 °K, at higher temperatures they gave less close fit with data than a computed straight line.

For use in calculating excess functions, a straight line,

$$\log_{10}\eta = -a' + b'(10^4/T),$$

$$\log_{10}\sigma = +f' \mp g'(10^4/T),$$

was fitted by least squares to the data in the temperature range 525 to 667 °K. Computed values of a' and b', f' and g' are recorded in tables 1 and 2.

In the following discussion, the difference is examined between the behaviour at low temperatures of mixed univalent nitrates, and that of mixtures containing

divalent cations such as Ca^{2+}. In the ultra-violet absorption studies, a thin film of the equimolar eutectic mixture of $KNO_3/NaNO_3$ was supercooled down to 100 °C (373 °K) without the formation of crystals (figure 3). (In the bulk phase however,

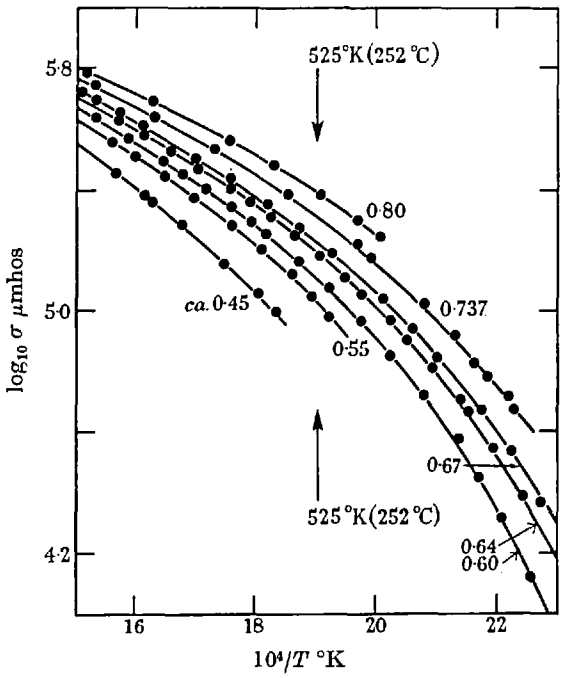

FIGURE 2. Conductivity of $KNO_3+Ca(NO_3)_2$ mixtures. Mole fraction KNO_3 as parameter.

TABLE 1. VISCOSITIES OF MIXED POTASSIUM AND CALCIUM NITRATE MELTS

Constants in the interpolation formula,

$$\log_{10}\eta \text{ mP} = a - b(10^4/T) + c(10^8/T^2) \text{ below } 525 \text{ °K},$$

and of the corresponding straight line,

$$\log_{10}\eta \text{ mP} = -a' + b'(10^4/T) \text{ between } 525 \text{ and } 667 \text{ °K}.$$

composition of mixture mole fraction KNO_3	lowest applicable temp. (°K)	temperature range up to 525 °K			525 to 667 °K	
		a	$10b$	10^2c	$10a'$	$10b'$
0·55	480	4·9175	5·1518	2·0182	9·7995	1·7628
0·60	450	5·3221	5·4829	2·0404	7·2050	1·1580
0·64	460	4·9700	5·0042	1·8654	6·3128	1·4790
0·67	440	5·1649	5·2060	1·8976	4·3050	1·3290
0·74	450	2·6364	2·3765	1·0890	3·4923	1·2460
0·80	500	1·3986	0·8495	0·6026	2·4940	1·1474
1·00	610	—	—	—	1·8949	1·0134

crystallization occurred in this melt at 490°K.) To allow comparisons of the viscosities of these melts at even lower temperatures, a ternary mixture of $NaNO_3$, KNO_3 and $RbNO_3$ (% mole fractions 37·8, 37·8 and 24·2 respectively) was prepared. This remained liquid down to about 465°K ($1/T = 21{\cdot}5 \times 10^{-4}$) as recorded in figure 4.

TABLE 2. ELECTRICAL CONDUCTIVITY OF MIXED POTASSIUM AND CALCIUM NITRATE MELTS

Constants in the interpolation formula,

$$\log_{10}\sigma\ \mu\text{mhos} = f + g(10^4/T) \mp l(10^8/T^2) \text{ below } 525\ °\text{K},$$

and the corresponding straight line,

$$\log_{10}\sigma\ \mu\text{mhos} = +f' \mp g'(10^4/T) \text{ between } 525 \text{ and } 667\ °\text{K}.$$

composition of mixture mole fraction KNO_3	lowest applicable temp. (°K)	temperature range up to 525 °K			temp. 525 to 667 °K	
		f	$10g$	$10^2 l$	f'	$10g'$
0·55	540	—	—	—	12·454	4·3319
0·60	450	1·8807	5·3420	1·9270	7·5314	1·2720
0·64	450	3·5145	3·4694	1·3728	7·5709	1·2588
0·67	440	3·7586	3·2305	1·3049	7·5506	1·2337
0·74	450	8·2629	7·9829	2·4700	7·5049	1·1664
0·80	500	5·8137	0·7559	0·5265	7·2698	0·9997
1·00	610	—	—	—	7·1188	0·8056

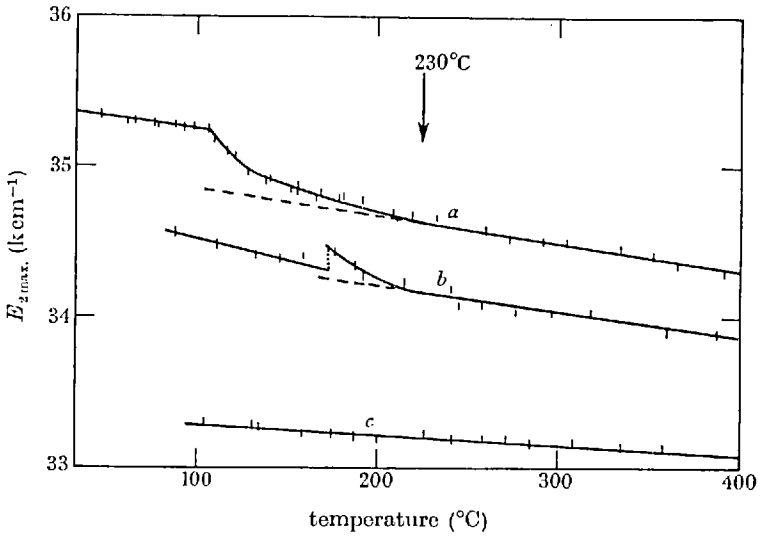

FIGURE 3. Ultra-violet spectra. $E_{2\,max.}$ variation with temperature for several mixtures: (*a*) $KNO_3 + Ca(NO_3)_2$ (0·64 mole KNO_3); (*b*) $KNO_3 + Ca(NO_3)_2$ (0·80 mole KNO_3); (*c*) $KNO_3 + NaNO_3$ (equimolar).

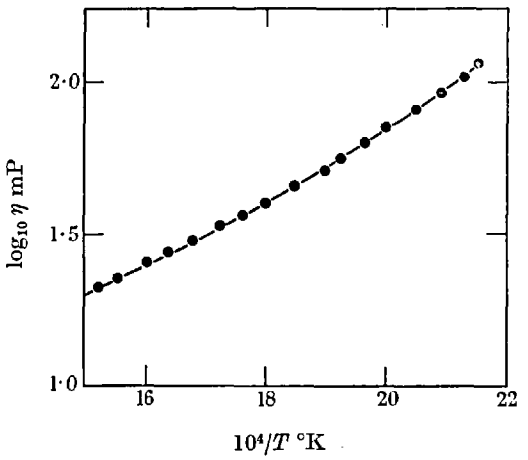

FIGURE 4. Viscosity of (Na + K + Rb) NO_3 mixture. Molo fractions of sodium, potassium and rubidium nitrates are 37·8, 37·8 and 24·2 % respectively.

DISCUSSION

Nitrate melts are liquids remarkable for following ideal mixture laws quite accurately with respect to excess volumes. In binary mixtures of $KNO_3 + Ba(NO_3)_2$ (Cleaver *et al.* 1961*b*), excess volumes do not exceed experimental error ($\pm 0{\cdot}01$ %) and similar behaviour has now been verified for the mixtures $KNO_3 + Ca(NO_3)_2$ (Al Mahdi 1964; McAuley, Rhodes & Ubbelohde 1965) and also $NaNO_3 + Ca(NO_3)_2$, $NaNO_3 + Ba(NO_3)_2$ and $RbNO_3 + Ba(NO_3)_2$ (McAuley *et al.* 1965). This ideal behaviour suggests a structural model for these melts, in which the nitrate anions form a negative plasma, squeezed together by the electrostatic forces exerted by an equivalent number of uni- and di-valent cations, packed at random in the interstices.

Calculations may be made of the volume requirements for the nitrate anion, using a repulsion volume swept out about all three principal axes as illustrated in figure 5 (cf. James & Janz 1962). Treating the nitrate ions as hexagonal close-packed spheres (radius 2·32 Å) with random orientations, the volume occupied by them is 42·6 ml. per gram ion. This may be compared with the measured volumes of the melts at different temperatures (table 3).

In table 3, for the mixed melts the additional equivalent volume allowance for the potassium cations has been estimated by assuming that in pure KNO_3 at 350 °C (molar volume 54·0 ml., Cleaver *et al.* 1961*b*) the hexagonally close packed nitrate anions (volume 42·6 ml.) rotate freely leaving the remaining volume (12·0 ml.) to be occupied by the cations only. This estimate of the volume requirement of the potassium cations is probably high, since no account has been taken of the small excess volume ($\Delta Vf/Vs \sim 3$ %) introduced on fusion (Davis *et al.* 1953). On the other hand, no allowance has been made for any additional space required by the calcium cations. The calcium ions (crystal contact radius 0·99 Å, Wells 1962) will practically fit into the interstices between the nitrate ions (maximum distance between spheres 1·92 Å).

From table 3 it can be seen that even at 350 °C there is no excess of actual volume over that calculated for the close-packed assembly of mixtures containing calcium ions. Clearly in the mixed melts at the lower temperatures tabulated, the nitrate ions are far from having freedom of orientation at random with respect to nearest neighbours. They must shrink by fitting together in various ways, to an extent which increases as the temperature falls. This conclusion is closely related to other evidence reported in the present paper pointing to cluster formation in the mixtures at lower temperatures.

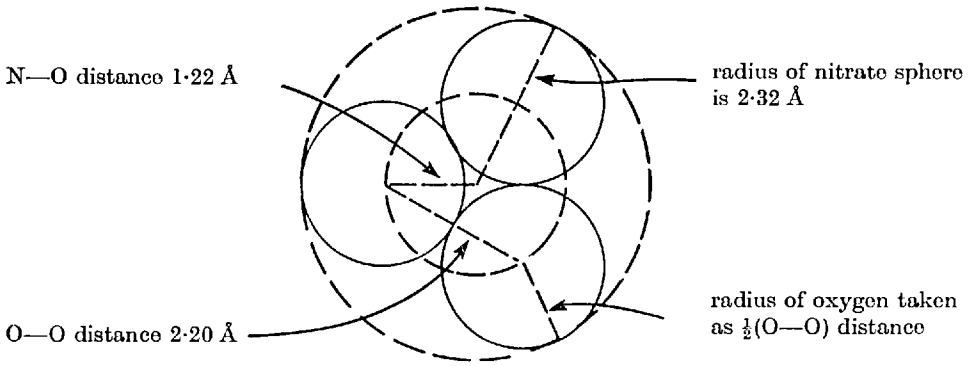

FIGURE 5. Nitrate anion considered as a rotating sphere.

TABLE 3. MOLAR VOLUMES OF MIXED NITRATE MELTS OF POTASSIUM AND CALCIUM

(volumes expressed as ml./g ion of NO_3^-, McAuley *et al.* 1965)

	mole % $Ca(NO_3)_2$		
T(°C)	20	30	40
150	—	43·9	42·5
250	—	45·6	44·1
350	49·2	47·3	45·6
Calculated for NO_3^- only hexagonally close packed (at all temperatures)	42·6	42·6	42·6
allowing for the additional volume estimated for K^+ (see text) at 350 °C	50·0	48·5	47·0

Above 250 °C, the tendency to local loss of freedom of the nitrate ions becomes progressively less as estimated from the molar volume calculations. Other properties such as viscosity and absorption spectra provide more sensitive tests for the structural changes occurring in the melts and may be briefly examined.

Transport properties

If the packing in these melts merely involved spherically randomized nitrate anions with interstitial cations, nitrate melts should provide ideal systems for testing simple models for transport processes, such as the 'hopping' model for

viscous flow (Glasstone, Laidler & Eyring 1941). Even if such models are open to serious criticisms, activation energies may be derived on a purely formal basis from simple Arrhenius-type equations

$$\log \eta = A_\eta + E_\eta/RT, \tag{1}$$

$$\log \sigma = A_\sigma + E_\sigma/RT. \tag{2}$$

Though E_η and E_σ are primarily to be regarded as empirical data defined by (1) and (2), they may be examined for any information they can give about the structure of the melts. This procedure has frequently been applied for various pure ionic melts

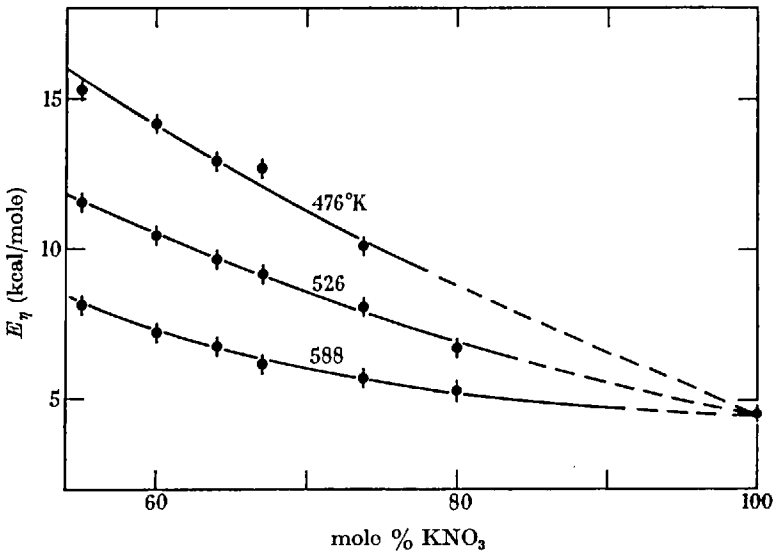

FIGURE 6. Computed values of E_η for $KNO_3 + Ca(NO_3)_2$ mixtures. T (°K) as parameter.

(e.g. Frame *et al.* 1959). Present results permit similar calculations for mixtures. Values of E_η are illustrated in figure 6 and corresponding trends for E_σ in figure 7.

It will be seen that nominal 'activation energies' calculated in this way rise steeply as the temperature falls particularly for mixtures containing most divalent cations. This might be attributed to the effects of electrostriction squeezing the anions together, thus raising the barrier opposing ion hopping, and also increasing the steric hindrance opposing rotation. Until measurements have been completed on the pressure coefficient of viscous flow, it is not possible to discard finally suggestions (Angell 1964) that uniform electrostatic squeezing can explain the whole of the anomalous behaviour of these nitrate melts. However, the present results suggest that models of uniform randomized packing of ions are much too simple to describe nitrate melts. It seems necessary to consider the micro-structure of domains or regions in the melt even to account for the data already available. Present findings lend considerable support to a model in which groups of ions are interlocked into transient clusters of higher density than the average, separated by regions of lower density. At the higher temperatures in the range investigated, such

tighter packed clusters appear to occupy only negligible fractions ϕ of the total volume. But on cooling, particularly in uni-divalent mixtures, the cluster volume fractions begin to influence some of the properties studied to a notable extent.

With this working hypothesis for the structure of the melts, two properties of particular significance appear to be the viscosity and the ultra-violet absorption. Viscosities would be enhanced by the presence of groups or clusters in a melt, whose relaxation time for aggregation and disaggregation is large compared with the relaxation time for ordinary shear relaxation in viscous flow (cf. Ubbelohde 1964, for examples).

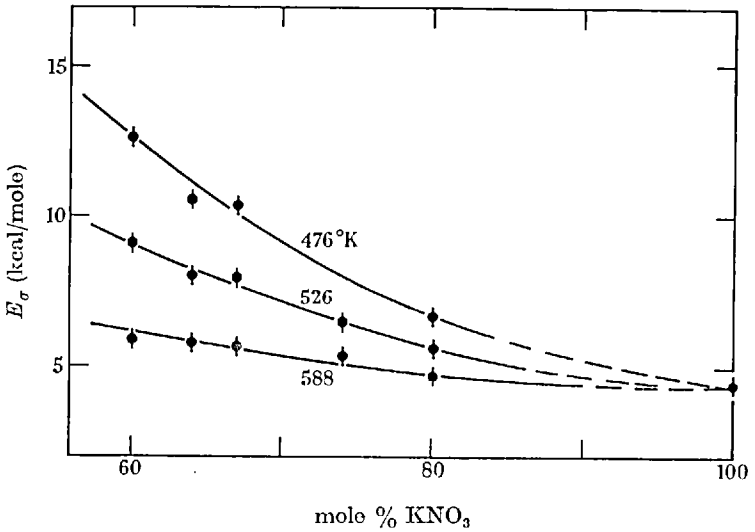

FIGURE 7. Computed values of E_σ for $KNO_3 + Ca(NO_3)_2$ mixtures. T (°K) as parameter.

A simple model treats molecules interlocked so as to obstruct fluid flow as particles in suspension in a liquid. The excess viscosity in such a suspension can be calculated by an equation, for spherical particles,

$$\eta/\eta_i = 1 + 2{\cdot}5\phi + 7\phi^2\ldots, \tag{3}$$

in which η is the actual viscosity at any temperature, and η_i is the 'ideal' viscosity of a fluid of similar composition but in which every part of the volume can relax in the same way under shearing stresses (Einstein 1911). In the present instance ϕ is calculated by extrapolating downwards data obtained at high temperatures using the data given in table 1. The analysis of equation (3) is based on the hypothesis that the fraction $(1-\phi)$ of the melt has 'simple' fluid structure and that ions in the blocked fraction ϕ must move together in the melt. Figure 8 illustrates a direct plot of ϕ against temperature; the proportion of blocked volume in the melt increasing rapidly as the temperature decreases.

The origin of this kind of transient structure of a fluid, consisting of a conglomerate of ions interlocked into clusters and ions packed more freely, can be seen in general terms in the statistical thermodynamics of fluctuations. It often happens that the

units, in this case non-spherical ions, can have their potential energy lowered by packing in certain arrangements closer than is given by the mean volume of the liquid. Except in the case of packing characteristic of crystal nucleus formation such clusters cannot grow very large; large assemblies cannot escape including voids unless they are based on a regular crystal lattice. Analogous non-crystalline clustering of molecules has been discussed for water, in which more detailed knowledge about force fields permits calculation of a range of cluster sizes. Near the freezing-point these range from about 25 to 100 molecules (Nementhy & Sheraga, 1962).

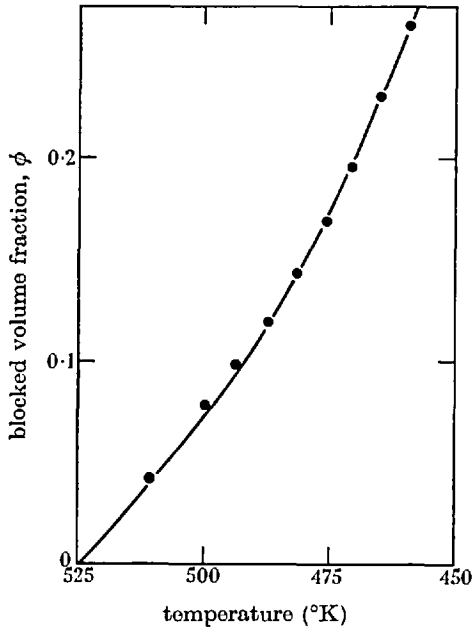

FIGURE 8. ϕ plot from computed values for 0·64 molo fraction KNO_3 in $KNO_3 + Ca(NO_3)_2$ mixture.

Ultra-violet absorption spectra

For mixed nitrate melts these can be interpreted on a corresponding basis. The results for three mixtures are recorded in figure 3. For the mixture of uni-univalent nitrates $KNO_3 + NaNO_3$, the slope dE_2/dT remains linear right down to 100 °C, where the melt is actually supercooled. This behaviour for mixtures may be regarded as additive and accords with the findings of other workers (Boston & Smith 1962). At higher temperatures similar behaviour is found for mixtures when divalent cations are present. But below about 230 °C regions of anomalous shift of $E_{2\,max.}$ in the $KNO_3 + Ca(NO_3)_2$ mixtures (figure 3) begin to be perceptible for the mixture with 0·64 mole fraction KNO_3; they appear at about the same temperature for the mixture with 0·80 mole fraction KNO_3. Temperatures of marked departure from linearity are also marked in figures 1 and 2 from which it can be seen that optical and transport anomalies begin to be prominent in about the same region of temperatures and concentrations. In this region it no longer seems possible to account

for all the observations on the assumption of perturbation of the nitrate anions by uniform electrostriction. Some kind of co-operative fluctuation of density and possibly of local distribution of univalent and divalent cations in the melt, would explain the anomalies observed. More direct methods of examining the conglomerate structure indicated, and of estimating the size of any clusters, or amplitude of co-operative fluctuations from uniform density, are being explored.

Thanks are due to the Royal Society for the loan of the spectrophotometer, to D.S.I.R. for a research bursary (W. E. S.) and to the Ministry of Aviation for other support.

References

Al Mahdi, A. A. K. 1964 *J. Appl. Chem.* **14** 269.
Angell, C. A. 1964 *J. Phys. Chem.* **68**, 218.
Bergmann, A. G. 1939 *C.R. Acad. Sci. U.R.S.S.* (*Doklady*), **38**, 304.
Borgen, O., Grjotheim, K. & Urnes, S. 1960 *Glasstechn. Ber.* **33**, 52.
Boston, C. R. & Smith, G.P. 1961 *Disc. Faraday Soc.* **32**, 14.
Cleaver, B., Rhodes, E. & Ubbelohde, A. R. 1961*a* *Disc. Faraday Soc.* **32**, 210.
Cleaver, B., Rhodes, E. & Ubbelohde, A. R. 1961*b* *Proc. Roy. Soc.* A, **262**, 435.
Cleaver, B., Rhodes, E. & Ubbelohde, A. R. 1963 *Proc. Roy. Soc.* A, **276**, 437.
Davis, W. J., Rogers, S. E. & Ubbelohde, A. R. 1953 *Proc. Roy. Soc.* A, **220**, 14.
Dietzel, A. & Poegel, H. J. 1953 *Proc. 3rd Int. glass congr., Venice*, p. 219.
Einstein, A. 1911 *Ann. Phys., Lpz.*, **34**, 591.
Frame, J. P., Rhodes, E. & Ubbelohde, A. R. 1959 *Trans. Faraday Soc.* **55**, 2039.
Frame, J. P., Rhodes, E. & Ubbelohde, A. R. 1961 *Trans. Faraday Soc.* **57**, 463.
Glasstone, S., Laidler, K. J. & Eyring, H. 1941 *Theory of rate processes.* New York: McGraw Hill.
Gross, E. F. & Kolesova, V. A. 1952 *Acad. Nauk. SSSR, Pamyati S.T. Vavilova*, p. 231.
James, D. W. & Janz, G. J. 1962 *Elektrochem. Acta*, **7**, 427.
Jones, G. O. 1956 *Glass.* London: Methuen Monograph.
McAuley, W. J., Rhodes, E. & Ubbelohde, A. R. 1965 (In publication.)
Nementhy, G. E. & Sheraga, H. A. 1962 *J. Chem. Phys.* **36**, 3382.
Rhodes, E. & Ubbelohde, A. R. 1959 *Proc. Roy. Soc.* A, **251**, 156.
Stevels, J. M. 1952 *Philips Tech. Rev.* **13**, 293.
Ubbelohde, A. R. 1960 Liversidge Lecture. *Proc. Chem. Soc.*, p. 332.
Ubbelohde, A. R. 1964 *J. Chim. Phys.*, p. 58.
Wells, A. F. 1962 *Structural inorganic chemistry* (3rd ed.), p. 70. Oxford: Clarendon Press.

PRINTED IN GREAT BRITAIN AT THE UNIVERSITY PRINTING HOUSE, CAMBRIDGE
(BROOKE CRUTCHLEY UNIVERSITY PRINTER)